DISSERTATION

submitted to the

Combined Faculties for the Natural Sciences and for Mathematics

of the Ruperto-Carola University of Heidelberg, Germany

for the degree of

Doctor of Natural Sciences

presented by

Diploma-Biologist **Verena Orth**,

born in Kruft

Oral-examination:

Influence of

Altered Hippocampal CKAMP44 Expression

on Spatial Reference- /Spatial Working-

and Recency-Dependent-Memory

Referees:

- **Prof. Dr. Peter Seeburg**
- **Prof. Dr. Hannah Monyer**

Declarations according to § 8 (3) b) and c) of the doctoral degree regulations: a) I hereby declare that I have written the submitted dissertation myself and in this process have used no other sources or materials than those expressly indicated, b) I hereby declare that I have not applied to be examined at any other institution, nor have I used the dissertation in this or any other form at any other institution as an examination paper, nor submitted it to any other faculty as a dissertation.

Heidelberg, _____

Acknowledgements

WORK. I thank my referees Prof. Dr. Hannah Monyer and Prof. Dr. Peter Seeburg. I thank Prof. Dr. Hannah Monyer for giving me the possiblity to work on this interesting project in her excellent lab and for her feedback on this work. I thank "the lab" and first and foremost Dr. Elke Fuchs and Dr. Antonio Caputi for teaching and supervising me, especially for many lessons on behavioral testing and virus injections. I thank Regina Hinz-Herkommer for cell culture support and Irmi Preugschat-Gumbrecht for help in everything concerning PCR- and Western-blot-troubleshooting. I thank Laura Winkel. I thank Dr. Elke Fuchs and Dr. Anne Herb for help with TierBase and the supply of animals.

PRIVATE. I thank Elke for correcting this piece of work, for moral support during the last years and for her friendship. I thank Antonio for discussions about movies and the lectures on rugby, as well as for tips and tricks on how to handle Italians and for the many cigarettes I "borrowed" during the years. I thank Julieta for sharing her secret knowledge about qPCR and picture-skills. I thank my fellow PhD-students Magda and Tina, and I thank Annalisa for moral support and evenings in which we tried not to talk about work. I thank Jakob for the shared interest in weird flicks and exchanging movies and movie-magazines with me. I thank the Schratt lab for keeping me sane during endless lonesome testing-periods back in 345. I thank the Italian Community & friends for the Belgian Beer-Weekend, Thursday Girls-Evenings, innumerous hours at Carlo's (I thank Carlo!), Monday-Beers, Negroni-Evenings, the Pole-Dancing-Trip, Little Lake Weekends, Jena-Trip, the Handschuhsheimer Kerwe, New-Years-Eve in Belgium, parties... fun! Special thanks to Roberto and Tati and Gabriele for the unforgettable time in Bari and Bologna, for being friends in good and bad times and for everything else. I thank Suse, Annika and Thomas for the best flat in Heidelberg and giving me a home. I thank Suse for convincing me to write this work in LaTeX. Thanks to my dormatory-flatmates Boa, Daniel, Sonja, Flo, Vadym & Joel for the nice time. I thank my best friends Doreen and Toni for simply being there when I needed them and for a long friendship. I thank Bine and Joe and my friends in Jena for making me still feel at home. I thank Didi for the latenight LaTeX-support and for giving me a place to stay in Munich.

I thank my parents, my sister and my grandma for being a lovely family.

I thank Daniele.

Contents

Abstract

The newly discovered brain-specific transmembrane protein CKAMP44 was shown to influence AMPA receptor function in the mouse hippocampus where the protein is differentially expressed. The low mRNA expression in CA1-neurons versus the high expression in DG-neurons gives reason to hypothesize that the different CKAMP44 levels influence memory processes assigned to these subfields. The DG has long been proposed to provide the cellular substrate for the process of spatial pattern separation, whereas CA1 is assumed to be the basis of temporal pattern separation. To investigate these hypotheses, two mouse models of altered CKAMP44 expression were analyzed.

Theoretically, a global knockout of CKAMP44 should influence a region with high endogenous CKAMP44 expression (DG) more than a region with low expression (CA1). Vice versa, CKAMP44 overexpression should exert a stronger influence on a region with low (CA1) than on a region with high expression (DG). Thus, the CKAMP44$^{-/-}$ mice served as a model to study the involvement of CKAMP44 in the DG-based spatial pattern separation. CKAMP44$^{-/-}$ mice failed to show any impairment in hippocampus-dependent spatial reference- and spatial working-memory tests including spatial pattern separation. In the second model, virus-mediated CKAMP44 overexpression was confined to the hippocampus. Compared to Controls, CKAMP44^{HCoex} mice made a similar number of errors during both spatial reference- and spatial working-memory test on the eight-arm radial arm maze. But a newly designed analysis of the working memory errors on the eight-arm radial arm maze and the chance-level performance during rewarded alternation revealed an impairment in the ability to process or retrieve stimulus-specific, recency-dependent memory in CKAMP44^{HCoex} mice.

Thus, the CKAMP44^{HCoex} model adds further proof to the implicated role for CA1 in temporal pattern separation, and also provides the hitherto only model of altered hippocampal memory funciton upon manipulation of an AMPA receptor auxiliary protein.

Zusammenfassung

CKAMP44 ist ein membrandurchspannendes Protein, welches im Gehirn von Mäusen entdeckt wurde, und dort die Funktion der AMPA-Rezeptoren beeinflusst. Das Protein wird in verschiedenen Regionen des Hippokampus unterschiedlich stark exprimiert. Die Menge nachweisbarer mRNA ist in CA1-Neuronen relativ gering, in DG-Neuronen hingegen sehr hoch. Auf Grund dieser Expressionsunterschiede wird vermutet, dass die CKAMP44-Level CA1- und DG-assoziierte Gedächtnisprozesse unterschiedlich beeinflussen. Seit langem wird dem DG eine wichtige Rolle im Prozess der Auftrennung räumlicher Muster (“ spatial pattern separation”) zugeschrieben. Wohingegen die Rolle von CA1 in der Auftrennung zeitlicher Muster (“ temporal pattern separation”) gesehen wird. Um diese Annahmen genauer zu untersuchen, wurden zwei Mausmodelle manipulierter CKAMP44-Expression analysiert.

Theoretisch sollte der globale Knockout von CKAMP44 die Region hoher Expression (DG) stärker beeinflussen als die Region niedriger Expression (CA1). Die umgekehrte Annahme gilt für die Überexpression von CKAMP44. Dementsprechend wurde anhand von CKAMP44$^{-/-}$ Mäusen der Einflusses von CKAMP44 auf die DG-basierte Auftrennung räumlicher Muster untersucht. Komplementär wurde anhand von CKAMP44^{HCoex} Mäusen die CA1-basierte Auftrennung zeitlicher Muster analysiert. Die CKAMP44$^{-/-}$ Mäuse zeigten keinerlei Beeinträchtigung in hippokampusabhängigen Tests des räumlichen Referenz- und Arbeitsgedächtnisses. Im Test zur Auftrennung räumlicher Muster erzielten die Tiere ein normales Ergebnis. Durch Injektion eines Viruskonstruktes in den dorsalen Hippokampus, konnte die Überexpression in den CKAMP44^{HCoex} Mäusen auf dieses Areal beschränkt werden. Verglichen mit Kontrolltieren zeigten CKAMP44^{HCoex} Mäuse die gleiche Anzahl an Fehlern während räumlichen Referenz- und Arbeitsgedächtnistests auf dem 8-Arm Radial-Maze. Eine Analyse der Fehler, welche die Tiere während des räumlichen Arbeitsgedächtnistests begingen, enthüllte eine Beeinträchtigung der Fähigkeit, stimulusspezifische Erinnerungen unmittelbar vorhergehender Ereignisse zu prozessieren oder abzurufen. Auf diese Schwäche ist auch das zufallsmäßige Alternieren der CKAMP44^{HCoex} Mäuse im T-Maze Test zurückzuführen.

Somit liefert das CKAMP44^{HCoex} Modell neue Beweise für die Rolle von CA1 im Prozess der Auftrennung zeitlicher Muster, und stellt das bisher einzige Modell veränderter hippokampusbasierter Gedächtnisfunktion durch Manipulation eines AMPA-Rezeptor-Hilfsproteins dar.

1 Introduction

The adult human brain has more than 100 billion (10^{11}) neurons. In the cortex, each neuron is connected to other neurons via up to 15.000 synapses. The estimated 10^{14} connections are everything but stable: Every day neurons die, neurons are born, neurons are rewired and synaptic strength is up- or down-regulated.

We constantly are in contact with an ever-changing world and integrate its signals to adapt our behavior, we sense and we interact. Therefore the most important feature of our nervous system is its flexibility. The constant modification of synapses contributes significantly to brain plasticity and is thus functionally relevant for behavioral changes. The strength of a synapse mirrors the activity experienced in the past. Efficacy of synaptic transmission is enhanced via long-term potentiation (LTP) or diminished via long-term depression (LTD). These changes can be manifested pre- or post-synaptically. Presynaptic alterations affect the release probability, composition and recycling of transmitters. The most powerful means of influencing synaptic strength is, however, located in the postsynapse. Ionotropic glutamate receptors (iGluRs) regulate the postsynaptic answer to presynaptic transmitter release. NMDA-type iGluRs (NMDARs) open upon rapid stimulation and allow Ca^{2+} to enter the cell. Intracellular Ca^{2+} levels influence the number of AMPA-type iGluRs (AMPARs) in the postsynaptic membrane and thus the excitability of a cell. Additionally to transport and abundancy of AMPARs, the efficacy of transmission exerts a great influence on synaptic plasticity. During the last few years, auxiliary proteins interacting with AMPARs were discovered to influence receptor trafficking and kinetics. The identification of TARPs (transmembrane AMPAR regulatory proteins) gave rise to a new area of research and by now, several members that belong to three classes of AMPAR-interacting auxiliary proteins were found and partially characterized. CKAMP44 (Cystine-knot AMPAR modulating protein; 44 kDa) is one of these members and is the foucus of this study, namely to investigate the functional role of CKAMP44 in hippomcampus-dependent learning and memory.

The following chapters of introduction will elaborate the above shortly mentioned neurobiological findings and lead the reader towards the results of this work and the subsequent discussion.

1.1 Synaptic Plasticity and the Substrates of Learning

Roger Sperry's ground-breaking and Nobel prize honored work lead him to the idea that every single connection in the nervous system is determined by the genes of the neurons. [Sperry, 1945]. With the proceeding in genome research it became evident that genes cannot provide the necessary capacity to store information for every single synapse [Changeux and Garey, 1985]. Sperry's ex-colleagues and co-laureates David Hubel and Torsten Wiesel unveiled in ground-breaking experiments that extended over two decades, the mechanisms of information processing in the visual system. Axons of developing retinal ganglion cells (RGCx) compete for space in their primary target, the superior colliculus, where a retinotopic map of visual information is established. Surplus connections wither (pruning) upon lack of usage [Hubel, 2004]. This research paved the way for a change of ideas from Sperry's genetic determinism to the notion of a more flexible and adaptable brain.

In the 40s, Canadian psychologist Donald Hebb postulated the "Hebbian synapse" [Hebb, 1949]. Hebb's theory is summarized as "neurons that fire together wire together" [reviewed by: Doidge, 2007]. This new idea lead to the quest for molecular substrates that allow neurons to detect synchronous activity and initiate change in synaptic plasticity. Furthermore, Hebb was the first to propose memory to be represented by the activity of cell assemblies. Two decades later, David Marr translated this concept into mathematical formulas to explain synaptic circuits [Marr, 1971]. In the 1970s, aspects of Hebb's theory were experimentally supported by the discovery of long-term potentiation (LTP) by the work of Timothy Bliss and Terje Lømo in hippocampal synapses [Bliss and Gardner-Medwin, 1973]. The hippocampus remained the region-of-choice for the following decades of LTP-research. Some years later a mechanism underlying the weakening of synaptic strength was discovered: Long-term-depression (LTD) was first described in the cerebellum [Ito et al., 1982] and subsequently in the hippocampus [Sejnowski, 1991].

In the 90s, ionotropic glutamate receptors have been identified as the molecular substrate for LTP and LTD. IGluRs comprise three families: N-methyl-D-aspartate receptors (NMDARs), Kainate receptors (KARs) and alpha-amino-3-hydroxy-5-methyl-4-isoxazolepropionicacid receptors (AMPARs). Metabotropic glutamate receptors (mGluRs) play a role in synaptic plasticity via activation of second messenger systems. They mediate mGluR-LTD [Gladding et al., 2009] at parallel fiber-Purkinje cell synapses [Ito et al., 1982] and in hippocampal subregion CA1 [Bashir et al., 1993]. MGluR-LTD differs from the earlier described NMDAR-LTP. **Figure 1.1** provides an overview of glutamate receptor subtypes.

According to their importance for the here presented work, further elaborations focus on NMDA- and especially AMPA-receptors.

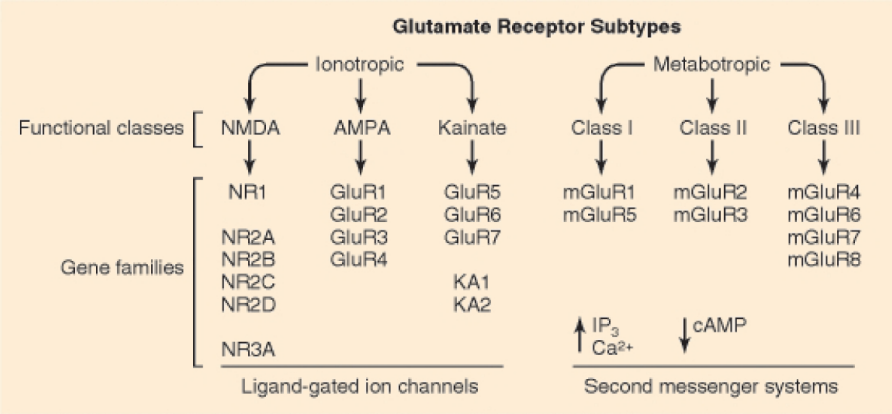

Figure 1.1: Molecular Families of Glutamate Receptors. Each of two main glutamate receptor divisions comprises three functionally defined groups (classes) of receptors. These are made up of numerous individual subunits, each encoded by a different gene. Taken from [Siegel et al., 1999]

1.1.1 NMDA Receptors

The NMDAR is a heterotetrameric receptor [reviewed by: Cull-Candy et al., 2001]. Pharmacological studies in the CA1 hippocampal subfield identified the NMDAR as a critical component for LTP-generation [Collingridge et al., 1983]. Shortly after, the first proof of the involvement of NMDARs in learning and memory-formation was provided [Morris et al., 1986]. Electrophysiological studies elucidated the key-features of the receptor: voltage dependent Mg^{2+} block [Nowak et al., 1984], high Ca^{2+} permeability [MacDermott et al., 1986], activation by glutamate and co-agonist glycine [Johnson and Ascher, 1987], and relatively slow activation and deactivation kinetics [Stern et al., 1992; Lester and Jahr, 1992]. Cloning of cDNAs encoding NMDAR components and consecutive experiments with recombinant NMDARs in heterologous expression systems lead to the unveiling of subunit composition [Moriyoshi et al., 1991; Monyer et al., 1992] and developmental expression [Monyer et al., 1994]. In summary, NMDARs serve as coincidence-detectors [Seeburg et al., 1995], modulate intracellular Ca^{2+} level and thus trigger signaling cascades leading to plastic changes at the synapse.

1.1.2 AMPA Receptors

NMDARs initiate long-term synaptic changes via changes of intracellular Ca^{2+} level. The major targets of the triggered signaling cascades are AMPARs. AMPARs are characterized by their fast kinetics and the blocking of Ca^{2+} permeability of the receptor upon involvement of GluA2, one of four possible subunits [Keinänen et al., 1990, reviewed by Hollmann and Heinemann, 1994]. The genetic sequence of GluA2 encodes for glutamine (Q) at the so-called Q/R-site.

During mRNA-editing, the codon for glutamine (Q) is changed to the codon for arginine (R). This small substitution makes the subunit and thus every GluA2-containing receptor impermeable for Ca^{2+} [Sommer et al., 1991]. Topology of the AMPAR and the role of the Q/R-site in Ca^{2+} permeability are summarized in **Figure 1.2**.

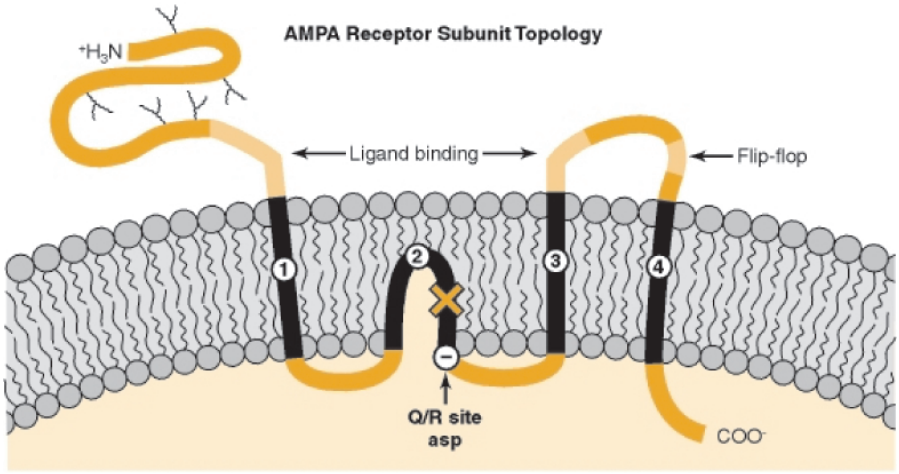

AMPA Receptors: Role of Q/R Site in Permeation

M2

GluR1	Q
GluR2	NEFGIFNSLWFSLGAFMRQGCDISPRSLS
GluR3	Q
GluR4	Q

Receptors	Internal polyamines	Pca	External polyamine spider toxins	γ (pS)
Lacking GluR2	Block	High	Block	7/16/27
+ GluR2 (R)	No block	Low	No effect	4/8
+ GluR2 (Q)	Block	High	Block	7/16/24

Figure 1.2: AMPAR Subunit Topology and Editing. Upper panel: Transmembrane topology and functional domains of AMPARs. X = Q/R site location in the 2nd membrane domain. Lower panel: Location and role of Q/R site in ion permeation through AMPARs. The amino acid sequences of GluR1 - GluR4 (GluA1 - GluA4) are identical within the pore loop except for the Q/R site, as shown. The phenotypes of AMPARs containing edited or unedited GluR2 (GluA2) or lacking GluR2 (GluA2) are summarized. Pca, calcium permeability; γ (pS) single channel conductance. Taken from [Siegel et al., 1999]

Not only mRNA-editing, alternative splicing [Sommer et al., 1990] and subunit composition but also trafficking and exit of the ER, transfer to the Golgi for glycosylation, cytoskeletal transport, synapse delivery [Greger and Esteban, 2007], lateral diffusion [Ashby et al., 2006] and eventual retention [Opazo and Choquet, 2011] influence the transmission at the synapse. AMPARs have no motor domains. Associating proteins thus must assist in the diverse trafficking processes. These putative partner proteins provide a wealth of possibilities to alter synaptic plasticity via AMPAR disposability. Currently, the idea of parallel AMPAR trafficking

pathways, serving two functionally distinct forms of synaptic plasticity, gained much interest. “Hebbian plasticity” (input-specific, associative, rapid LTP) and “homeostatic synaptic scaling” (not input-specific, slow and accumulative) are thought to cooperate to promote information storage and circuit refinement. Studies suggested that LTP and synaptic scaling indeed manifest themselves via different trafficking pathways; with LTP being GluA1-dependent [Zamanillo et al., 1999; Shi et al., 2001] and operating on a time scale of minutes [Malenka and Bear, 2004], whereas synaptic scaling depends on GluA2 and gradually increases the number of synaptic AMPARs over a period of many hours [Turrigiano and Nelson, 1998; Ibata et al., 2008]. Thus, the distinct regulation of these processes via different proteins is of major importance for synaptic plasticity, learning and memory. Initially, the trafficking-assistants were thought to be cytosolic proteins interacting with the C-terminal domain (CTD) of the receptor subunits. Despite the lack of direct interaction between scaffolding proteins like PSD-95 and PSD-93 and AMPARs, it has been shown that the number of synaptic AMPARs crucially depends on the expression of these auxiliary proteins [Stein et al., 2003; Ehrlich and Malinow, 2004].

In 2000, stargazin, the first transmembrane protein to interact with AMPARs, was identified [Chen et al., 2000]. This solved the discrepancy in the lack of interaction but dependence between scaffolding proteins and AMPARs and added a new topic in the research field of AMPARs, namely the TARPs (transmembrane AMPAR regulatory proteins). TARPs and other AMPAR-interacting auxiliary proteins, referred to as “AMPAR auxiliary proteins”, will be introduced in detail in the next chapter with focus on the protagonist of this work, CKAMP44.

1.2 TARPs and AMPAR Auxiliary Proteins

”The whole is more than the sum of its parts”. Aristotle’s famous quote is easily applicable to the function of AMPARs. For a long time it was believed that the biophysiological properties are solely based on the subunit composition and withstand – once spliced, edited, and assembled – further changes. Only recently this theory has been shaken by the discovery of TARPs and AMPAR auxiliary proteins (**Figure 1.3**).

Interactions between these proteins and the AMPAR subunits interfere not only with trafficking but – and this is of highest importance – also profoundly modulate the functional properties of the receptors in a flexible fashion. This opens a variety of possibilities to shape the kinetics of synaptic AMPARs and thus to adapt the synapse to ever-changing activation realities. For the sake of comprehension, the diverse mechanisms by which TARPs and AMPAR auxiliary

proteins influence AMPAR-trafficking and -gating are not addressed in the text but are itemized in **Table 1.1**.

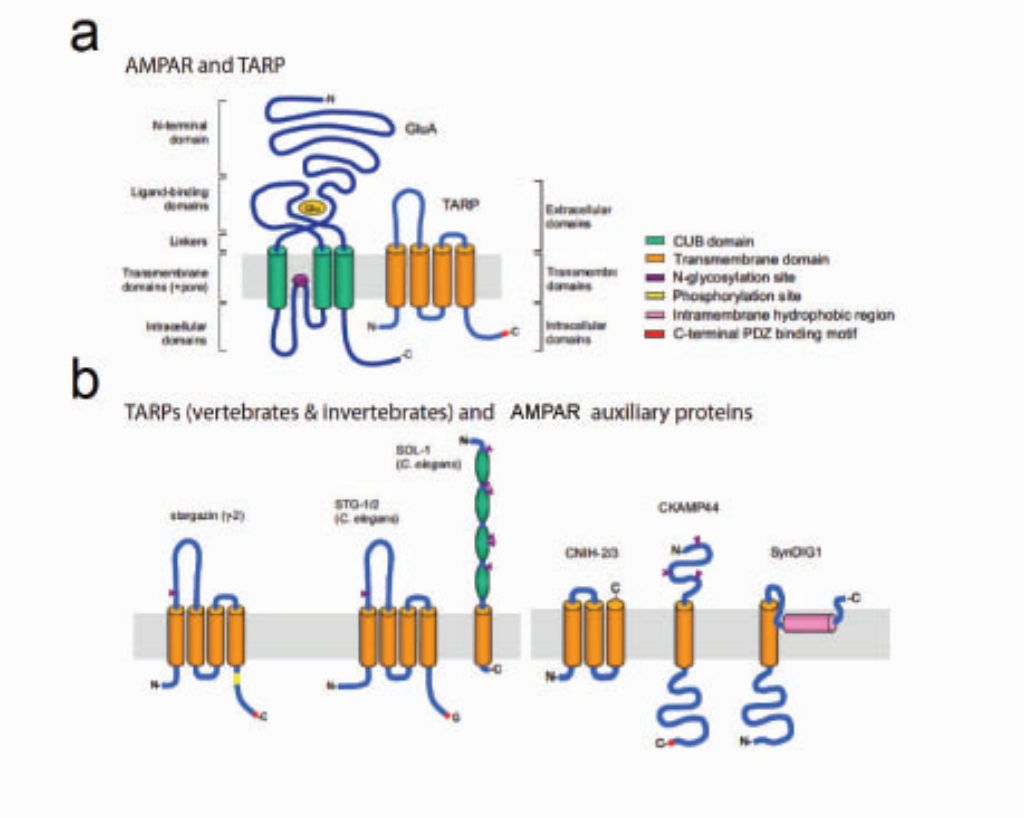

Figure 1.3: TARPs and AMPAR Auxiliary Proteins. (a) Illustration of the structural features of a closely opposed individual GluA subunit and a canonical TARP. The GluA subunit of a tetrameric AMPAR is composed of a large extracellular N-terminal domain (NTD), the ligand-binding core, transmembrane (TM) domains, linker regions, and several intracellular domains including the C-terminal tail (CTD). Agonists such as glutamate (yellow) bind within the ligand-binding core to mediate channel opening. The Q/R site (magenta) is the narrowest constriction of the AMPAR pore and is an important determinant of its functional properties. The TARP auxiliary subunit consists of four TM domains with a large extracellular loop, essential for TARP modulation of AMPAR gating. The tip of the TARP CTD contains a PDZ binding motif (red), which is known to bind to PDZ domain-containing proteins such as PSD-95, and which is essential for the synaptic targeting of AMPARs. (b) Illustration of the proposed secondary structures of TARPs and AMPAR auxiliary proteins mentioned in the text. Adapted from [Jackson and Nicoll, 2011]

	Type I TARPs				Type II TARPs		Candidate AMPAR Auxiliary Proteins		
	stargazin (γ-2)[a]	γ-3[b]	γ-4[c]	γ-8[d]	γ-5[e]	γ-7[f]	CNIH-2/3[g]	CKAMP44[h]	SynDig1[i]
PDZ binding motif	Class I-TTPV	Class I-TTPV	Class I-TTPV	Class I-TTPV	Atypical-SSPC	Atypical-TSPC	none	Class II-EVTV	none
Surface trafficking of AMPARs	↑	↑	↑↑	↑↑	↔	↑	↔	↓↓	unknown
Enriched at synapses/PSD fractions	↑↑	↑↑	↑↑	↑↑	↔	↑	↑	↑↑	↑↑
Synaptic targeting of AMPARs	↑↑	↑↑	↑↑	↑↑	↔	↑	↔	unknown	↑↑
Desensitization and deactivation rates	↓	↓	↓↓	↓↓	↑	↓	↔	↑ desensitization ↓ deactivation	unknown
mEPSC decay	↓	↓	↓↓	↓	↔	unknown	↔	no effect	unknown
Resensitization	no effect	no effect	↑	↑	no effect	↑	no effect	unknown	unknown
Mean channel conductance	↑	↑	↑	↑	↑	↑	↑	unknown	unknown
Peak open probability	↔	no effect	no effect	no effect	↓	no effect	no effect	unknown	unknown
Intracellular polyamine affinity	↓↓	↓↓	↓↓	↓↓	↓	↓↓	↓↓	unknown	unknown
Glutamate affinity	↑↑	↑↑	↑	↑	↓	no effect	unknown	↑↑	unknown
Kainate efficacy	↑↑	↑↑	↑↑	↑↑	no effect	↑	no effect	unknown	unknown
CNQX efficacy	↑	↑	↑	↑	unknown	unknown	↔	unknown	unknown
Polyamine toxin efficacy	↑	↑	↑	↑	unknown	unknown	unknown	unknown	unknown

Table 1.1: Modulation of AMPAR Surface Trafficking, Synaptic Targeting and Gating by Mammalian TARPs and AMPAR Auxiliary Proteins. Upwards arrows indicating increase, downwards arrows indicating decrease, horizontal arrows incicating variable effects or conflicting reports. Taken from Jackson and Nicoll, 2011. References: [a] [Hashimoto et al., 1999]; Chen et al., 1999, 2000; [Schnell et al., 2002]; [Tomita et al., 2003, 2005]; [Yamazaki et al., 2004]; [Priel et al., 2005]; [Turetsky et al., 2005]; [Bedoukian et al., 2006]; [Kott et al., 2007, 2009]; [Soto et al., 2007], [Soto et al., 2009]; [Koerber et al., 2007]; [Milstein et al., 2007]; [Cho et al., 2007]; [Menuz et al., 2007]; [Suzuki et al., 2008]; [Jackson and Nicoll, 2011]. [b] [Tomita et al., 2003]; [Kott et al., 2007, 2009]; [Kato et al., 2007, 2010]; [Milstein et al., 2007]; [Cho et al., 2007]; [Menuz et al., 2007]; [Suzuki et al., 2008]; [Soto et al., 2009]; [Shi et al., 2009]; [Jackson and Nicoll, 2011]. [c] [Tomita et al., 2003]; [Kott et al., 2007, 2009]; [Kato et al., 2007, 2010]; [Koerber et al., 2007]; [Milstein et al., 2007]; [Cho et al., 2007]; [Menuz et al., 2007]; [Suzuki et al., 2008]; [Soto et al., 2009]; [Shi et al., 2009]; [Jackson and Nicoll, 2011]. [d] [Tomita et al., 2003]; [Rouach et al., 2005]; [Kott et al., 2007]; [Milstein et al., 2007]; [Cho et al., 2007]; [Menuz et al., 2007]; [Suzuki et al., 2008]; [Soto et al., 2009]; [Kott et al., 2009]; [Shi et al., 2009, 2010]; [Kato et al., 2010]; [Jackson and Nicoll, 2011]. [e] [Tomita et al., 2003, 2005]; [Kato et al., 2007, 2008, 2010]; [Soto et al., 2009]. [f] [Priel et al., 2005]; [Kato et al., 2007, 2008, 2010]; [Soto et al., 2009]. [g] [Schwenk et al., 2009]; [Shi et al., 2010]; [Kato et al., 2010]. [h] [Von Engelhardt et al., 2010]. [i] [Kalashnikova et al., 2010].

1.2.1 Stargazin and the γ-Family of TARPs

A spontaneous mutation in an inbred mouse strain lead to the discovery of stargazin, the prototypical TARP (alternatively named "$\gamma-2$" due to its homology to the voltage-gated calcium channel (VGCC) subunit $\gamma-1$). Stargazer mice display a unique behavioral phenotype comprising the eponymous head-tossing, ataxia and dyskinesia [Noebels et al., 1990]). A decade later the lack of stargazin was linked to the AMPARs: Despite normal expression levels of the GluA subunits, functional AMPARs were absent in cerebellar granule cells (CGN) [Hashimoto

et al., 1999]. This was the first hint to the involvement of stargazin in surface-delivery of AMPARs [Chen et al., 2000]. Stargazin belongs to a family of tetrameric membrane-spanning proteins with cytosolic N- and C-termini ($\gamma-2$ to $\gamma-8$). Some of them appear to be functionally redundant. For instance, $\gamma-3$, $\gamma-4$ and $\gamma-8$ rescued AMPAR-mediated surface currents in stargazer CGNs, and thus were defined as initial TARPs [Tomita et al., 2003]. Not only because they influence trafficking but also because they change functional properties of the channel [Priel et al., 2005; Turetsky et al., 2005; Zhang et al., 2006; Milstein et al., 2007], $\gamma-3$, $\gamma-4$ and $\gamma-8$ can be truly classified as auxiliary subunits of the AMPARs. Recent studies showed that although $\gamma-5$ $\gamma-7$ failed to compensate the lack of stargazin, both proteins mildly modulated AMPAR trafficking and gating and were thus categorized as type II TARPs, complementary to the initial TARPs, now termed type I TARPs [Kato et al., 2010]. The widespread and extensively overlapping expression of different TARP subtypes raised the question regarding the potential subtpye-specific modulation of AMPARs. Indeed, distinct TARP subtypes differentially modulate channel properties of GluA2-containing (Ca^{2+} impermeable) AMPARs, adding yet another possibility to vary synaptic AMPAR-mediated transmission across neuronal cell-types, depending on the associated TARP subtype, its expression level and the AMPAR/TARP stoichiometry [Jackson and Nicoll, 2011]. For detailed reviews on TARPs see the work of Nicoll and colleagues [Milstein and Nicoll, 2008; Jackson and Nicoll, 2011].

1.2.2 Invertebrate TARP Homologs

Lurcher mice display ataxia as a result of apoptotic death of cerebellar Purkinje cells during postnatal development. This is due to a gain-of-function mutation in GluR$\delta-2$ [Zuo et al., 1997]. Although sharing roughly 30% sequence identity with AMPARs and NMDARs, GluRδ -1 and -2 are not activated by glutamate and thus termed "orphan" iGluRs. The lurcher-defect was successfully copied in *C. elegans* by mutating the AMPAR-homolog GLR-1. The worm showed aberrant movements. By screening for rescue-mutations and consecutive analysis, SOL-1 (suppressor of lurcher) has been identified as a transmembrane protein modulating GRL-1 gating [Zheng et al., 2006]. In the course of further experiments [Walker et al., 2006a,b; Wang et al., 2008] Ce STG-1 and Ce STG-2 (*C. elegans* stargazin-like proteins) proved to be crucial for GLR-1 function. It seems that the role of stargazin in modulating AMPAR gating is evolutionary older than the influence on receptor trafficking.

1.2.3 Cornichon Homologs CNIH-2 and CNIH-3

The quest for further TARPs or other AMPAR auxiliary proteins gained momentum by the discovery that only roughly 30% of AMPARs in the rat brain are associated with $\gamma-2$ or $\gamma-3$, i.e. with TARPs exhibiting ubiquitous expression [Fukaya et al., 2005]. Proteomic analysis identified transmembrane AMPAR-binding proteins that are homologs to the highly conserved *Drosophila* cargo receptors "cornichon" and thus were named CNIH-2 and CNIH-3 (cornichon homologs) [Schwenk et al., 2009]. Additionally to the 30% of AMPARs assembling with TARPs, 70% bind to cornichons. Schwenk and colleagues concluded that the interaction of TARPs and cornichons is mutually exclusive in the majority of AMPARs.

Recent experiments showed that endogenous CNIH-2 localizes in part to the surface of hippocampal neurons and acts synergistically with $\gamma-8$ to regulate AMPAR-pharmacology and -gating [Kato et al., 2010]. Whereas in cerebellar granule cells (CGCs), overexpressed CNIH-2 was shown to promote Golgi trafficking of AMPARs but did not reach the surface [Shi et al., 2010]. The controversy of CNIH-2 function in hippocampal neurons versus its function in CGCs was solved in 2011 by Gill and colleagues. They showed that CNIH-2 modulates stoichiometry of TARPs within AMPAR-complexes in diverse neuronal subtypes. But the protein associates at the cell surface exclusively with specific TARP-containing AMPARs – like $\gamma-8$/AMPAR complexes – that are expressed in hippocampal CA1-neurons but not in CGCs [Gill et al., 2011].

1.2.4 Novel AMPAR Auxiliary Protein Candidate: SynDIG1

Differential gene expression analysis of the already mentioned lurcher mouse lead to the discovery of yet another potential AMPAR auxiliary protein, namely synDIG1 (synapse differentially induced gene 1). SynDIG1, member of a family comprising 4 genes, is a transmembrane protein regulating synapse development by promoting synaptic localization of AMPARs [Diaz et al., 2002]. SynDIG1 either works via AMPAR trafficking or by "'priming' nascent synapses for delivery of AMPA receptors via other molecules such as TARPs". The expression of SynDIG1 is activity regulated. Proof for a modulatory effect of SynDIG1 on AMPAR-kinetics is still missing [reviewed by: Diaz, 2011].

1.2.5 CKAMP44 and the Cystine-Knot Family

CKAMP44 (cystine knot AMPAR modulating protein of 44 kDa) is a brain-specific transmembrane protein recently found in our lab by using proteomic approaches [Von Engelhardt

et al., 2010]. The structural idiosyncrasy of the protein is an accumulation of 8 cysteine residues (see **Figure 1.4a**) similar to the Cys-knot structure in ω-conotoxins, which function as Ca^{2+} channel blockers [reviewed by: Heinemann and Leipold, 2007]. CKAMP44-mRNA is expressed widely throughout the brain with prominent levels in hippocampus (**Figure 1.4b**). Neurons in CA1 express low levels and neurons in DG express particularly high levels of CKAMP44mRNA.

Upon coexpression with GluAs (GluA1, GluA2 or GluA3) in a heterologous expression system (*Xenopus* oocytes), CKAMP44 reduced AMPAR-mediated steady-state currents by influencing AMPAR desensitization. In neurons it was shown that CKAMP44 influenced AMPAR transmission by allowing stronger and faster AMPAR desensitization and slower recovery from desensitization. All other TARPs and AMPAR auxiliary proteins reduce desensitization (**Table 1.1**). Based on the observation that AMPAR subunit mutations that stabilize the close cleft conformation have the same effect, it is hypothesized that CKAMP44 stabilizes the close cleft conformation of the ligand-binding core.

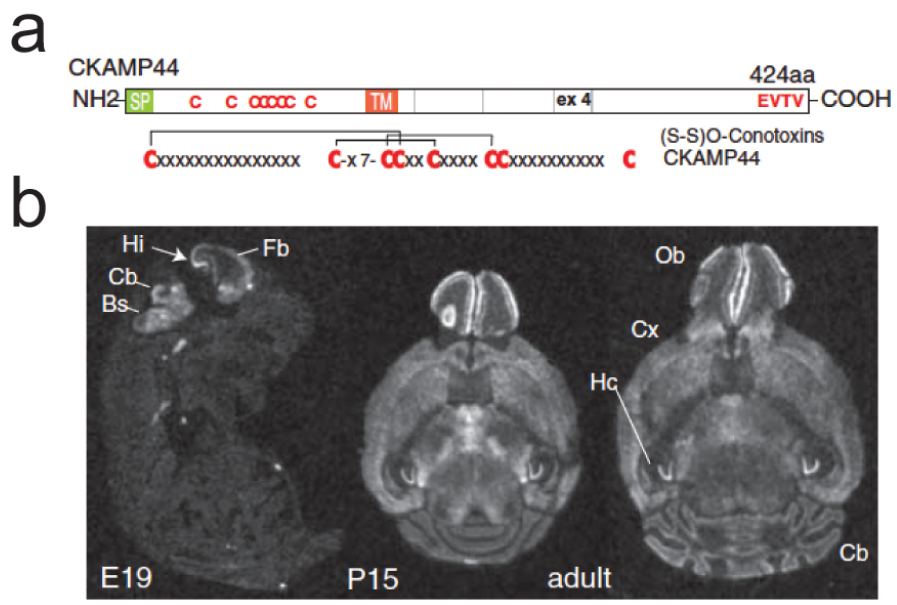

Figure 1.4: Novel AMPAR Auxiliary Protein CKAMP44. (a) Schema of the 424 amino acid residue CKAMP44. SP, signal peptide; extracellular domain with cysteine-rich region (red Cs); TM, single transmembrane region; intracellular domain containing a C-terminal PDZ domain interaction site. Grey lines indicate separated exons encoding protein regions. Below: Cys-knot motif of CKAMP44. Brackets indicate proposed disulfide bridges. (b) CKAMP44-mRNA expression by in situ hybridization on sagittal section of a mouse at E19, on brain sections of P15 and adult mouse. Adapted from Von Engelhardt et al., 2010.

To investigate CKAMP44-mediated effects on hippocampal function, overexpression and knockout studies were performed in CA1- (low expression) and DG-principal cells (high expression) in acute brain slices. CKAMP44 was shown to differentially modulate short-term plasticity in these synapses. In CA1 neurons, the paired pulse ratio was reduced upon CKAMP44 overexpression, whereas in DGCs, the paired pulse ratio was increased upon CKAMP44 knockout. The effect on short-term plasticity of EPSCs by reducing paired-pulse facilitation is stunning because this kind of plasticity is normally expressed presynaptically by changes in transmitter release. The subfield-confined CKAMP44 expression raises the question as to the CKAMP44 involvement in hippocampal learning and memory.

1.2.6 The Merits of Mutant Models

Spontaneous mutations enabled the discovery of TARPs and other AMPAR auxiliary proteins (stargazer- and lurcher-mice). These mice offer insight into the importance of AMPAR auxiliary proteins in behavior dependent on synaptic AMPARs, and thus contribute to link AMPAR auxiliary proteins to neurological and psychiatric diseases.

In the course of TARP research, many single and combinatorial $\gamma-$mutants have been generated. **Table 1.2** shows the consequences of mutations in one or several TARPs for AMPAR trafficking and behavior. It is worth noting, that the knockout of one or more TARPs resulted in lethality or severe impairments whenever $\gamma-2$ (stargazin) was affected, whereas double and even triple-knockouts of non-$\gamma-2$ TARPs had no effect on the phenotype. For the mammalian cornichon homologs CNIH-2 and CNIH-3, no deficient mouse models have been described so far. Behavioral studies in mice with targeted deletion of the SynDIG1 gene are ongoing in the Diaz lab [Diaz, 2011] but have not resulted in publications.

The redundancy and possible combinatorial effects of TARPs make it hard to show their involvement in expression of distinct behavioral functions. Tissue-specific mutants may be able to shed light upon the complexity of AMPAR auxiliary proteins. The here discussed CKAMP44^{HCoex} mouse is the first model linking tissue-specific misexpression of an AMPAR auxiliary protein to a distinct behavioral phenotype.

Mutant Mouse	Targeting	Viability/ Survival	Behavioral Phenotype	Cell-Type Specific AMPAR Trafficking Phenotype
stargazer (γ-2)[a]	spont	viable	dyskinesia, head-tossing, severe ataxia, spike-wave discharges (seizures), low body weight	CGN: severe loss of synaptic and extrasynaptic AMPARs; PC: reduction in CF and PF synaptic AMPARs with no loss of extrasynaptic AMPARs; SC: severe reduction in PF synaptic AMPARs, with no loss of extrasynaptic AMPARs; CA1: normal; nRT: reduction in synaptic AMPARs; TRN: normal
γ-3[b]	KO	viable	normal	GoC: normal; CA1: normal
γ-4[c]	KO	viable	normal	MSN: loss of synaptic AMPARs in neonates (P5–6), normal in juveniles (P14–16)
γ-7[d]	flox (global)	viable	normal	PC: normal
γ-8[e]	KO	viable	normal	CA1: modest reduction in synaptic AMPARs but severe loss of extrasynaptic AMPARs
γ-2/γ-3[f]	spont/KO	failure to thrive	more severe ataxic phenotype than *stg*, low bodyweight	GoC: reduction in PF synaptic AMPARs; CA1: normal
γ-2/γ-4[g]	spont/KO	failure to thrive/viable (see references)	enhancement in seizures in *waggler* and *stargazer3J* mutants	N/A
γ-2/γ-7[d]	flox/flox (global)	viable	more severe ataxic phenotype than *stg*, low bodyweight	PC: severe loss of CF synaptic AMPARs
γ-2/γ-8[h]	spont/KO	failure to thrive		CA1: more severe reduction in synaptic AMPARs than γ-8 KO alone
γ-3/γ-4[i]	KO/KO	viable	normal	CA1: normal
γ-2/γ-3/γ-4[i]	spont/KO /KO	lethal	newborns do not breathe or move	CTX: normal synaptic and extrasynaptic AMPARs in cultured embryonic neurons; SpC: normal synaptic and extrasynaptic AMPARs in embryonic slices
γ-2/γ-3/γ-8[i]	spont/KO /KO	lethal	N/A	N/A
γ-3/γ-4/γ-8[i]	spont/KO /KO	viable	normal	CA1: modest reduction in synaptic AMPARs, similar to loss of γ-8 alone

Table 1.2: Summary of Behavioral- and AMPAR Trafficking-Phenotypes Observed in TARP Mutant Mice. Abbreviations: spont, spontaneous mutation; KO, knockout; flox, conditional knockout; CGN, cerebellar granule neurons; PC, cerebellar Purkinje cells; SC, cerebellar stellate cells; GoC, cerebellar Golgi cells; CF, cerebellar climbing-fiber pathway; PF, cerebellar parallel-fiber pathway; CA1, hippocampal CA1 pyramidal neurons; nRT, thalamic nucleus reticularis neurons; TRN, thalamic relay neurons; MSN, striatal medium spiny neurons; CTX, cortical neurons; SpC, spinal cord neurons. Taken from Jackson and Nicoll, 2011. [References:[a] [Noebels et al., 1990]; [Letts et al., 1998]; [Hashimoto et al., 1999]; [Chen et al., 1999, 2000]; [Menuz et al., 2008; Menuz and Nicoll, 2008], [Jackson and Nicoll, 2011]. [b] [Menuz et al., 2008]. [c] [Letts, 2005], [Milstein et al., 2007]. [d] [Yamazaki et al., 2010]. [e] [Rouach et al., 2005]. [f] [Menuz et al., 2008, 2009]. [g] [Letts, 2005], [Menuz et al., 2009]. [h] [Rouach et al., 2005]; [Menuz et al., 2009]. [i] [Menuz et al., 2009].]

1.3 The Hippocampus

Famous patient H.M. – inevitable to mention in a text introducing the hippocampus – provided fame for those scientists studying his case and who founded modern neuropsychology and memory research based on their findings. In 1953, Henry Molaison underwent radical experimental brain surgery to cure his epilepsy. The amygdala, entorhinal- and perirhinal-cortices and 2/3 of the hippocampus were removed. This alleviated the symptoms but left him with devastating memory problems making a normal life impossible. H.M. displayed profound anterograde amnesia: He was unable to store new information for more than a few minutes, leaving him "chained to the past" (Brenda Milner). Additionally, partial retrograde amnesia hindered him in remembering the decade preceding the surgery. Brenda Milner and William Scoville (who performed the operation) discovered that the degree of memory impairment in H.M. and other patients undergoing the same kind of surgery, varied with the amount of tissue removed from a specific area, namely the hippocampus [Scoville and Milner, 1957]. These findings contradicted the dogma of Karl Lashey, who failed to find the "engram" (the trace of memory) and thus concluded that memory is not to be assigned to a defined brain structure but that memory is dispersed all over the brain. Instead, Scoville's and Milner's work supported the dual memory model of short-term to long-term memory transfer, introducing the hippocampus as the structure in charge. Up to day, Scoville's and Milner's case-study of patient H.M. has been cited over 2500 times (Web of Science).

To wrest secrets from the hippocampus, scientists continued to use a similar approach by applying lesions to defined areas in brains of rodents. Nowadays, lesion studies are often replaced by more sophisticated methods. Tissue-specific knockout, knockdown, mutations and overexpression of proteins related to memory functions provide the tools for unraveling the "engram". The relatively new field of optogenetics even makes it possible to manipulate a defined group of cells in real-time, in the behaving animal.

1.3.1 Anatomy and Connectivity

The hippocampal formation consisting of hippocampus proper (CA1 and CA3), dentate gyrus (DG), subicular complex and entorhinal cortex (EC), is at large comparable in all mammals. This allowed the rodent hippocampus to become a model system for understanding hippocampal function in learning and memory. The connectivity of the hippocampus subfields CA1, CA3 and DG (**Figure 1.5**) is traditionally described as an excitatory feed-forward trisynaptic loop [Andersen et al., 1966; Swanson et al., 1978]. Neurons in layer II of entorhinal cortex (EC, the major input region to the hippocampus) build the "perforanth path" [Steward and Scoville, 1976] and convey polymodal sensory information to the dendrites of DGCs (1^{st} synapse). DGCs

project through their axons, the mossy fibers, to dendrites of CA3 pyramidal neurons (2^{nd} synapse) which project to CA1 pyramidal cells (3^{rd} synapse) through the Schaffer collaterals [De No, 1934; Blackstad, 1956; Amaral, 1978]. CA1 pyramidal axons connect with entorhinal cortex layer V as the major output region. CA3 has additionally to the DG input a dense interconnected network and receives direct input from EC layer II. Via the temporoammonic pathway, neurons of EC layer II synapse on CA1 pyramidal neurons which send their axons back to EC layer V (monosynaptic pathway).

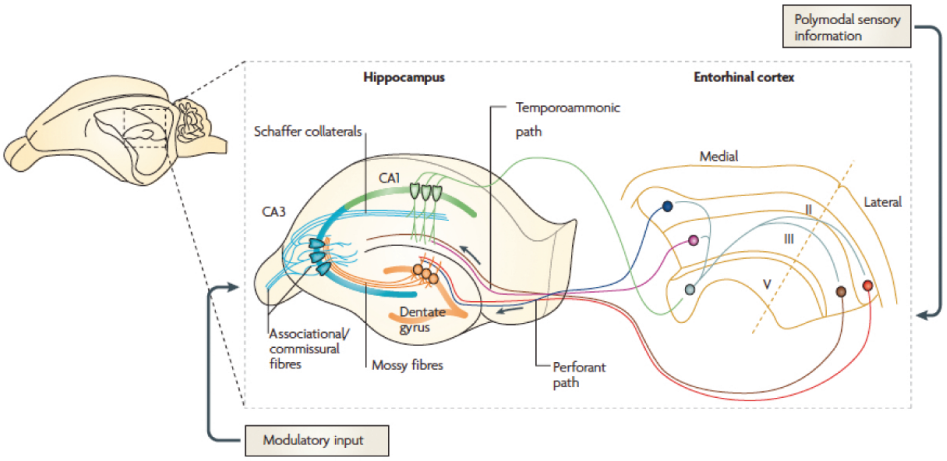

Figure 1.5: Basic Anatomy of the Hippocampus. Wiring diagram of the hippocampus as trisynaptic loop. Major input is provided by axons of the perforant path, conveying polymodal sensory information from layer II entorhinal cortec (EC) neurons to the dentate gyrus (DG) and CA3 (not shown). DG granule cells (DGCs) project through their axons (mossy fibers) to dendrites of CA3 pyramidal neurons, which in turn project to CA1 pyramidal cells through Schaffer collaterals. CA1 pyramidal cell axons connect with layer V EC as the major output region. CA3 principal neurons project contralateral to other CA1 and CA3 pyramidal cells (commissural fibers) and ipsilateral within the CA3 subfield, building a dense interconnected network (associational fibers). CA3 also receives direct input from layer II EC neurons (temporoammonic pathway, not shown). Distal apical dendrites of CA1 pyramidal cells receive a direct input from layer III EC. A rich diversity of interneurons (not shown) provides further modulatory input. Taken from Neves and Bliss,2008.

1.3.2 Place Cells and Spatial Behavior

The discovery of “place cells” assigned the task of spatial navigation to the hippocampus, by creating a “cognitive map” [Tolman, 1948] of the environment [O’Keefe and Dostrovsky, 1971]. Whenever the animal passes a particular place in the local environment, certain place cells fire, representing the entire environment as a pattern of activity of the local cell population

[O'Keefe, 1976; Wilson and McNaughton, 1993]. Place cells are flexible: They participate in representations of different environments [O'Keefe and Conway, 1978]. From then on, the hippocampus was regarded as a processing and storing-unit of spatial memory – a type of declarative memory dealing with spatial locations – consistent with Scoville's and Milner's proposal based on the case study of patient H.M.. To gain insight into the mechanisms affected by diseases of the human brain and resulting in memory deficits, testing of rodents in tasks designed to unveil the mechanisms responsible for two distinct cognitive learning and memory processes, became in-vogue. Spatial reference memory is the ability to incrementally learn the association between a distinct location in space and the environment throughout several repetitions. To access this memory in rodents the Morris water maze (MWM) was developed. The animals learn the position of a hidden escape-platform in a water-filled pool surrounded by spatial cues [Morris et al., 1982]. Spatial working memory is defined as flexible, one trial-based form of short-term memory. This is traditionally tested on the "delayed non-matching-to-place T-Maze" as introduced by Rawlins and Olton [Rawlins and Olton, 1982]. Correct performance in this test (choice of one out of two arms in the T-shaped maze) is reliant on the ability to remember unique information from a single preceding trial (recently explored arm on the T-Maze).

Based on increasing anatomical knowledge, it was possible to apply computational approaches to mimic hippocampal networks. Results from these studies suggested distinct roles for the different subfields. Studies in which a lesion was confined to a hippocampal subfield and genetic engineering which confined iGluR deletions not only spatially but also temporally, unveiled the involvement of NMDARs and AMPARs, and the differential influence of hippocampal subfields step by step. The more research is done on the hippocampus, the more it presents itself as a complex system organizing spatial learning and memory and memory processes beyond.

1.3.3 Subfield-Specificity: Building and Processing of Episodic Memory

The hippocampus organizes spatial memory by forming "cognitive maps" [O'Keefe and Conway, 1978] and integrates temporal aspects, thus being responsible for generation, storage and retrieval of spatio-temporal context-dependent (episodic) memory [reviewed by: Squire, 1994; Eichenbaum, 2001; Nadel and Moscovitch, 2001]. Information is stored as neuronal representations and new information has to be compared to already existing information in order to (1) identify new information as different from already existing representations, or in order to (2) identify new information as a part of already existing representations. These processes are called "pattern separation" and "pattern completion", respectively.

Based on the hippocampal structure and connectivity of the subregions (CA1, CA3 and DG), they have been proposed to be the substrate for distinct functions [Marr, 1971; McNaughton and Morris, 1987; Treves and Rolls, 1992; Amaral et al., 2007]. Indeed, in course of the last decades, many behavioral and electrophysiological studies supplied evidence for distinct processing functions of the subfields [reviewed by: Gilbert and Brushfield, 2009]. CA3, for example, contains extensive recurrent connections and receives direct inputs from entorhinal cortex via the perforanth path and DG derived input via mossy fibers. Based on its connectivity, CA3 was proposed to be an autoassociator [McNaughton and Nadel, 1990; Treves and Rolls, 1994] and comparator [Vinogradova, 2001]. CA3 is believed to retrieve entire patterns from partial input (pattern completion). The sparse and powerful mossy fiber connections from the DGCs onto CA3 principal neurons orthogonalize various inputs, i.e. makes them more different. Thus DG is proposed to be the basis for pattern separation.

CA3 recurrent collaterals: spatial pattern completion
Pattern completion allows retrieval of a complete representation of stored information using partial or degraded cues [Kesner and Hopkins, 2006].

Computational models attributed a pivotal role in pattern completion to the CA3 subfield [Marr, 1971; Rolls et al., 1998; Wallenstein et al., 1998]. To verify this hypothesis, contextual and spatial information procession was investigated in CA3 and CA1 neuronal ensembles by behavioral studies of rodents with subfield-specific lesions or genetically engineered lack of plasticity in CA3 [Lee et al., 2005; Gold and Kesner, 2005; Nakazawa et al., 2002]. Electrophysiological recordings in CA3 pyramidal cells of monkeys and rats hinted at the role of the subfield in completion of a scene in the absence of the visual input and in coherent representation of an environment even when the animal faces different degrees of mismatch in environmental cues [Robertson et al., 1998; Rolls, 1996; Lee and Kesner, 2004]. Experiments measuring the time course of activation of neuron ensembles by using an immediate-early-gene-based imaging method supported these findings [Vazdarjanova and Guzowski, 2004]. Environmental changes seemingly needed to overcome a certain threshold to trigger remapping in CA3 (DG-based pattern separation). If the changes in environment were subtle, CA3 representations remained stable and de-emphasized the perturbations, which is – per definition – a process of pattern completion [Vazdarjanova and Guzowski, 2004].

Dentate gyrus: spatial pattern separation
Pattern separation allows the separation of similar information (partially overlapping pattern of neuronal activity) into discrete representations.

The interconnectivity of CA3 neurons has been suggested to be ideal for encoding and retrieval of memory representations [Marr, 1971]. Soon it became evident that CA3 cannot fulfill this task without an upstream separation device. Based on its anatomy and the mossy fiber projections

to CA3, the DG seems to be tailor-made for this role. The DGC population faces a high level of tonic inhibition and is essentially silent with sparse coding [Jung and McNaughton, 1993]. Each DGC terminates on only a dozen CA3 neurons, but the activity of a single mossy fiber is able to trigger the firing of a downstream CA3 neuron [Henze et al., 2002]. All these anatomical idiosyncrasies make the DG prone to establish de-correlated patterns in the CA3 network and thus subserve CA3 in pattern separation [McNaughton and Morris, 1987; Treves and Rolls, 1992; Amaral et al., 2007, reviewed by Treves et al., 2008].

Pattern separation is manifested in the substantial change of place cell firing (CA1 and CA3) upon minor changes in the sensory input or motivational context [Muller et al., 1991]. This "remapping" is realized in two distinct forms in the DG-CA3 network: "global remapping" and "rate remapping'" [Leutgeb et al., 2005, 2007; Leutgeb and Leutgeb, 2007]. "Global remapping" is defined as the complete redistribution of both firing locations and firing rates in the CA3 cell population. It is associated with a change of spatial inputs from the EC [Fyhn et al., 2007]. During "rate remapping" only the rate, but not the location of active neurons changes, based on altered synaptic input weights (Non-Hebbian plasticity). Rate remapping has been suggested to originate in the DG, but to be independent of EC-input [Fyhn et al., 2007; Leutgeb and Leutgeb, 2007]. Early lesion studies functionally dissociated the DG from the CA1 and provided experimental evidence for a pivotal role of the DG in pattern separation [Gilbert et al., 2001]. DG-*NR1*-KOs in which synaptic plasticity was abolished in DG were unable to distinguish between a shocked and a non-shocked context over time [McHugh et al., 2007]. Recently, adult neurogenesis in DG was proven to be crucial for pattern separation [Clelland et al., 2009; Deng et al., 2010; Tronel et al., 2010; Sahay et al., 2011]. It is hypothesized that the constant gain of new DGCs provides the means for increasing "memory resolution", a term proposed to replace "pattern separation" [Aimone et al., 2011].

CA1: Temporal integration

It was suggested that although the hippocampus processes various types of sensory information, it does so to extract and associate especially spatial and temporal information [Leutgeb et al., 2005; Kesner and Hopkins, 2006]. Studies on DG-based pattern separation and CA3-based pattern completion focused on the spatial component of memory formation and processing, neglecting the temporal context of episodic memory.

Lesion studies gave a first clue about how the temporal component of an experienced episode is processed in the hippocampus. Kesner and colleagues showed that rats with dorsal CA1 lesions were unable to perform non-spatial pair-associated learning if a time component was involved [Kesner et al., 2005]. Further studies supported the implication of CA1 in processing temporal information by a mechanism – somewhat confusingly – called temporal order pattern separation. Results from computational modelling suggested that involvement of CA3 might be required for temporal decay and temporal sequence memory [reviewed by: Rolls and Kesner,

2006]. This was supported by results obtained from behavioral testing of rats with either CA3- or CA1-lesion. All lesioned animals were impaired in a temporal-context dependent task. CA1-lesioned rats performed even worse than CA3-lesioned rats. This indicates that the CA3 subfield is not as critical as the CA1 subfield for the episodic recall of spatio-temporal sequences [Hunsaker et al., 2008].

1.3.4 Knockout-Studies to Dissociate Spatial Working- and Reference-Memory

Results obtained from diverse experiments with hippocampal subfield-specific NR1- and GluA1-knockouts were reviewed in detail by Nakazawa and Sanderson & Bannerman respectively [Nakazawa et al., 2004; Sanderson and Bannerman, 2010] and are summarized in the following sections.

Region-specific NR1-knockouts: The global knockout of the mandatory NMDAR subunit NR1 was lethal [Forrest et al., 1994]. Temporally and spatially restricted NR1 ablation in the murine hippocampus differentialy influenced memory expression and offered insight into different hippocampal memory mechanisms.

Postnatal CA1-specific knockout of NR1 in CA1-*NR1*-KO mice resulted in severe impairment in the hidden-platform MWM test for reference memory [Tsien et al., 1996]. This contradicts results obtained by Bannerman and colleagues: Blocking NMDARs in dorsal hippocampus by NMDAR-antagonist (AP5) infusion did not influence the performance when the mice underwent spatial or non-spatial pre-training in a different environment [Bannerman et al., 1995]. Furthermore, the behavioral impairment of CA1-*NR1*-KOs might have been based on the spread of the mutatation to cortical areas with advancing age [Fukaya et al., 2003].

CA3-*NR1*-KO mice showed normal MWM-performance but failed in the transfer test in which cues were removed after successful learning of the task [Nakazawa et al., 2002]. This specific impairment hints at the involvement of CA3 in pattern completion. The anatomical idiosyncrasies of the subfield support this idea: CA3 displays a robust recurrent network [Miles and Traub, 1986] whose synapses were shown to express NMDAR-dependent plasticity, whereas plasticity at DGC mossy fibre-CA3 synapses proved to be NMDAR-independent [Harris and Cotman, 1986; Williams and Johnston, 1988; Zalutsky and Nicoll, 1990]. Furthermore, CA3-NMDARs were shown to be crucial for rapid hippocampal encoding of novel information, because they support the spatial refinement of CA1-placefields, which is necessary for rapid learning of one-time experience [Nakazawa et al., 2003].

Computational models proposed the DG to be the main source for pattern separation [Marr, 1971; McNaughton and Nadel, 1990]. DG-*NR1*-KO mice expressed normal pattern separation but showed a spatial working memory deficit and intact spatial reference memory performance as assessed simultaneously on the 6-arm radial arm maze [Niewoehner et al., 2007]. In an other study, DG-*NR1*-KOs were impaired in distinguishing two similar contexts early during training although the animals showed normal contextual fear conditioning [McHugh et al., 2007].

CKAMP44$^{-/-}$: The global knockout of GluA1 resulted in animals whose synapses and dendrites were well developed despite a reduction in number of functional AMPARs [Zamanillo et al., 1999]. NMDAR induced AMPAR-delivery to the synapse is GluA1-dependent [Shi et al., 2001] and thus is impaired in GluA1$^{-/-}$ mice; excitatory synaptic transmission is attenuated [Andrasfalvy et al., 2003; Jensen et al., 2003; Romberg et al., 2009]. In the MWM, GluA1$^{-/-}$ mice showed normal reference memory performance in acquisition as well as in retention [Zamanillo et al., 1999]. Rodents with hippocampal lesions needed more time to find the platform. Mice devoid of fast synaptic transmission (upon AMPAR-antagonist infusion) performed at chance level [Riedel et al., 1999]. These findings suggest that the loss of GluA1 is not comparable with the loss of all functional AMPARs. Reisel and colleagues showed that normal performance on spatial reference memory tests in GluA1$^{-/-}$ mice is accompanied by impairment in a "delayed non-matching-to-place forced alternation task", a task that was introduced by Olton [Olton and Papas, 1979] to assess short-term working memory [Reisel et al., 2002]. On the T-Maze and on the RAM (radial arm maze), GluA1$^{-/-}$ mice resembled animals with hippocampal lesions [Rawlins and Olton, 1982; Deacon et al., 2002; Schmitt et al., 2003]. Schmitt and colleagues tested GluA1$^{-/-}$ mice in both spatial reference- and spatial working-memory simultaneously on the RAM, thus providing a "within-subjects, within-task demonstration of intact spatial reference memory and impaired spatial working memory" [Schmitt et al., 2003]. These and previous findings suggest distinct neuronal mechanisms within the hippocampus: A rapid GluA1-dependent form of information processing and an incrementally strengthened spatial reference memory mechanism.

In the following chapter, results obtained from mice with altered CKAMP44 expression provide further insight into the influence the very fine-graded manipulation of AMPARs exerts on distinct forms of memory processes.

2 Materials and Methods

2.1 Materials

2.1.1 Mouse Strains

CKAMP44$^{-/-}$ Mice: The CKAMP44$^{-/-}$ mice were generated by gene targeting. In 129 SvEvBrd ES cells the CKAMP44 promoter region and exon1 were replaced by the PGKbgeo/ puro selection cassette [Von Engelhardt et al., 2010]. ES cell-derived chimeric mice were back-crossed with C57Bl6 mice and F6 and F7 were analysed.

C57Bl/6 Mice: The CKAMP44^{HCoex} mice and the Controls were generated by injecting viral constructs into the dorsal hippocampus of C57Bl/6 mice from Charles River. For virus description and method of injection see subchapters **"AAV Production**" and **"AAV Injection into Dorsal Hippocampus"**.

2.1.2 Antibodies

Primary antibodies and dilutions:

mouse anti-Calbindin (Swant) 1:5000
mouse anti-Calretinin (Swant) 1:5000
mouse anti-Parvalbumin (Sigma) 1:3000
rabbit anti-NPY (Immunostar) 1:5000
mouse anti-NeuN (Chemicon) 1:1000
goat anti-Doublecortin (Santa Cruz) 1:500
rabbit anti CKAMP44 (kindly provided by Dr. Sprengel, MPI) 1:2000
mouse anti-Dynein (Chemicon) 1:8000
mouse anti-GFP (Invitrogen) 1:1000

Secondary antibodies and dilutions:

Cy3TM-conjugated goat anti-mouse rabbit (Dianova) 1:1000
Cy3TM-conjugated goat anti- rabbit (Dianova) 1:1000
Cy3TM-conjugated donkey anti-goat (Dianova) 1:1000
AlexaFluor 488 donkey anti-goat (Invitrogen) 1:1000
Peroxidase anti-mouse/rabbit IgG (H+L) (Vector Laboratories) 1:20000
Biotinylated anti-mouse/rabbit/rat IgG (H+L) (Vector Laboratories) 1:400
DyLightTM549-conjugated donkey anti-mouse
(Jackson ImmunoResearch Laboratories) 1:1000

2.1.3 Plasmids

Both plasmids syn:CKAMP44-IRES-Venus and syn:GFP were modified from the AAV vector pAAV-6P-SEWB [Kügler et al., 2003]. Syn:CKAMP44-IRES-Venus: The full-length coding cDNA for CKAMP44 was obtained by RT-PCR from brain RNA of adult BALB/c mice [see Von Engelhardt et al., 2010]. The human synapsin I promotor and the coding cDNA followed by the bovine growth hormone polyadenylation site were inserted as XbaI-BpiI fragment into pAAV-6P-SEWB. An internal ribosome entry site (IRES) preceding the Venus-sequence supported the bicistronic expression units. Syn:GFP: GFP under the control of human synapsin I promoter was inserted into the pAAV-6P-SEWB-backbone.

2.1.4 Oligonucleotides for Genotyping of CKAMP44$^{-/-}$ Mice

Primers (5' to 3')

1: GAGTCCTGCAGCTGAAACC (19 nt)
2: CGACATCCTCACCGAGGTTG (20 nt)
3: CCCTAGGAATGCTCGTCAAGA (21 nt)

Fragments

Pr. 1 + 2 = 343 bp on wildtype allele
Pr. 1 + 3 = 452 bp on mutant allele

2.2 Methods

2.2.1 Molecular Biological Methods

Standard molecular biological methods were performed as described in Sambrock et al. [Sambrook et al., 1989]. The isolation and purification of plasmid-DNA (for the AAV production) were performed with the Plasmid Maxi-Kit Qiagen (Hilden, Germany) according to the manual provided by the manufacturer.

2.2.2 Genotyping of CKAMP44$^{-/-}$ Mice by PCR Analysis

Mouse tail biopsies were digested by incubating them for two hours at 55°C in TENS buffer (50 mM TRIS-HCl pH 8.0, 100 mM EDTA, 100 mM NaCl, 1% SDS) that contained proteinase K (1 mg/ml). After precipitation with one volume of isopropanol and washing with 70% ethanol, the genomic DNA was resuspended in 250 μl 1x TE buffer (1 mM TRIS, 0.1 mM EDTA pH7.6) for one hour at 55°C. For PCR analysis 2 μl of the dissolved genomic DNA were used in a total volume of 25 μl reaction mix that contained PCR buffer (Invitrogen), 2 mM MgCl2, dNTPs (0.2 mM per nucleotide), specific oligonucleotides (0.4 μM each), 0.5U Taq polymerase (Invitrogen) and sterile water. The conditions for the PCR on CKAMP44$^{-/-}$ mice were as follows:

1. Initial denaturating step : 98°C , 5 min

2. Denaturing: 94°C , 15 sec

3. Annealing : 55°C , 20 sec

4. Elongation : 72°C , 30 sec

Steps 2 to 4 were repeated 34 times, followed by a final elongation step at 72°C for 5 minutes. The PCR product was determined by gel electrophoresis. The PCR product of homozygous CKAMP44$^{-/-}$ mice had a length of 452 bp, the product of Wts had a length of 343 bp.

2.2.3 AAV Production

For rAAV particle production, HEK293 cells were co-transfected with an AAV vector carrying the transcription units of interest and helper plasmids in equimolar ratios by calcium phosphate-mediated plasmid transfection. Cells were lysed 72 hrs after transfection by three freeze-thaw cycles. The cell debris was removed by centrifugation. The supernatant containing the viral particles was treated with benzonase, and viral particles were purified by iodixanol density centrifugation (S6, S7) in a Ti70 rotor at 60.000 rpm. Iodixanol was removed, and the virus was concentrated in PBS buffer in an Amicon Ultra 15 centrifugation filter. The remaining 500 μl solution containing the viral particles was filtered through a Milex GV 0.22 μm pore size. The rAAV particles were stored at -20°C and thawed prior to infection.

2.2.4 AAV Injection into Dorsal Hippocampus

Mice (8 - 9 weeks old at the time of surgery) were anesthetized with isoflurane. One μl of AAV was stereotactically injected into the dorsal hippocampus at a rate of 0.3 - 0.5 μl/min using glass capillaries with a tip resistance of 2-4 M Ω. The injection coordinates were 2.4 mm posterior to bregma, 2 mm lateral from midline, 1.6 mm below the surface of the cortex [Paxinos and Franklin, 2001, modified]. C57/Bl6 littermates were injected with one of the two viral constructs (syn:CKAMP44-IRES-Venus or with syn:GFP). For subsequent behavioral experiments, mice were analysed 7-8 weeks after virus injection.

2.2.5 Immunohistochemistry (IHC)

Fluorescent IHC staining: Mice were transcardially perfused with 4% paraformaldehyde. The brain was postfixed in 4% paraformaldehyde over night and stored in phosphate buffered saline (PBS). 45 μm thick coronal sections were cut on a vibratome (Leica VT1000S, Heidelberg, Germany) and washed with PBS. Free-floating slices were permeabilized and blocked for 2 hours with PBS containing 5% BSA and 0.2% Triton X-100. The incubation of the sections with primary antibodies was performed over night at 4°C. The antibody dilutions were: mouse anti-Calbindin (1:5000), mouse anti-Calretinin (1:5000), mouse anti-Parvalbumin (1:3000), mouse anti-NeuN (1:1000), goat anti-Doublecortin (1:500), mouse anti-GFP (1:1000). Sections were washed with PBS and incubated for 2 hours with Cy3TM-, DyLightTM-594- or AlexaFluor-488-conjugated secondary antibodies (all in 1:1000 dilution). After repeated washing with PBS, slices were transferred onto 0.1% gelatin-coated glass slides and mounted in Mowiol 40-88

(Aldrich, Taufkirchen, Germany). Images were taken using a BX 51 microscope (Olympus, Japan). The applied software was MagnaFire 2.1C.

Peroxidase IHC staining: Expression of marker proteins in the DG of CKAMP44$^{-/-}$ mice was analysed using the avidin-biotin-peroxydase technique (Elite ABC, Vector Laboratories Burlingame, CA). Brains were blocked in 4% agar (dissolved in 1x PBS), cut on the vibratome (45μm; Leica VT1000S) and sections were either stored in 1x PBS at 4°C or washed four times for 10 minutes in order to proceed with the immunohistochemical staining. Sections were incubated first in 10% sucrose/1xPBS for 15 minutes at room temperature and in 30% sucrose/1xPBS over night at 4°C. Permeabilisation of the sections was performed by repeated (4-5 times) freezing (over liquid nitrogen) and defrosting (55°C). To remove the sucrose, four washing steps with 1x PBS (each 10 minutes) followed. Sections were incubated in 1% H_2O_2 in 1x PBS for 10 minutes and washed with 1x PBS four times for 10 minutes. To block unspecific binding sites, sections were incubated 45 minutes in 5% BSA/1x PBS at room temperature. Primary antibodies were diluted in 1x PBS and incubated for 24 hours at 4°C. The antibody dilution was 1:5000 for rabbit anti-NPY. After washing three times with 1x PBS, sections were incubated for two hours at room temperature with the secondary antibody for the DAB staining: biotinylated anti-rabbit IgG, 1:400 in 1x PBS. To enhance the staining reaction sections were incubated with an avidin-biotin complex (ABC Elite Kit, Vector Laboratories) for 90 minutes. Two washing steps with 1x PBS and two with 20 mM TRIS-HCl buffer pH 7.6 (TRIS), each for 10 minutes, followed. Sections were incubated in DAB solution (0.4 mg/ml, Sigma) for 20 minutes. The staining reaction was initiated by adding 0.01% H_2O_2 and stopped by transferring the sections to TRIS-buffer. Three washing steps with TRIS buffer followed. Three final washing steps in TRIS buffer were performed before sections were mounted with gelatin on microscopic glass slides. After the sections were dried, they were cover-slipped with Mowiol 40-88 (Aldrich, Taufkirchen, Germany). For imaging an Olympus BX51 microscope connected to a camera system from INTAS was used. The applied software was MagnaFire 2.1C.

2.2.6 Western Blot (WB)

We analysed CKAMP44 expression by Western blot in the hippocampus and in the cerebellum. Lysate was generated after the mice underwent behavioral testing and thus were minimum 6 months of age. Brain areas were dissected, homogenized in buffer A (0.32 M sucrose, 10 mM HEPES, pH 7.4 plus Complete protease inhibitors; Roche, Mannheim, Germany), and centrifugated at 2000 x g for 10 min. Supernatant was recovered and protein concentration was measured using the Bradford method (Bio-Rad, Munich, Germany). Lysate was analysed

by semi-quantitative Western blot. For immunoblot analysis 10- 20 μg of the protein samples were boiled in SDS gel Laemli buffer for 5 min at 95°C and subsequently separated by SDS-PAGE (10% gel). The transfer of the proteins onto PVDF membranes (Mini-PROTEAN Electrophoresis System; Mini trans blot; Immun-Blot PVDF Membrane; Bio-Rad, Munich Germany) was realized over night. After 2 hours of blocking with 5% skimmed milk powder in PBS the incubation with the specific primary antibodies occurred in 0.1% Tween 20 PBS (PBS-T) for 2 hours. The dilutions of the primary antibodies were as follows: polyclonal rabbit anti-CKAMP44 (1:1000) and monoclonal mouse anti-Dynein antibody (1: 8000). In order to detect the specific antibody binding, horseradish-peroxidase labelled secondary antibodies were used. After washing the membrane 3 times with PBS-T for 10 min, the membrane was probed with the secondary antibodies in PBS-T for 45 min. The dilution of the secondary antibodies was 1: 20000 for the peroxidase-conjugated anti-mouse- and anti-rabbit-antibodies (Vector, Burlingame, CA). Amersham ECL plus Western Blotting Detection Reagents (GE Healthcare Life Sciences, Freiburg, Germany) were used for blot development. Semi-quantitative evaluation was performed using ImageJ.

2.2.7 Behavioral Analysis

MICE

CKAMP44$^{-/-}$ Mice: Behavioral tests were conducted with male littermates of the CKAMP44$^{-/-}$ line. Mice underwent exploratory behavior testing and testing for rewarded alternation on the T-maze as well as spatial working- and spatial reference- memory testing on the eight-arm radial arm maze (RAM). Up to four littermates were held in one cage. The experimenter was blind to the identity of the mice.

CKAMP44^{HCoex} Mice: Behavioral tests were conducted with male C57/Bl6 littermates which were previously injected with either of the two viral constructs. 11 control-injected (syn:GFP-AAV) and 11 CKAMP44^{HCoex} mice (syn:CKAMP44-IRES-Venus-AAV) underwent exploratory behavior testing and testing for rewarded alternation on the T-maze as well as spatial working- and spatial reference-memory tests on the eight-arm radial arm maze (RAM). Four littermates were held in one cage. Two of these four mice were Controls and two were CKAMP44^{HCoex} mice. The experimenter was blind to the identity of the injected construct and blind to the identity of the mice.

TESTS

Open field: The open field consisted of a gray PVC enclosed arena (50 x 30 x 18 cm), which was divided into 10 x 10 cm squares. Since our aim was to assess activity and exploration and not to subject the mice to a strongly anxiogenic situation, normal room illumination was used.

Mice were placed individually into the middle of the box and observed for 5 min. The total number of squares traversed and the total number of rearings were recorded. The test was run on two consecutive days.

Novel object recognition tasks: Mice were individually habituated to an open field box (50 x 30 x 18 cm) for 3 days. During the training session, two different objects A and B were placed into the open field and the mouse was allowed to freely explore for 5 min. The time spent exploring each object was recorded. After a 5 min break during the test phase the animals were placed back into the same box, in which object A "familiar object" was replaced with a copy of A and object B was replaced with the "novel object" C. The animal was free to explore for 5 min. A camcorder was used to evaluate the performance of the animals on a computer screen by an observer blind to the genotype of the animals. The time exploring the familiar and the novel object was recorded. A duplicate of the original familiar object was used to avoid the use of odour cues. The time spent with the new object compared with the time spent with the familiar object during the retention test was used to measure recognition memory (discrimination ratio). All objects presented were of similar surface structures and sizes, but had distinctive shapes and colors, and the objects were presented in a counterbalanced order to prevent spontaneous object preference.

Spontaneous alternation on the elevated T-maze: Mice were maintained on a restricted feeding schedule at 85% of their free-feeding weight. Spatial working memory was assessed on an elevated wooden T-maze. This consisted of a start arm (47 x 10 cm) and two identical goal arms (35 x 10 cm), surrounded by a 10 cm high wall. A metal food well was located 3 cm from the end of each goal arm. The maze was located 1 m above the floor in a well-lit laboratory that contained various prominent distal extra-maze spatial cues. The mice were habituated to the maze, and to drinking sweetened water over several days before spatial nonmatching-to-place testing. Each trial consisted of a sample run and a choice run. On the sample run, the mice were forced either left or right by the presence of a wooden block, according to a pseudorandom sequence (with equal numbers of left and right turns per session, and with not more than two consecutive turns in the same direction). A reward (0.1 ml of 30% sucrose in water) was available in the food well at the end of the arm. The time interval between the sample run and the choice run was approximately 10 s. The animal was rewarded for choosing the previously unvisited arm (that is, for alternating). Mice were run one trial at a time with an ITI (inter-trial interval) of approximately 10 min. Each daily session consisted of 2 to 3 trials, and mice received 50 trials in total. Data were analysed in blocks of 10 trials.

Assessment of spatial reference- and spatial working-memory on the eight-arm radial arm maze (RAM): Spatial reference- and spatial working-memory were assessed using a grey eight-arm radial maze made of plastic (TSE Systems, Bad Homburg, Germany). Each arm (30

x 6 cm) had walls constructed from transparent Perspex and extended from a circular platform (19 cm diameter). A plastic food well was located at the end of each arm. Mice were rewarded with 0.1 ml of sugared (30% sucrose) water. The maze was elevated 80 cm above the floor in a well-lit laboratory that contained various extramaze cues (e. g. laboratory equipment, stools, table and posters). At the entrance of each arm of the maze there was a gray Perspex door that could be controlled by the experimenter using a series of strings. Mice were maintained on a restricted feeding schedule at 85% of their free-feeding weights. The mice were habituated to drink sweetened water on two arms of an elevated Y-maze in a room (i.e. not the testing room) and went through the rewarded alternation on the T-maze before being tested on the RAM.

The mice were trained on a radial arm maze task in which the same four arms were always baited and the reward was not replaced within a trial. The four baited arms were allocated such that two of the arms were adjacent, and the other two arms were 90 degrees apart from the adjacent arms (e.g. arms 1,3,6,8). For each mouse, the position of the baited arms relative to each other and relative to extra-maze spatial cues stayed the same for all trials. At the start of a trial, a mouse was placed on the central platform. The mouse was allowed to explore freely and consume all rewards available. During acquisition phase, Perspex doors prevented mice from re-entering an arm they already visited during the very same trial [Niewoehner et al., 2007; Schmitt et al., 2003]. All doors were closed each time the mouse returned to the central platform where the mouse was confined for 10 s until the next choice. Once an arm had been visited, its door remained closed for subsequent choices. Thus all eight doors were open for the first choice, seven for the second choice, six for the third choice and so on. Using this testing procedure it was not possible for the mice to make spatial working memory errors. This provides a test for spatial reference memory acquisition. Spatial reference memory errors were defined as entries into arms that were never baited (maximum of 4 errors per trial). The maze was rotated periodically to prevent the mice from using intra-maze cues to solve the task. Data were analysed in blocks of 4 trials. By this stage all animals had acquired the spatial reference component of the task and made few errors.

A special condition was then introduced to the spatial reference memory test. To investigate the performance upon deprivation of extra-maze spatial cues, the see-through walls of the arms were veiled with white paper. The mice received 4 trials (one block) in which the same 4 out of 8 arms were baited. After this, the mice received 2 trials in the unveiled condition before introducing the spatial working memory component.

The spatial working memory component of the task was then introduced. The mice received further 28 trials (with an inter-choice interval of 10 sec) in which the same 4 out of 8 arms were baited but in the new task the mice were no longer prevented from re-entering a previously explored arm. The doors were solely used to retain the animals on the central platform between

choices. Spatial working memory errors were scored when a mouse entered an arm that was already visited on the very same trial. A reference spatial working memory error was defined as re-entry into a never baited arm. A non-reference spatial working memory error was defined as re-entry into a previously baited arm. Spatial reference memory errors were scored as before.

Analysis of spatial pattern separation performance during spatial reference- and spatial working-memory test on the eight-arm radial arm maze (RAM): Spatial pattern separation performance was analyses as described in Niewoehner et al., 2007. The analysis is based on the spatial distribution of baited versus unbaited arms. Spatial reference memory errors and spatial working memory errors made during the tests on the eight-arm radial arm maze were categorized as wrong entries made into adjacent or wrong entries made into single arms, thus introducing a spatial pattern separation component. For further description of the analysis, see "Results: 3.1.2.4 and 3.2.2.5 Pattern Separation Performance on the Eight-Arm Radial Arm Maze".

Analysis of recency-dependent choice of arms during spatial working memory test on the eight-arm radial arm maze (RAM): Spatial working memory performance was analysed with focus on the recency of re-entering a previously visited arm. The analysis was based on the assumption that the visit of an arm prevents re-entry into that very same arm in a recency-dependent manner, termed "recency dependent choice of arms". The most severe recency-dependent error ("type 0"-error) was defined as a direct re-entry into a previously visited arm without entering any other arm. A "type 3"-error represents any working memory mistake in which 3 arms were visited between the first entry to an arm and the re-entry to this very same arm. Types of errors comprised "type 0"- to "type 6"-errors. For further description of the analysis, see "Results: 3.2.2.6 Recency-Dependent Choice of Arms during the Working Memory Test on the Eight-Arm Radial Arm Maze".

3 Results

3.1 CKAMP44$^{-/-}$ Mice

3.1.1 CKAMP44 Expression in Hippocampus of CKAMP44$^{-/-}$ Mice and Anatomy of the Hippocampus

The AMPAR auxiliary protein CKAMP44 exhibits a brain specific expression. In situ hybridizations performed on horizontal brain sections of C57/Bl6 mice showed highest levels of CKAMP44-mRNA expression in olfactory bulbs, cerebellum and hippocampus. In the hippocampus, DG-neurons express high levels of CKAMP44 and CA1-neurons express low levels (**Figure 1.4**). Complete ablation of CKAMP44 was achieved by removing the promoter region and exon 1 of the gene. Homozygous CKAMP44$^{-/-}$ mice were viable and did not show major abnormalities [Von Engelhardt et al., 2010].

Western blot analysis of whole hippocampi proved the absence of CKAMP44 in Knockouts and showed reduced protein level in Heterozygous compared to Wildtypes (Wt) (**Figure 3.1**). Immunostainings revealed normal hippocampal anatomy in CKAMP44$^{-/-}$ mice. Overall neuron number and distribution were assessed by neuronal nuclei (NeuN) staining. GABAergic interneurons were stained with antibodies against calcium-binding proteins calretinin (CR) and parvalbumin (PV), addressing different interneuronal subgroups (**Figure 3.2**). There was no difference between CKAMP44$^{-/-}$ and Wt mice.

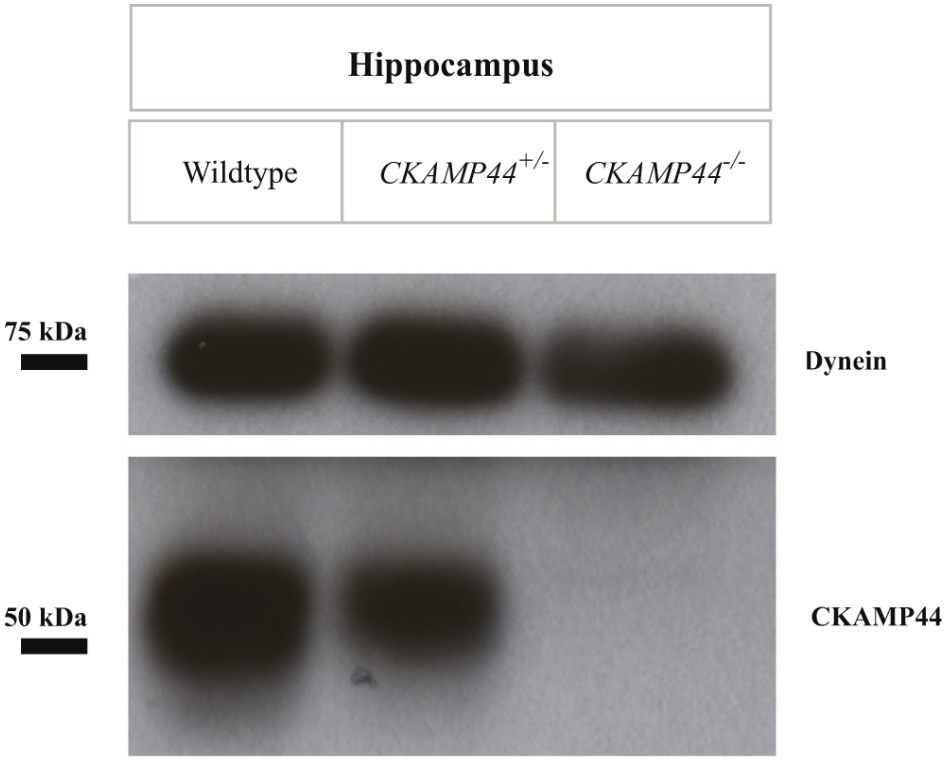

Figure 3.1: Absence of CKAMP44 in the Hippocampus of CKAMP44$^{-/-}$ Mice. Representative Western Blot analysis for comparison of CKAMP44 level in hippocampal lysates of Wt mice, Heterozygots (CKAMP44$^{+/-}$ mice) and Homozygots (CKAMP44$^{-/-}$ mice). CKAMP44$^{+/-}$ mice expressed, relative to the Wt mice, a reduced level of CKAMP44.The protein was not detectable in CKAMP44$^{-/-}$ mice.

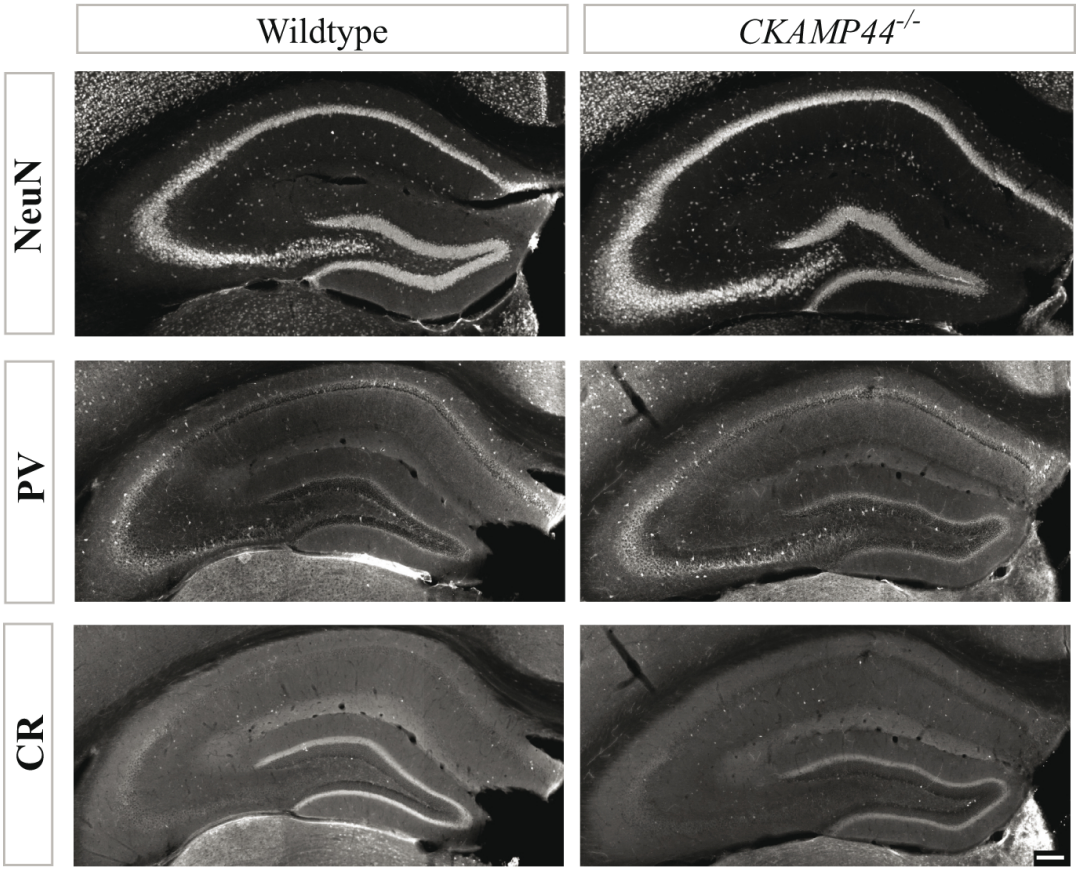

Figure 3.2: Unaltered Hippocampal Anatomy in CKAMP44$^{-/-}$ Mice. Immunostainings for NeuN, PV and CR in dorsal hippocampus of Wt and CKAMP44$^{-/-}$ mice showed no alterations in number and distribution of NeuN-, PV- and CR-positive cells. Sections, 45 μm; scale bar, 25 μm.

Because the DG is the subfield with highest native CKAMP44-mRNA expression [Von Engelhardt et al., 2010], further analysis focused on this subregion. The DG was stained with antibodies for the following DG-specific marker proteins that are generally used to check the integrity of the DG: Doublecortin (DCX) is expressed in neuronal progenitor cells and immature neurons and thus serves as a marker for neurogenesis, calcium-binding protein calretinin (CR) is mainly expressed in dentate granule cells (DGCs) and their dendrites, neuropeptide Y (NPY) is expressed in hilar cells and mossy fibers. The lack of CKAMP44 did not cause obvious anatomical changes in DG. Expression of CB, DCX (**Figure 3.3a**) and NPY (**Figure 3.3b**) in DG of CKAMP44$^{-/-}$ mice was comparable to the expression in Wts.

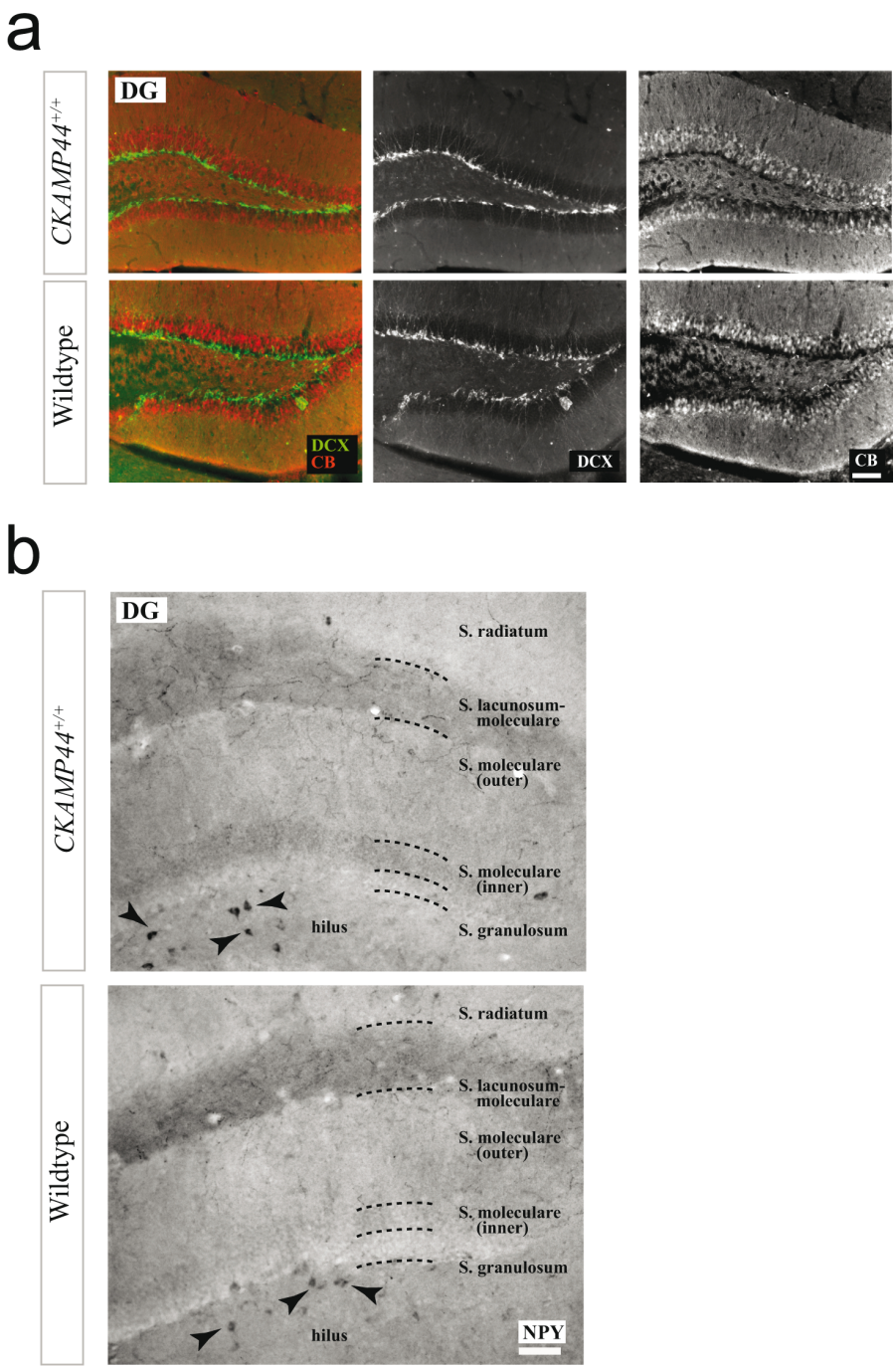

Figure 3.3: Unaltered Expression of Marker Proteins in Dentate Gyrus of CKAMP44$^{-/-}$ Mice. (a) Detailed view of hippocampal subregion DG. Immunostainings for DCX and CB showed no alterations in number and distribution of DCX- and CB-positive cells in CKAMP44$^{-/-}$ mice. Sections, 45 μm; scale bar, 25 μm. (b) Detailed view of the DG hilus and upper blade. Immunostainings for NPY showed no alterations in number and distribution of NPY-positive cells and neurites. S., Stratum; Sections, 45 μm; scale bar, 15 μm.

3.1.2 Behavioral Characterization of CKAMP44$^{-/-}$ Mice

Wts (n = 11) and CKAMP44$^{-/-}$ mice (n = 12) were subjected to behavioral tests addressing exploratory behavior as well as spatial reference- and spatial working-memory performance. **Figure 3.4** provides an overview of applied tests and temporal order of testing.

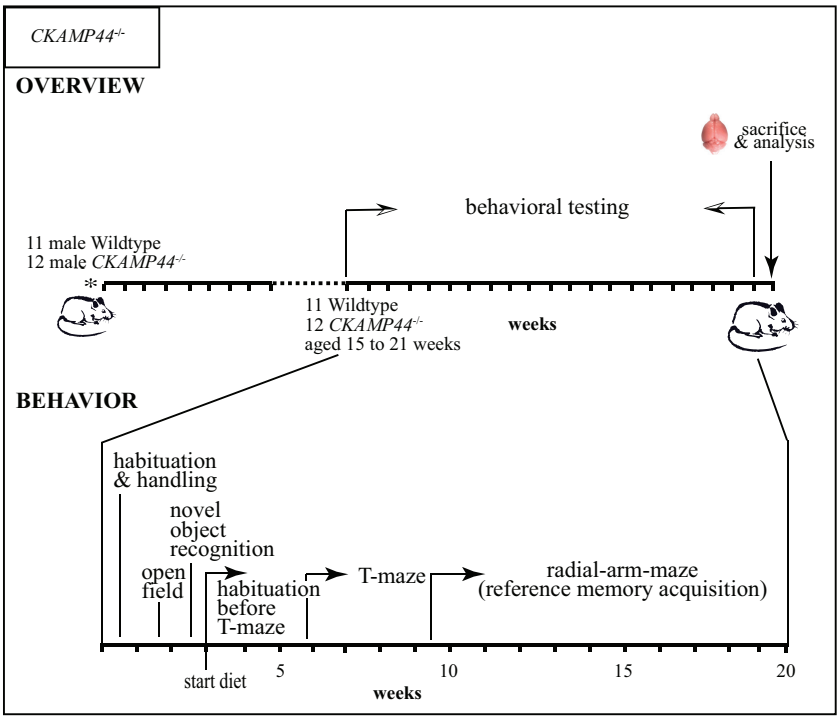

Figure 3.4: Time Course of Experiments for CKAMP44$^{-/-}$ Mice. Diagrams outline the course of experiments from birth of the mice and behavioral testing to the sacrifice of the animals. The upper part provides an overview and the lower part focuses on the temporal order of behavioral experiments.

3.1.2.1 Exploratory Behavior

Compared to Wts, CKAMP44$^{-/-}$ mice displayed normal exploratory behavior in a novel environment as measured in the open field box by the number of traversed squares and rearings within 5 minutes on two consecutive days of testing. Boxplots are shown to underline the similarity of the datasets (mean number of squares day 1, Wt 83.73 $\pm$ 8.33, CKAMP44$^{-/-}$ 88.00 $\pm$ 6.74, t(21) = 0.40, p = 0.69, day 2, Wt 53.55 $\pm$ 9.29, CKAMP44$^{-/-}$ 68.17 $\pm$ 6.69, t(21) = 1.29, p = 0.210 (**Figure 3.5a**); mean number of rearings day 1: Wt 27.91 $\pm$ 5.80, CKAMP44$^{-/-}$

27.33 ± 3.24, $t_{(21)} = 0.09$, $p = 0.930$, day 2: Wt 22.27 ± 5.94, CKAMP44$^{-/-}$ 24.17 ± 2.98, Welch-corrected $t_{(14)} = 0.29$, $p = 0.780$ (**Figure 3.5**)).

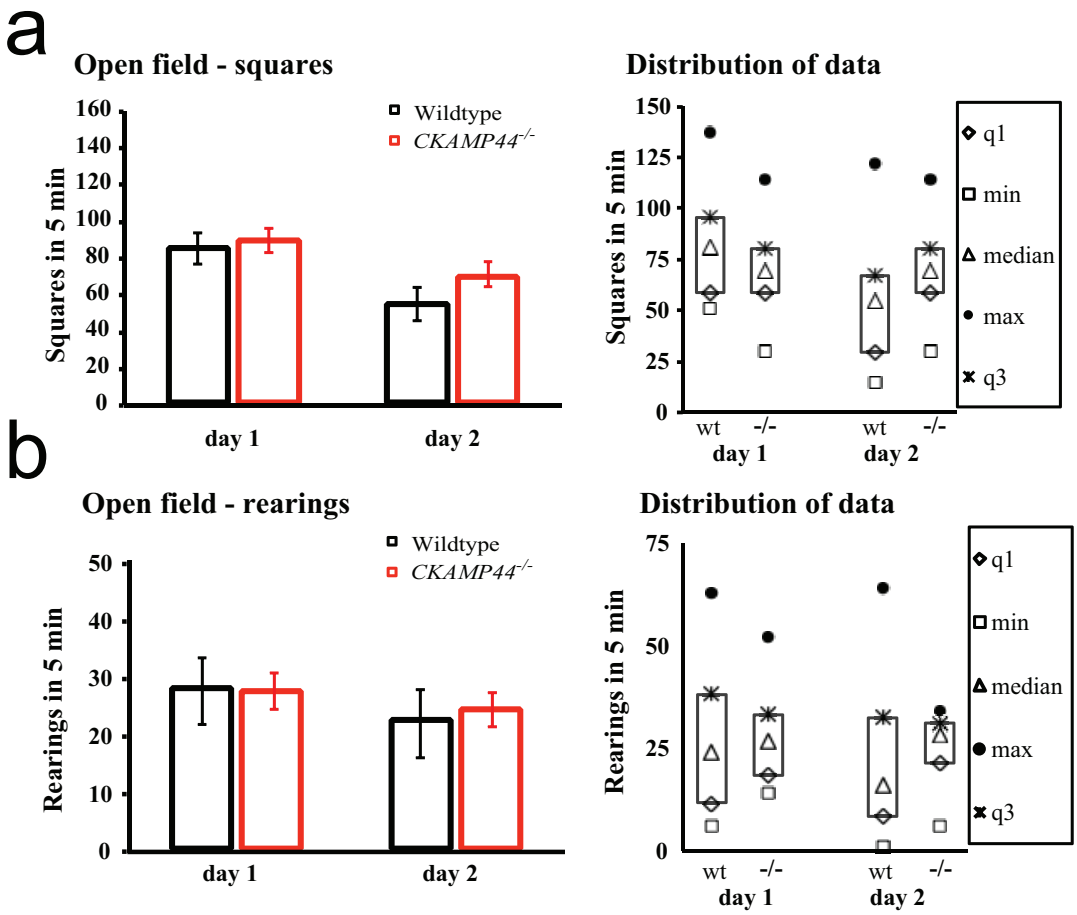

Figure 3.5: Unaltered Behavior of CKAMP44$^{-/-}$ Mice in Free Exploration in the Open Field Box. (a) Mean number of traversed squares (± SEM) in 5 minutes showed no altered performance in CKAMP44$^{-/-}$ mice on both testing days. Boxplot diagram depicts distribution of group data depending on genotype. Wt, n = 11; CKAMP44$^{-/-}$, n = 12. (b) Mean number of rearings (± SEM) in 5 minutes showed no alteration in CKAMP44$^{-/-}$ mice on both testing days. Boxplot diagram depicts distribution of group data depending on genotype. Q1, first quartile; min, minimum; max, maximum; q3, third quartile. Wt, n = 11, CKAMP44$^{-/-}$, n = 11.

Furthermore, novel object recognition test was performed to test the ability to recognize novel objects [Alarcon et al., 2004; Rampon et al., 2000] and to obtain another measure of free exploratory activity. Based on the natural exploratory behavior of rodents and on their memory for previously encountered objects, the mice were allowed to freely explore two different objects in a 5 minutes training phase. After a break of 5 minutes in the home cage, the mice were confronted with a copy of the familiar object and a novel object for 5 minutes of test phase (**Figure 3.6a**). The exploration times in both phases were taken and exploration performance was calculated by comparing the time spent exploring the novel object to the time spent exploring novel and familiar object during the test phase (discrimination ratio). There was no significant difference in total exploration time in Wt and CKAMP44$^{-/-}$ mice in the training and the test phase (total exploration time in seconds: Training: Wt 13.64 $\pm$ 2.34, CKAMP44$^{-/-}$ 18.42 $\pm$ 3.17, $t_{(21)} = 1.20$, $p = 0.245$, test: Wt 10.36 $\pm$ 2.09, CKAMP44$^{-/-}$ 9.58 $\pm$ 2.32, $t_{(21)} = 0.25$, $p = 0.806$ (**Figure 3.6b**)). The discrimination ratio of Wt and CKAMP44$^{-/-}$ mice was equally high and above chance level (mean discrimination ratio: Wt 0.63 $\pm$ 0.05, CKAMP44$^{-/-}$ 0.66 $\pm$ 0.055, $t_{(17)} = 0.49$, $p = 0.630$ (**Figure 3.6c**)). Mice that showed exploration behavior for 3 seconds or less in the training or the testing phase were excluded from the analysis.

These data suggest normal exploratory behavior and normal novelty preference in CKAMP44$^{-/-}$ mice.

3.1.2.2 Rewarded Alternation on the T-Maze

To analyse hippocampus dependent spatial working memory, the mice were tested on the appetitively rewarded alternation on the T-Maze test (Deacon et al., 2002). Animals were trained to run on the T-shaped maze. In order to get a food reward, they had to choose the arm, which was not encountered in the previous (10 seconds delayed) forced run (**Figure 3.7a**). Analysis with 2-way-ANOVA showed a significant effect for interaction ($F_{(4,100)} = 4.25$, $p = 0.003$), genotype ($F_{(1,100)} = 10.96$, $p = 0.001$) and block ($F_{(4,100)} = 7.11$, $p = 0.0001$). Bonferroni multiple comparison analysis revealed equal performances of Wt and CKAMP44$^{-/-}$ mice in all blocks except for block II. Here the performance differed significantly (mean percent correct, Wt 81.82 $\pm$ 3.52, CKAMP44$^{-/-}$ 56.36 $\pm$ 3.38, $t_{(21)} = 4.93$, $p = 0.0001$). As depicted in the line-graph (**Figure 3.7b**, upper graph) CKAMP44$^{-/-}$ mice performed above chance level (50%) and were comparable to Wts in all blocks except block II. For better illustration of the differences in performance in block II, a column-graph was generated (**Figure 3.7b**, lower panel).

The data suggest an overall normal spatial working memory as assessed by the rewarded alternation on the T-Maze.

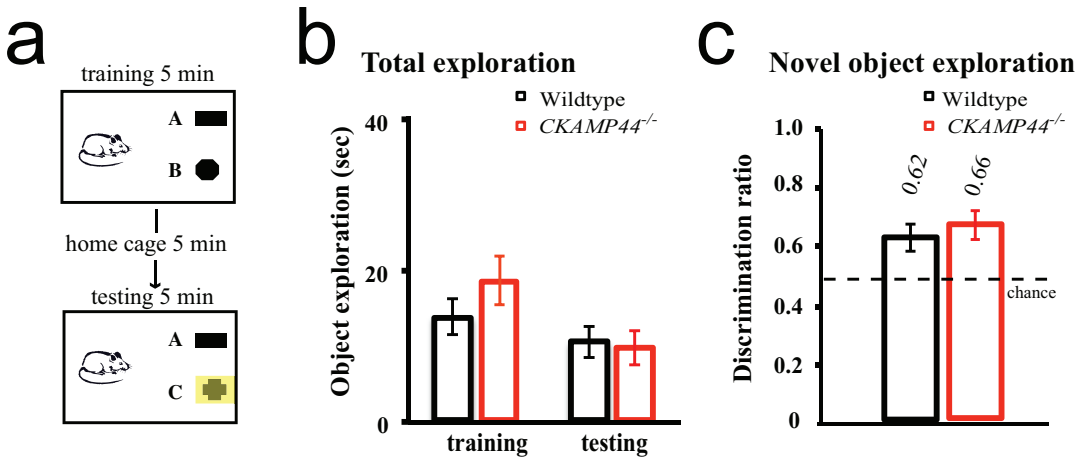

Figure 3.6: Unaltered Total Exploration Time and Discrimination Ratio in CKAMP44$^{-/-}$ Mice during Novel Object Recognition Test (NOR). (a) Schema depicting the paradigm of NOR. Objects "A" and "B" were first encountered in the training phase in which the mouse had 5 minutes of free exploration. After 5 minutes in the home cage, a copy of the familiar object "A", and the novel object "C" were presented in the 5 minutes test phase. (b) Total exploration time in seconds (± SEM) during the training and the test phase (5 minutes each). In both phases Wts (n = 11) did not differ from CKAMP44$^{-/-}$ mice (n = 12). (c) Novel object exploration performance was measured by the mean discrimination ratio (± SEM): time spent exploring the novel object relative to time spent exploring both, novel and familiar objects during the test phase. There was no difference in the performances of Wts (n = 11) and CKAMP44$^{-/-}$ mice (n = 12). Both performed above chance level (dotted line).

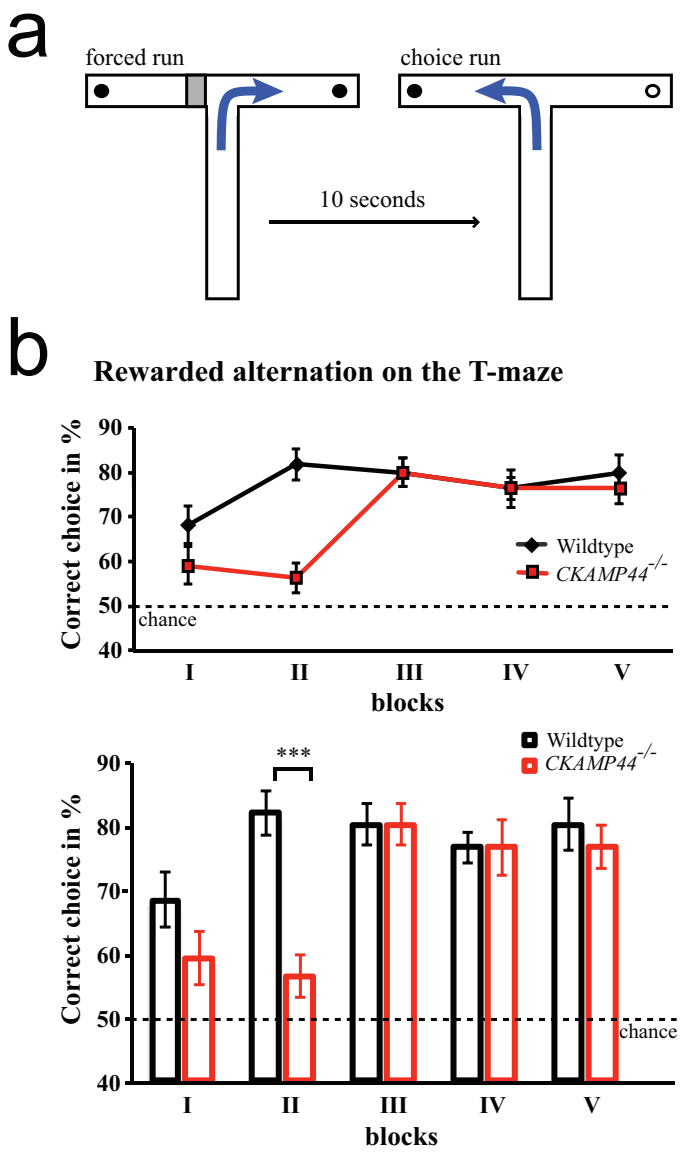

Figure 3.7: Unaltered Performance of CKAMP44$^{-/-}$ Mice in the Rewarded Alternation on the T-Maze Test. (a) Schema depicting the paradigm of the rewarded alternation on the T-Maze test. By blocking (grey rectangle) one arm, the mouse was forced to choose the baited (filled circle) arm. The animal was removed from the maze for 10 seconds. In the choice run, the mouse could freely decide between both arms. Correct choice (blue arrow) is the decision for the previously not visited, baited arm. The arm accessible in the forced run of a trial is chosen in pseudo-random fashion. One block consistes of 10 trials. (b) Line-graph: Mean percent correct choice (± SEM) in rewarded alternation on the T-Maze. Wts (n = 11) and CKAMP44$^{-/-}$ mice (n = 12) perform above chance level (50%, dotted line). The percentages of correct choice of Wt and CKAMP44$^{-/-}$ mice differed, due to the significantly impaired performance of CKAMP44$^{-/-}$ mice in block II (see column graph).

3.1.2.3 Spatial Reference Memory on the Eight-Arm Radial Arm Maze

To further examine whether CKAMP44 ablation was associated with defects in hippocampus dependent behavior, CKAMP44$^{-/-}$ mice were tested for spatial reference memory acquisition on the eight-arm radial arm maze (RAM) [Olton and Samuelson, 1976; Becker et al., 1980]. The animals had to learn the position of four baited arms and avoid entering four unbaited arms (spatial reference memory error) by navigation according to extra-maze spatial cues (**Figure 3.8a**). The pattern of baited arms varied among animals, but always consisted of two adjacent and two single baited arms. The delay between the choices of arms within one trial was 10 seconds. One block consisted of 4 trials. Wts and CKAMP44$^{-/-}$ mice learned equally well and the number of spatial reference memory errors was reduced over 25 blocks (mean number of spatial reference memory errors, 2-way-ANOVA $F_{(1,425)} = 0.40$, $p = 0.526$ (**Figure 3.8b**)). The performance did significantly depend on the block ($F_{(24,425)} = 12.63$, $p = 0.0001$), which reflects the learning progress with an advancing number of trials. The test was completed as soon as the animals showed a baseline error rate for a minimum of 3 blocks (blocks XXIII - XXV).

The RAM-data show normal reference memory in CKAMP44$^{-/-}$ mice.

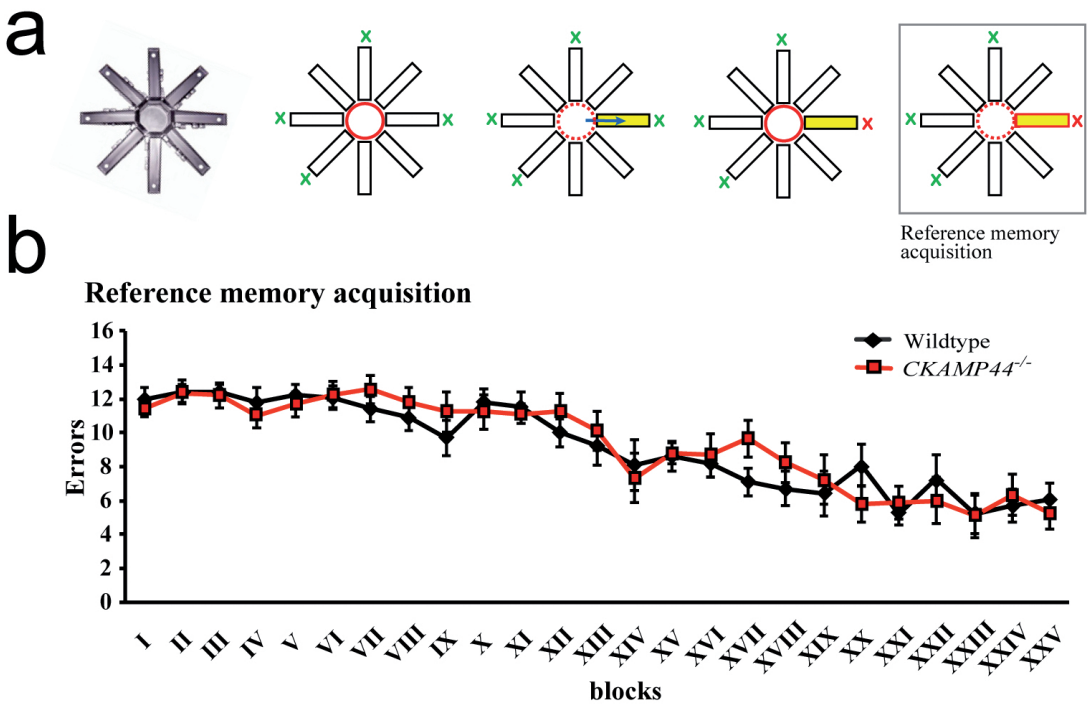

Figure 3.8: Unaltered Performance of CKAMP44$^{-/-}$ Mice in Spatial Reference Memory Acquisition on the Eight-Arm Radial Arm Maze (RAM). (a) Schema depicting spatial reference memory acquisition on the eight-arm RAM. Two adjacent and two single arms were baited (green X). The animal was placed on the platform with all doors closed (red circle). After 10 seconds, doors opened (dotted red circle) and the animal was free to choose any arm (blue arrow). After returning from the explored arm to the platform, doors closed again (red circle) for 10 seconds, followed by the second round of choice. Reference memory acquisition (grey box, left): In the subsequent round of choice only doors to unvisited arms opened. This prevented re-entry into previously explored arms (red rectangle). The visit of an unbaited arm is defined as spatial reference memory error. During the acquisition of spatial reference memory the animals ideally learned to exclusively enter baited arms. When the performance remained constantly high (low error rate for 3 consecutive blocks), the spatial working memory test started. (b) Mean number of spatial reference memory errors (± SEM) during reference memory acquisition. Wts (n = 10) and CKAMP44$^{-/-}$ mice (n = 9) performed equally well.

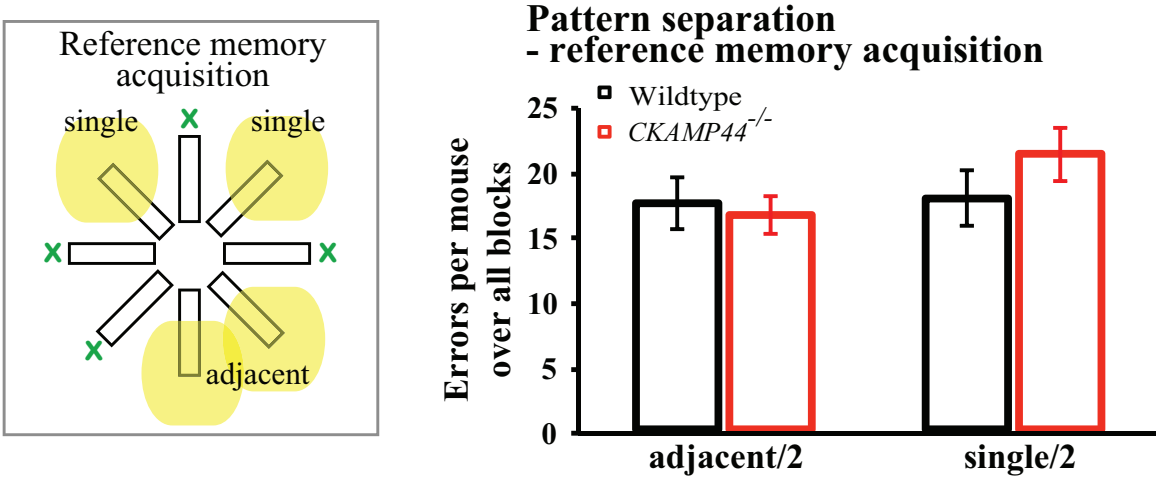

Figure 3.9: Unaltered Pattern Separation Performance of CKAMP44$^{-/-}$ Mice on the eight-arm Radial Arm Maze (RAM). Pattern separation performance during spatial reference memory acquisition. Left panel: Schema depicting the pattern separation analysis of spatial reference memory acquisition. Identifying one of two adjacent baited arms with overlapping spatial cues is assumed to challenge the pattern separation ability of the animals more than identifying a single baited arm with unique spatial cues [Niewoehner et al., 2007]. Graph: Mean spatial reference memory error per mouse (± SEM) over all blocks into adjacent/2 and single/2 arms showed no difference in pattern separation performance of Wt (n = 10) and CKAMP44$^{-/-}$ mice (n = 9).

3.1.2.4 Pattern Separation Performance on the Eight-Arm Radial Arm Maze

Based on the functional implication of the DG in pattern separation [Leutgeb and Moser, 2007; Bakker et al., 2008], data obtained during reference memory acquisition on the eight-arm RAM were further analysed for possible impairment in the ability for pattern separation. The pattern separation analysis is based on the spatial distribution of baited versus unbaited arms in the eight-arm RAM (**Figure 3.9**, grey box). Distinguishing between adjacent baited arms (overlapping shared spatial cues) and single baited arms (non overlapping arm-specific spatial cues) is assumed to differeantially challenge the pattern separation ability of the animals [Niewoehner et al., 2007]. Summed over all 25 blocks of spatial reference memory acquisition, errors made into adjacent arms and errors made into single arms (divided by 2) were comparable between Wts (n = 10) and CKAMP44$^{-/-}$ mice (n = 9) (mean sum of errors per animal into adjacent/2 arms: Wt 52.80 ± 3.13, CKAMP44$^{-/-}$ 50.83 ± 4.53, $t_{(17)} = 0.36$, $p = 0.721$, mean sum of errors per animal into single/2 arms: Wt 62.35 ± 3.22, CKAMP44$^{-/-}$ 65.94 ± 2.97, $t_{(17)} = 0.82$, $p = 0.426$ (**Figure 3.9**, graph)).

The data suggest normal spatial pattern separation in CKAMP44$^{-/-}$ mice.

3.2 CKAMP44^{HCoex} Mice

3.2.1 CKAMP44 Overexpression upon AAV Injection and Hippocampal Anatomy in CKAMP44^{HCoex} Mice

Hippocampal overexpression of CKAMP44 in CKAMP44^{HCoex} mice was achieved by AAV injection into dorsal hippocampi of 8 weeks old male C57Bl/6 mice. AAV-CKAMP44-IRES-Venus was designed to express CKAMP44 and (IRES-inserted) Venus-protein under the synapsin promoter. Control mice were injected with AAV-GFP: a construct expressing GFP under the synapsin promoter (further information in **Materials and Methods**). To verify the precise targeting of the chosen injection site (**Figure 3.10a**) and the distribution of virus-mediated expression in Controls and CKAMP44^{HCoex} mice, immunostainings for the fluorescent protein were performed. Venus and GFP expression were restricted to the hippocampus with high levels in the dorsal and very low levels in the ventral hippocampus, as shown in a series of coronal sections from Bregma -1.15 mm to Bregma -3.95 mm. Bregma -2.50 mm was the targeted injection site (**Figure 3.10b**).

These data show the restriction of CKAMP44-overexpression to the hippocampus.

Western blot analysis of CKAMP44 expression in hippocampal versus cerebellar lysates of Controls and CKAMP44^{HCoex} mice revealed the extent of the overexpression and proved its confinement to the hippocampus (**Figure 3.11a**). The level of overexpression was similar amongst CKAMP44^{HCoex} animals (**Figure 3.11b**). Serial dilution of the hippocampal lysate of a representative CKAMP44^{HCoex} mouse (oex #B2, **Figure 3.11c**) allowed estimation of the overexpression factor. Compared to the normal hippocampal protein level (con #4, **Figure 3.11a**), AAV-CKAMP44-IRES-Venus injection resulted in an approximately 50fold increase of CKAMP44 expression.

To check for a putative undesired influence of CKAMP44 overexpression, immunostainings were performed and the hippocampal anatomy of CKAMP44^{HCoex} mice was investigated. Venus/GFP expression in the hippocampus was proven to be robust in all subregions and comparable in Controls and CKAMP44^{HCoex} mice. In situ hybridizations [Von Engelhardt et al., 2010] showed a differential expression of CKAMP44-mRNA in the rodent hippocampus. Thus AAV-mediated overexpression of CKAMP44 might exert a greater influence on CA1-neurons (low level of CKAMP44-mRNA) than on DGCs (high level of CKAMP44-mRNA). Immunostainings for neuronal nuclei (NeuN) showed a normal distribution of neurons within hippocampal subfields (**Figure 3.12a**). Overall number and distribution of NeuN-positive cells in CA1 and DG were comparable in Controls and CKAMP44^{HCoex} mice (**Figure 3.12b**).

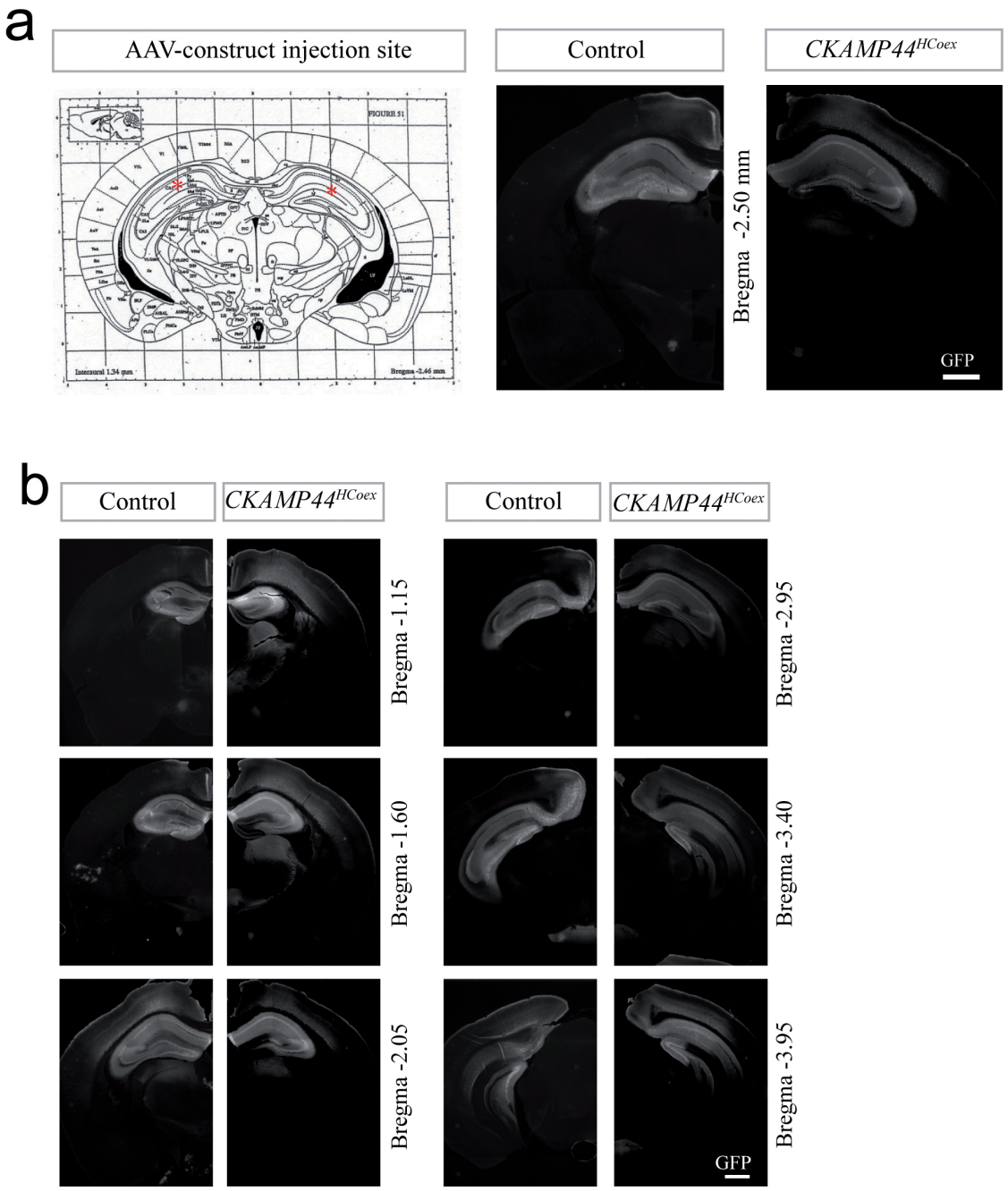

Figure 3.10: AAV-Mediated Gene Expression is Mainly Restricted to the Dorsal Hippocampus. (a) Injection site (red asterisks) of AAV-constructs (graphic taken from the Allen Brain Atlas). Coordinates for injection (1μl): Bregma - 2.4 mm, lateral 2 mm, depth 1.4 mm. Lower panel: Corresponding coronal brain-sections of Controls and CKAMP44^{HCoex} mice. Sections, 45 μm; scale bar, 50 μm. (b) Expression of GFP (AAV:GFP) and Venus (AAV:CKAMP44-IRES-Venus) throughout coronal sections of dorsal to ventral hippocampus. Staining was performed with anti-GFP. Dorso-ventral position of the section in distance from Bregma $\pm$ 5 μm. Sections, 45μm. Scale bars, 50 μm.

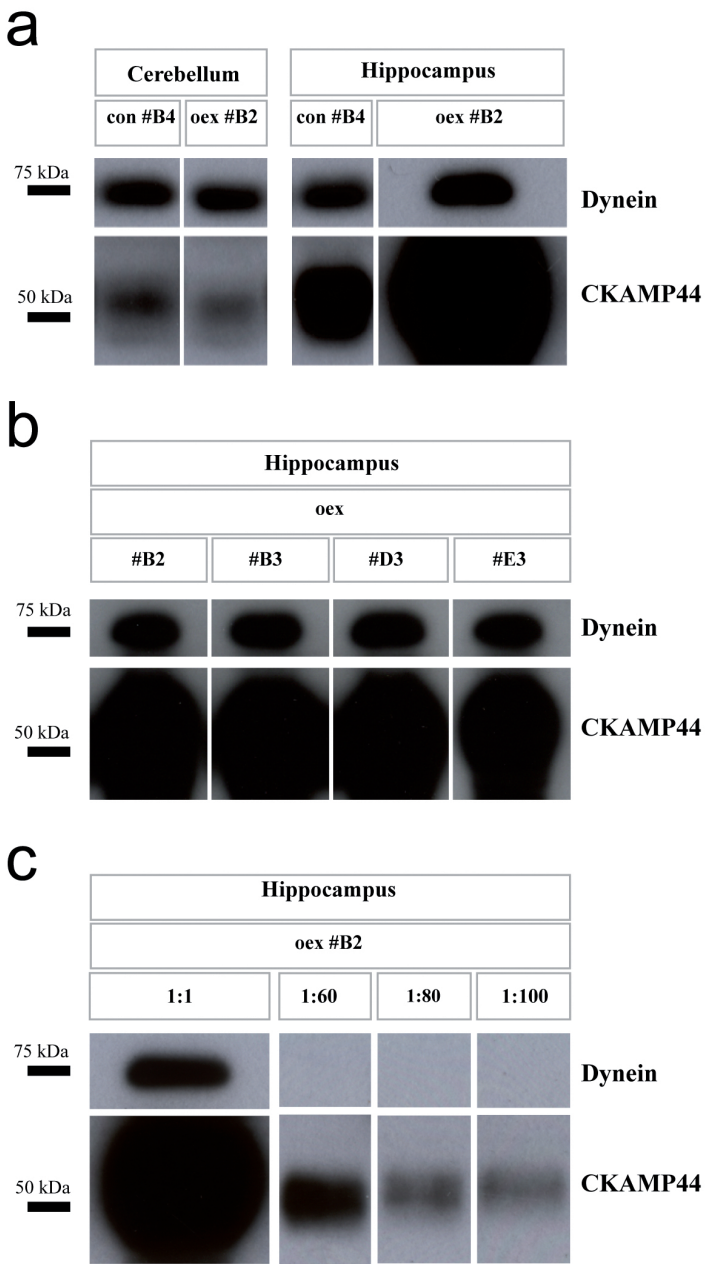

Figure 3.11: Hippocampal Overexpression of CKAMP44 upon Injection of the AAV:CKAMP44-IRES-Venus Construct. (a) Representative Western blot analysis showed similar levels of CKAMP44 in cerebellar lysates of Controls (#B4) and CKAMP44^{HCoex} (#B2) mice. Comparison of hippocampal lysates of the same animals showed much higher expression of CKAMP44 in CKAMP44^{HCoex} than in Control mice. (b) Hippocampal overexpression of CKAMP44 resulted in equal amount of protein in individual CKAMP44^{HCoex} animals (#B2, #B3, #D3, #E3). (c) Dilution of the hippocampal lysate of a representative CKAMP44^{HCoex} mouse for estimation of the overexpression factor. Dynein was used as a housekeeping gene.

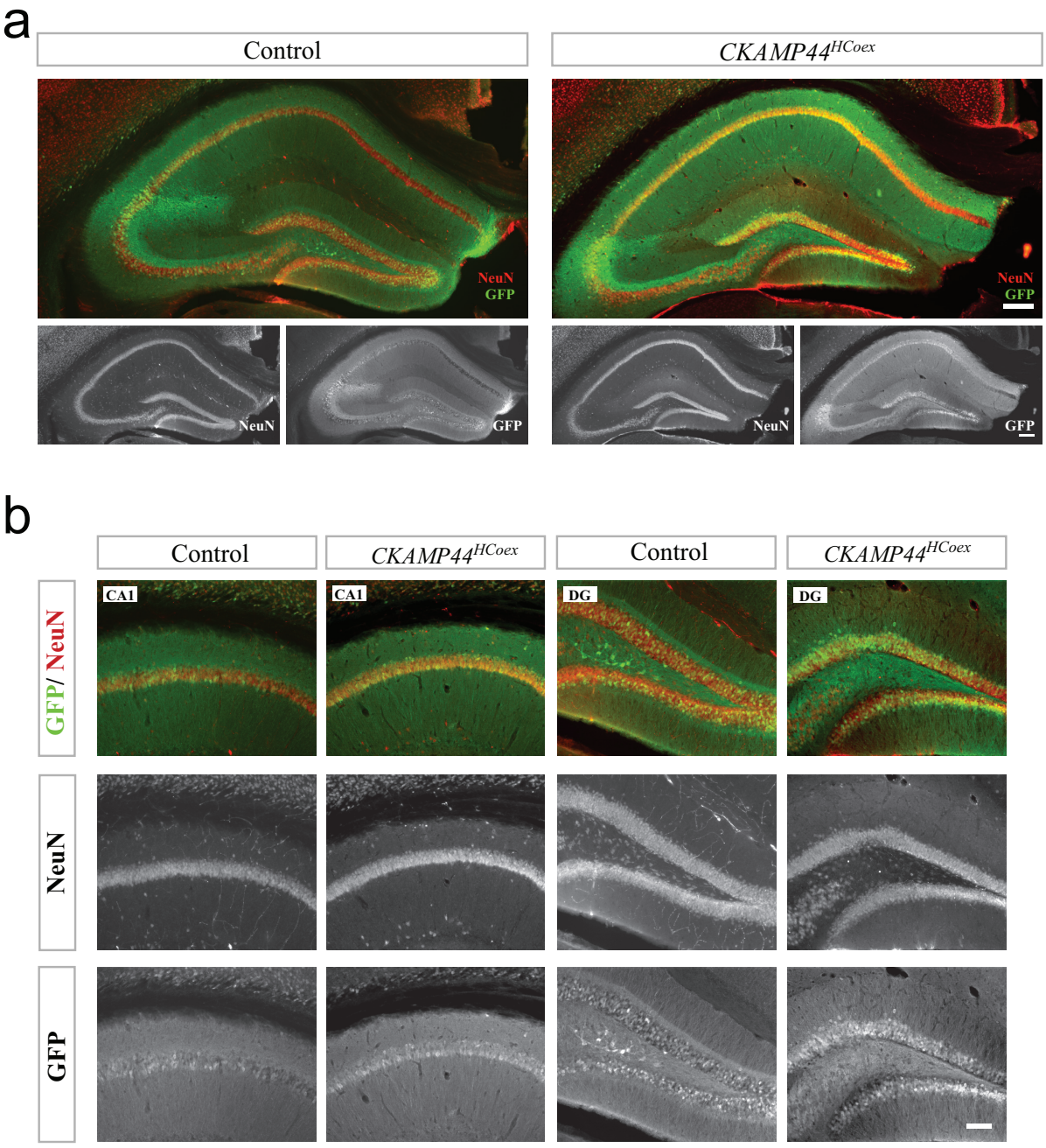

Figure 3.12: Unaltered Hippocampal Anatomy in CKAMP44^{HCoex} Mice. (a) Immunostainings for NeuN and GFP in dorsal hippocampus of Controls and CKAMP44^{HCoex} mice showed no obvious differences in number and distribution of NeuN-positive cells. Sections, 45 μm; scale bars, 25 μm. (b) Detailed view of hippocampal subregions CA1 and DG showed no obvious differences in number and distribution of NeuN-positive cells in Controls and CKAMP44^{HCoex} mice. Sections, 45 μm; scale bar, 25 μm.

Staining for calcium-binding protein parvalbumin (PV) was performed to verify the distribution and number of the most prominent type of GABAergic fast-spiking interneurons (**Figure 3.13a**). For quantitative analysis, PV-positive cells were counted in CA1, CA3 and DG. Hippocampal CKAMP44 overexpression upon AAV injection did not influence the number of PV-positive cells in either subregion (mean cell number per hemisphere in Control (10 hemispheres) and CKAMP44^{HCoex} mice (9 hemispheres): CA1: Controls 86.50 ± 4.40, CKAMP44^{HCoex} 77.78 ± 6.26 $t_{(17)} = 1.16$, $p = 0.264$, CA3: Controls 183.43 ± 12.59, CKAMP44^{HCoex} 199.70 ± 10. 96 $t_{(17)} = 0.97$, $p = 0.344$, DG: Controls 44.90 ± 9.22, CKAMP44^{HCoex} 38.33 ± 6.54 $t_{(17)} = 0.57$, $p = 0.577$ (**Figure 3.13b**)). Only a small fraction of PV-positive interneurons expressed GFP (**Figure 3.13c**). GFP/PV-positive cells were confined to stratum oriens and stratum pyramidale of CA1.

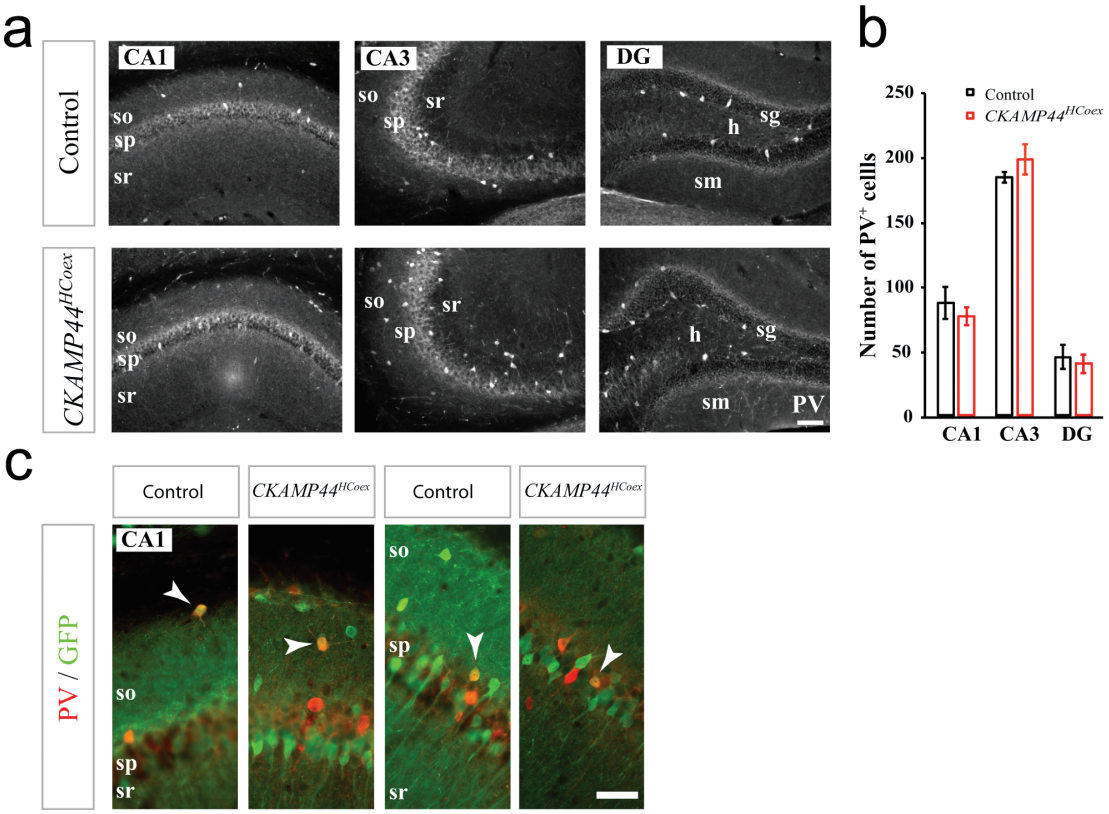

Figure 3.13: Unaltered PV-Positive Cell Number in Hippocampal Subregions of CKAMP44^{HCoex} Mice. (a) Immunostainings for PV in hippocampal subregions of Controls and CKAMP44^{HCoex} mice showed no alterations in number and distribution of PV-positive cells in CA1, CA3 and DG. So, stratum oriens; sp, stratum pyramidale; sr, stratum radiatum; sg, stratum granulosum; h, hilus; sm, stratum moleculare. Sections, 45 μm. Scale bar, 25 μm. (b) Cell count (mean number $\pm$ SEM) of PV-positive cells in CA1, CA3 and DG of Controls (hemispheres, n = 10) and CKAMP44^{HCoex} mice (hemispheres, n = 9) showed no difference in neither of the subregions. (c) Immunostainings for PV and GFP in dorsal hippocampus of Controls and CKAMP44^{HCoex} mice revealed sparse colocalization. GFP-expressing PV-positive interneurons were confined to CA1 stratum oriens and stratum pyramidale. So, stratum oriens; sp, stratum pyramidale; sr, stratum radiatum. Sections, 45 μm. Scale bar, 25 μm.

3.2.2 Behavioral Characterization of CKAMP44^{HCoex} Mice

Controls (n = 11) and CKAMP44^{HCoex} mice (n = 11) were subjected to behavioral tests addressing exploratory behavior as well as spatial reference- and spatial working-memory performances. **Figure 3.14** provides an overview of treatment, applied tests and temporal order of testing.

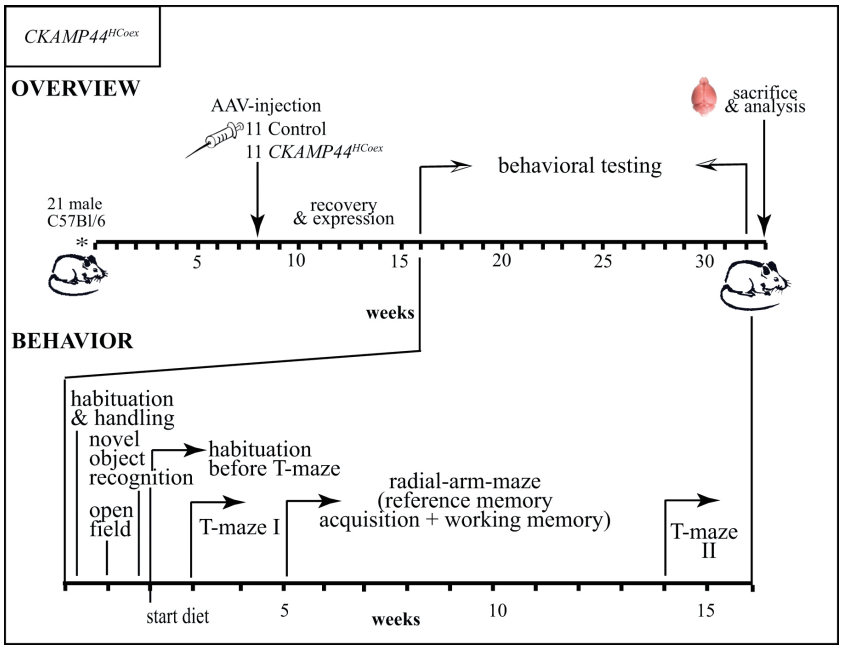

Figure 3.14: Time Course of Experiments (Treatment and Behavior) for CKAMP44^{HCoex} Mice. Diagram outlining the course of experiments from birth of the C57Bl/6 mice, injection of AAV-construct and behavioral testing to the sacrifice of the animals. The upper part provides an overview and the lower part focuses on the temporal order of behavioral experiments.

3.2.2.1 Exploratory Behavior

To address the exploratory behavior of the animals in a novel environment, Controls (n = 11) and CKAMP44^{HCoex} mice (n = 11) were tested in an open field box. Compared to Controls, CKAMP44^{HCoex} mice displayed highly significant hyperactivity, measured by the number of traversed squares and rearings within 5 minutes on two consecutive days of testing (mean number of squares day 1: Controls 105.18 $\pm$ 7.27, CKAMP44^{HCoex} 228.91 $\pm$ 12.96, $t_{(20)}$ = 8.33, p = 0.0001, day 2: Controls 70.18 $\pm$ 5.26, CKAMP44^{HCoex} 175.64 $\pm$ 14.20, Welch corrected $t_{(12)}$ = 6.96, p = 0.0001(**Figure 3.15a**); mean number of rearings day 1: Controls 43.18 $\pm$ 4.78, CKAMP44^{HCoex} 62.45 $\pm$ 4.77, $t_{(20)}$ = 2.86, p = 0.01, day 2: Controls 29.64 $\pm$ 3.00, CKAMP44^{HCoex} 53.36 $\pm$ 3.56, $t_{(20)}$ = 5.10, p = 0.0001 (**Figure 3.15b**)). On both

days of testing, the number of squares CKAMP44^{HCoex} mice traversed was twice as high as the number of squares Controls traversed . This hyperactivity made it possible to identify the AAV-CKAMP44-IRES-Venus-treated mice by mere observation in the open field box. Boxplots are shown to underline the big difference of the datasets obtained from Controls and CKAMP44^{HCoex} mice. The performance of Controls was comparable to the open field performance of other models (GluA1$^{PVCre+/+}$, GluA1$^{PVCre-/-}$and GluA4$^{+/+}$) tested in this lab [Fuchs et al., 2007].

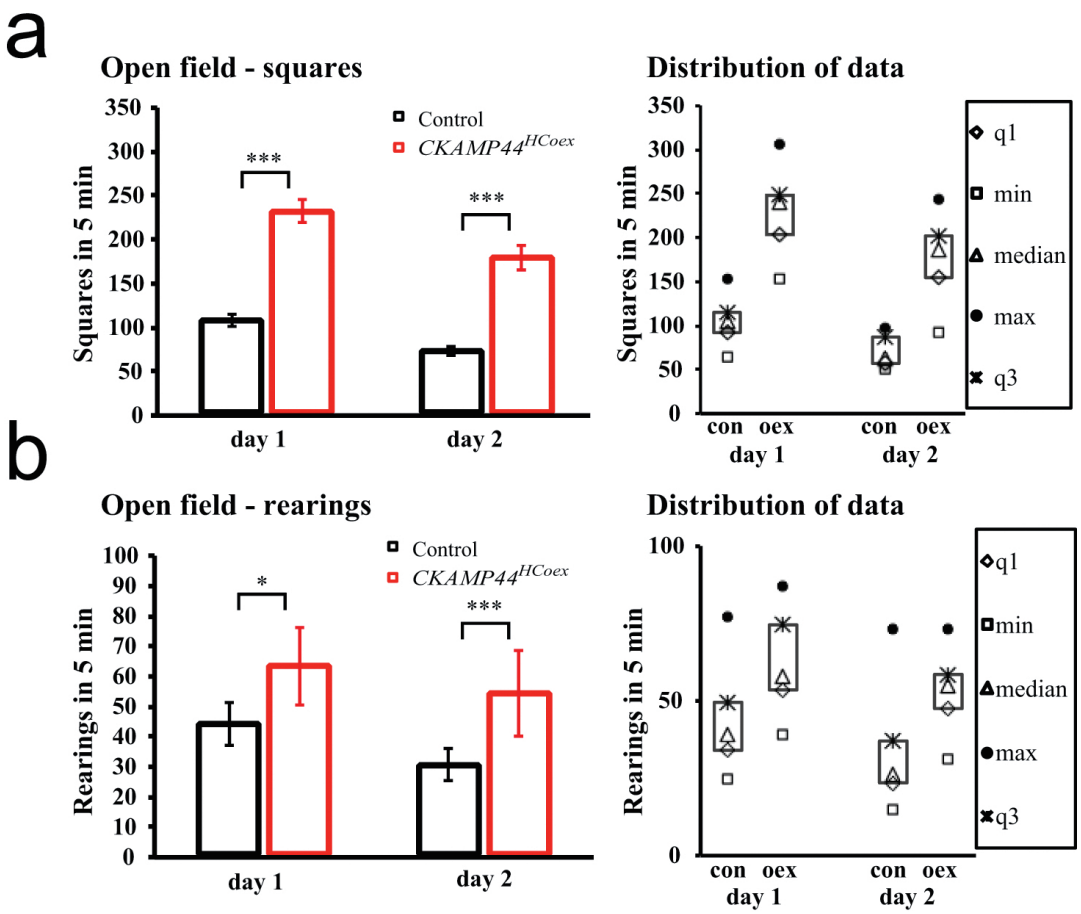

Figure 3.15: Hyperactivity of CKAMP44^{HCoex} Mice in Free Exploration in the Open Field Box. (a) Mean number of traversed squares (± SEM) in 5 minutes reveals hyperactivity of CKAMP44^{HCoex} mice on both testing days. ***$p = 0.0001$. Boxplot diagram depicts the highly restricted distribution of group data depending on the injected AAV-construct. Control, n = 11; CKAMP44^{HCoex}, n = 11. (b) Mean number of rearings (± SEM) in 5 minutes revealed hyperactivity of CKAMP44^{HCoex} mice on both testing days. *$p = 0.01$, ***$p = 0.0001$. Boxplot diagram depicting the distribution of group data depending on the injected AAV-construct. Q1, first quartile; min, minimum; max, maximum; q3, third quartile. Control, n = 11, CKAMP44^{HCoex}, n = 11.

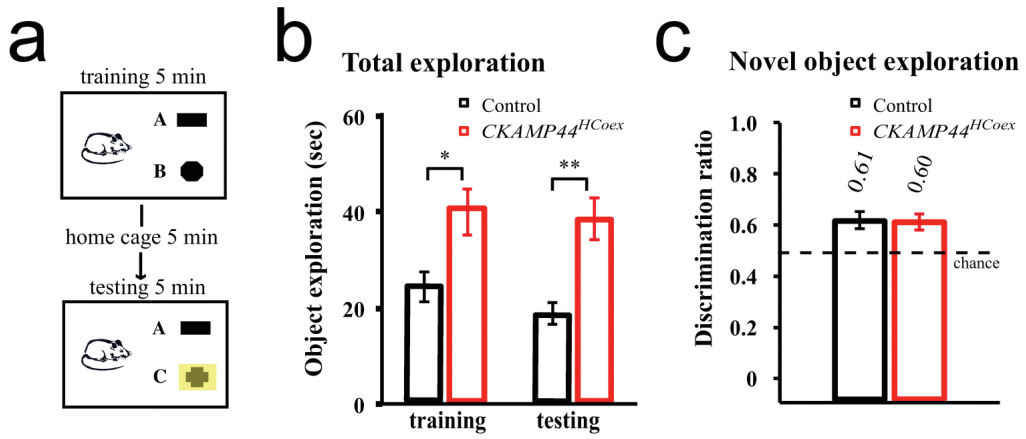

Figure 3.16: Enhanced Total Exploration Time but Normal Discrimination Ratio in CKAMP44^{HCoex} Mice during Novel Object Recognition Test (NOR). (a) Schema depicting the paradigm of NOR. Objects "A" and "B" were first encountered in the training phase in which the mouse had 5 minutes of free exploration. Following 5 minutes in the home cage, a copy of the familiar object "A" and novel object "C" were presented for 5 minutes (test phase). (b) Total exploration time in seconds (± SEM) during training and test phase (5 minutes each). In both phases Controls (n = 11) differed significantly from CKAMP44^{HCoex} mice (n = 11) in exploration time. *p = 0.01, **p = 0.001. (c) Novel object exploration performance was measured by the mean discrimination ratio (± SEM): time spent exploring the novel object relative to the time spent exploring both novel and familiar objects during the test phase. There was no difference in the performances of Controls and CKAMP44^{HCoex} mice. Both performed above chance level.

Furthermore, novel object recognition test was performed (**Figure 3.16a**). The exploration times in both phases were measured and exploration performance was calculated by comparing the time spent exploring the novel object to the time spent exploring the novel and the copy of the familiar object during the test phase (discrimination ratio). Also in this test, CKAMP44^{HCoex} mice showed a significantly higher level of exploratory activity, measured by total exploration time in both training and test phase (total exploration time in seconds: Training: Controls 23.64 ± 3.02, CKAMP44^{HCoex} 40.00 ± 4.83, $t_{(20)}$ = 2.88, p = 0.05, test: Controls 18.00 ± 2.37, CKAMP44^{HCoex} 37.91 ± 4.34, $t_{(20)}$ = 4.02, p = 0.001 (**Figure 3.16b**)). Both Controls and CKAMP44^{HCoex} mice expressed a discrimination ratio above chance level and thus favoured the novel object without any significant difference (mean discrimination ratio: Controls 0.600 ± 0.03, CKAMP44^{HCoex} 0.615 ± 0.03, $t_{(20)}$ = 0.34, p = 0.735 (**Figure 3.16c**)).

The above-chance discrimination ratio reflects the unaltered novelty preference of the animals. The simultaneously expressed hyperactivity in exploration is not surprising, because the open field box test already revealed hyperexploratory behavior in CKAMP44^{HCoex} mice.

3.2.2.2 Rewarded Alternation on the T-Maze

To analyse hippocampus dependent spatial working memory, the mice were subjected to the appetitively rewarded alternation on the T-Maze test [Deacon et al., 2002]. For detailled explanation of the testing paradigm, see "3.1.2.2 Rewarded Alternation on the T-Maze" for CKAMP44$^{-/-}$ mice and the schema of the T-Maze (**Figure 3.17a**). Controls (n = 11) showed a normal and steady performance of 71.62 $\pm$ 3.68 percent correct choices summed over a total of 5 blocks, whereas CKAMP44^{HCoex} mice (n = 11) performed at chance level (54.16 $\pm$ 3.64) (**Figure 3.17b**). Data-analysis by 2-way-ANOVA showed a significant effect for treatment ($F_{(1,100)}$ = 53.77, p = 0.0001). To check if this impairment in rewarded alternation changed with the level of training, the test was repeated after the intensive training on the eight-arm RAM (see time course of experiments **Figure 3.14a**). Compared to the results obtained in the predating T-Maze I, Controls (n = 11) displayed lower but still normal and steady performance of 67.05 $\pm$ 5.25 percent correct choices summed over all 4 blocks in T-Maze II, whereas CKAMP44^{HCoex} mice (n = 11) continued to be impaired and performed at chance level (52.96 $\pm$ 3.26) (**Figure 3.17c**). Data analysis by 2-way-ANOVA showed (as in T-Maze I) a significant effect for treatment ($F_{(1,80)}$ = 20.15, p = 0.0001).

These data reveal a robust impairment of CKAMP44^{HCoex} mice in spatial working memory as assessed by the rewarded alternation on the T-Maze, independent of the experimental naivety or experience of the animals.

3.2.2.3 Spatial Reference- and Spatial Working-Memory on the Eight-Arm Radial Arm Maze

To test spatial reference memory and to further validate the spatial working memory impairment of the mutants, the performance of Controls and CKAMP44^{HCoex} mice in both tasks was simultaneously assessed by an elegant within-task within-subject test on the eight-arm RAM (rats: [Jarrard, 1983, 1993], mice: [Schmitt et al., 2003]).

Mice were trained to remember the position of four baited arms and to avoid entry into any of the four unbaited arms (spatial reference memory error) by navigation according to extra-maze spatial cues (**Figure 3.18a**). After the exploration of one arm, the animal returned to the central platform of the maze and all entrances were blocked for 10 seconds (temporal delay). The trial was accomplished when the animals visited all four baited arms. This was repeated until the number of reference memory errors remained steady for three blocks (one block = 4 trials). Controls (n = 11) and CKAMP44^{HCoex} mice (n = 11) learned equally well and spatial reference memory errors were reduced over 13 blocks (mean number of spatial reference memory errors, 2-way-ANOVA $F_{(1,260)} = 0.17$, $p = 0.685$ (**Figure 3.18b**, graph)). The block significantly influenced the performance ($F_{(12,260)} = 36.29$, $p = 0.0001$), reflecting the learning progress with the increasing number of trials. The test was completed as soon as the animals showed a baseline error rate for a minimum of 3 blocks (mean number of spatial reference memory errors averaged over blocks XI - XIII: Controls 2.18 ± 0.23, CKAMP44^{HCoex} 2.24 ± 0.08, $t_{(4)} = 0.23$, $p = 0.827$).

After concluding the spatial reference memory test, Controls (n = 11) and CKAMP44^{HCoex} mice (n = 11) were subjected to the working memory test on the eight-arm RAM (**Figure 3.18c**, working memory schema). During the spatial reference memory acquisition mice were prevented to commit spatial working memory errors (re-entry into a previously visited arm) by blocking the entrance of already visited arms in the following choice runs (**Figure 3.18a**, reference memory schema). After the animals reliably learned the pattern of baited arms, opening the doors to all arms in every choice run made re-entries possible (**Figure 3.18c**, working memory schema). Thus, both spatial reference and spatial working memory errors could be made in the course of one trial.

The number of spatial reference memory errors served as inbuilt control for steady performance during the spatial working memory test. Controls and CKAMP44^{HCoex} mice did not differ in their spatial reference memory performance during spatial working memory test (mean number of spatial reference memory errors, 2-way-ANOVA $F_{(1,140)} = 0.52$, $p = 0.473$ (**Figure 3.18c**, left graph)). Averaged over all blocks, CKAMP44^{HCoex} mice displayed a low number of spatial reference memory errors comparable to the baseline error rate of spatial reference memory acquisition (mean number of spatial reference memory errors during spatial working memory test

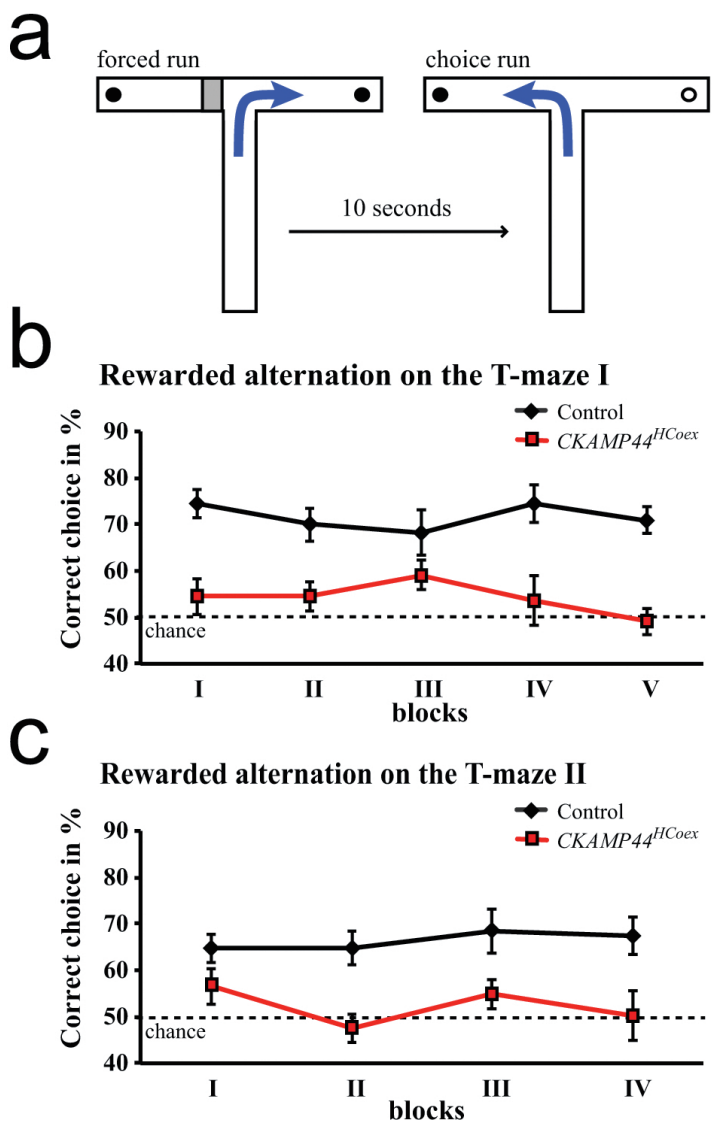

Figure 3.17: Chance Level Performance of CKAMP44^{HCoex} Mice in the Rewarded Alternation on the T-Maze test before (naïve) and after (experienced) Training on the Eight-Arm Radial Arm Maze (RAM). (a) Schema depicting the paradigm of the rewarded alternation on the T-Maze test. By blocking (grey rectangle) one arm, the mouse was forced to choose the baited (filled circle) arm. The animal was removed from the maze for 10 seconds. In the choice run, the mouse could freely decide between both arms. Correct choice (blue arrow) was the decision for the previously not visited, baited arm. The arm accessible in the forced run of a trial was chosen in pseudo-random fashion. One block consists of 10 trials. (b) Mean percent correct choice (± SEM) of experimentally naïve mice (before RAM). CKAMP44^{HCoex} mice (n = 11) performed at chance level (50%, dotted line), significantly different from Controls (n = 11). ***$p = 0.0001$. (c) Mean percent correct choice (± SEM) of experimentally experienced mice (after RAM). CKAMP44^{HCoex} mice (n = 11) performed at chance level (50%, dotted line), significantly different from Controls (n = 11). ***$p = 0.0001$.

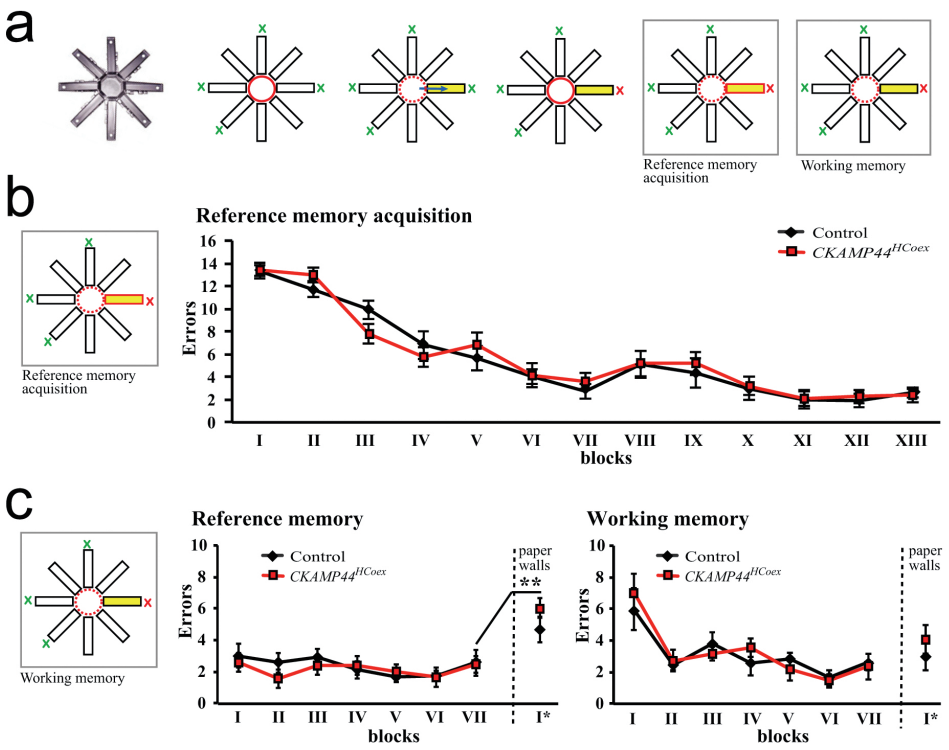

Figure 3.18: Unaltered Performance of CKAMP44^{HCoex} Mice in Spatial Reference Memory Acquisition and Spatial Working Memory Test on the Eight-Arm Radial Arm Maze (RAM). (a) Schema depicting spatial reference memory acquisition spatial and working memory test on the eight-arm RAM. Two adjacent and two single arms were baited (green X). The animal was placed on the platform with closed doors (red circle). After 10 seconds, doors opened (dotted red circle) and the animal was free to choose any given arm (blue arrow). After the mouse returned to the platform, doors closed again (red circle) for 10 seconds before the second round of choice. Reference memory acquisition (grey box, left): In the subsequent round of choice only doors to unvisited arms opened to prevent re-entry into previously explored arms (red rectangle). Spatial reference memory error: Visit of an unbaited arm. During the acquisition of spatial reference memory the animals ideally learned to exclusively enter baited arms. When the performance of the mice reached baseline-level (constantly few errors for 3 consecutive blocks), the spatial working memory test started. One block consisted of 4 trials. Working memory (grey box, right): In the subsequent round of choice, all doors opened. Spatial working memory error: re-entry into previously visited arm. One block consisted of 4 trials. (b) Left panel: Testing paradigm. Graph: Mean number of spatial reference memory errors (± SEM) during spatial reference memory acquisition. Controls (n = 11) and CKAMP44^{HCoex} mice (n = 11) performed equally well. (c) Left panel: Testing paradigm. Left graph: Mean number of spatial reference memory errors (± SEM) during spatial working memory. Block I to VI: RAM with all extra-maze spatial cues visible through the acrylic-glass walls of the arms and through the open ceiling. Block I*: Partly deprivation of extra-maze spatial cues by veiling the acrylic-glass walls with white paper (“paper walls”). Controls (n = 11) and CKAMP44^{HCoex} mice (n = 11) performed equally well in the unveiled and veiled version. *Continued on page 56.*

averaged over blocks I to VII: Controls 2.82 ± 0.65, CKAMP44^{HCoex} 2.35 ± 0.32, $t_{(20)}$ = 0.45, p = 0.655, mean number of spatial reference memory errors during spatial reference memory acquisition averaged over block XI to XIII (baseline): Controls 2.18 ± 0.23, CKAMP44^{HCoex} 2.24 ± 0.08, $t_{(4)}$ = 0.23, p = 0.827 (**Figure 3.18b**)).

CKAMP44^{HCoex} mice showed normal spatial reference memory as well as normal spatial working memory performance during the spatial working memory test (in contrast to the chance-level performance on the T-Maze). The number of spatial working memory errors did not differ between Controls and CKAMP44^{HCoex} mice ((**Figure 3.18b**, right graph), mean number of working memory errors, 2-way-ANOVA $F_{(1,140)}$ = 0.05, p = 0.815). The 2-way-ANOVA revealed a significant difference between blocks ($F_{(5,140)}$ = 9.66, p = 0.0001). Bonferroni multiple comparison analysis assigned this effect to a significant difference in block I compared to all other blocks (Controls: Mean spatial working memory error for block I: 6.00 ± 1.14, blocks II - VII: 2.65 ± 0.37, Welch corrected $t_{(12)}$ = 2.77, p = 0.017, CKAMP44^{HCoex} : Mean working memory error for block I: 7.09 ± 1.32, blocks II - VI: 2.58 ± 0.32, Welch corrected $t_{(11)}$ = 3.33, p = 0.007).

To prove the dependence of spatial reference memory on extra-maze spatial cues, a change was introduced between block VII and block I* of the spatial working memory paradigm. The acrylic-glass walls of the maze were veiled with white paper to deprive the animals of extra-maze spatial cues. Both Controls and CKAMP44^{HCoex} mice showed a higher number of spatial reference memory errors in the veiled compared to the unveiled condition (**Figure 3.18c**, left graph). This difference between blocks is significant for CKAMP44^{HCoex} mice (mean number of spatial reference 0.62, $t_{(20)}$ = 4.30, p < 0.001). Controls showed a trend to commit more spatial reference memory errors under the cue-deprived conditions (mean number of spatial reference memory errors block VII: 2.55 ± 0.84, block I*: 4.64 ± 0.81, $t_{(20)}$ = 1.08, p = 0.08).

In contrast to the spatial reference memory performance, the spatial working memory performance was not significantly influenced by the deprivation of extra-maze spatial cues in both Controls and CKAMP44^{HCoex} mice(Controls: mean number of spatial working memory errors block VI 2.64 ± 0.83, block I* 3.091 ± 0.91, $t_{(20)}$ = 0.37, p = 0.716 (**Figure**

Figure 3.18 (cont.): Hippocampus-dependent navigation by spatial cues was proven by the difference between block VI (unveiled) and block I* (veiled): significant impairment in block I* for CKAMP44^{HCoex}. **p = 0.001. Controls showed a tendency to make more spatial reference memory errors upon change of conditions. Right graph: Mean number of spatial working memory errors (± SEM). Controls (n = 11) and CKAMP44^{HCoex} mice (n = 11) performed equally well. There was no significant difference in the performances under normal condition (block I - VI) and veiled condition (block I*).

3.18c, right graph), CKAMP44^{HCoex} mice: mean number of spatial working memory errors block VI 2.36 ± 0.54, block I* 4.09 ± 0.98, $t_{(20)}$ = 1.54, p = 0.138 (**Figure 3.18c**, right graph)).

Summarizing, in both spatial memory tests, assessed simultaneously on the eight-arm RAM, CKAMP44^{HCoex} mice showed normal performances. Depriving the mice of most extra-maze spatial cues resulted in augmentation of spatial reference memory errors (significant for CKAMP44^{HCoex} mice but only tendentially in Controls) but did not influence spatial working memory errors significantly. This proves that the mice used extra-maze spatial cues for navigation to learn the pattern of baited arms.

3.2.2.4 Reference- and Non-Reference-Working Memory Errors on the Eight-Arm Radial Arm Maze.

To further dissect spatial working memory performance, the spatial working memory errors were divided into two groups. The spatial reference working memory (SRWME) error is defined as the repeated entry into an arm that was never baited (**Figure 3.19a**, left box). The spatial non-reference working memory (SNRWM) error is defined as the repeated entry into a formerly baited arm (**Figure 3.19a**, right box). After switching from spatial reference memory acquisition to the spatial working memory paradigm, Controls (n =11) and CKAMP44^{HCoex} mice ($n = 11$) continued to show a low baseline level of spatial reference memory errors (mean number of spatial reference memory errors averaged over blocks I to VII: Controls 2.82 ± 0.65, CKAMP44^{HCoex} 2.35 ± 0.32, $t_{(20)}$ = 0.45, p = 0.655 (**Figure 3.19b**, top graph)). SRWM errors did not differ between Controls and CKAMP44^{HCoex} mice (mean number of SRWM errors averaged over block I to VII: Controls 0.10 ± 0.04, CKAMP44^{HCoex} 0.09 ± 0.03, $t_{(20)}$ = 0.23, p = 0.818(**Figure 3.19b**, middle graph)). SRWM errors represented only a very small fraction, smaller than 5%, of all spatial working memory errors (Controls 3.85 ± 1.50%, CKAMP44^{HCoex} 3.26 ± 1.23%). SNRWM errors did not differ between Controls and CKAMP44^{HCoex} mice ((**Figure 3.19b**, bottom graph). Data-analysis by 2-way-ANOVA showed no significant interaction ($F_{(6,140)}$ = 0.57, p = 0.751) and no significant difference in condition ($F_{(1,140)}$ = 0.06, p = 0.810). Significance in blocks ($F_{(6,140)}$ = 10.17, p = 0.0001) arose from the high number of errors made in block I, directly after switching the paradigms. Averaged over block I to VII, Controls and CKAMP44^{HCoex} mice did not display any significant difference in mean number of SNRWM errors (Controls 3.04 ± 0.43, CKAMP44^{HCoex} 3.10 ± 0.38, $t_{(20)} = 0.11$, p = 0.911). SNRWM errors represented over 95% of all spatial working memory errors (Controls 96.92 ± 0.02%, CKAMP44^{HCoex} 96.46 ± 0.01%).

There was no difference in performance of Controls and CKAMP44^{HCoex} mice in the veiled condition (block I*), neither in SNRWM errors nor in SRWM errors (mean number of SNRWM errors in block I*: Controls 2.82 ± 0.71, CKAMP44^{HCoex} 3.64 ± 0.85, $t_{(20)} = 0.74$, $p = 0.467$; mean number of SRWM errors in block I*: Controls 0.36 ± 0.20, CKAMP44^{HCoex} 0.45 ± 0.21, $t_{(20)} = 0.31$, $p = 0.757$).

In summary, this analysis suggests unaltered composition of spatial working memory errors in CKAMP44^{HCoex} mice compared to Controls: 95% of all spatial working memory errors were spatial non-reference working memory (SNRWM) errors.

3.2.2.5 Pattern Separation Performance on the Eight-Arm Radial Arm Maze

Based on the functional implication of the DG in pattern separation [Leutgeb and Moser, 2007; Bakker et al., 2008], data obtained during spatial reference memory acquisition on the eight-arm RAM were further analysed to check for any possible impairment in pattern separation ability during spatial reference memory acquisition (**Figure 3.20a**) and assessment of spatial working memory (**Figure 3.20b**). The different distribution of baited versus unbaited arms (adjacent and single arms) provides the basis for the pattern separation analysis. Distinguishing between adjacent baited arms (overlapping shared spatial cues) and single baited arms (non overlapping arm-specific spatial cues) is assumed to challenge the pattern separation ability of the mice in different degrees ([Niewoehner et al., 2007] see schemata of overlapping spatial cues in **Figure 3.20a+b**).

Summed over all 13 blocks of spatial reference memory acquisition, errors made into adjacent arms and errors made into single arms (divided by 2) were comparable between Controls (n = 11) and CKAMP44HCoes mice (n = 11) (mean sum of reference memory errors per animal into adjacent/2 arms: Controls 17.41 ± 2.04, CKAMP44HCoes 16.45 ± 1.42, $t_{(20)} = 0.38$, $p = 0.705$, mean sum of reference memory errors per animal into single/2 arms: Controls 19.27 ± 2.11, CKAMP44^{HCoex} 21.14 ± 2.04, $t_{(20)} = 0.63$, $p = 0.533$ (**Figure 3.20a**)).

Summed over all 7 blocks of the spatial working memory test, errors made into adjacent arms and errors made into single arms (divided by 2) were comparable between Controls (n = 11) and CKAMP44^{HCoex} mice (n = 11) (mean sum of working memory errors per animal into adjacent/2 arms: Controls 4.82 ± 0.60, CKAMP44^{HCoex} 5.64 ± 0.75, $t_{(20)} = 0.85$, $p = 0.406$, mean sum of working memory errors per animal into single/2 arms: Controls 5.59 ± 1.06, CKAMP44^{HCoex} 5.32 ± 0.87, $t_{(20)} = 0.20$, $p = 0.844$ (**Figure 3.20b**)).

The data suggest normal spatial pattern separation in CKAMP44^{HCoex} mice.

3.2.2.6 Recency-Dependent Choice of Arms during the Working Memory Test on the Eight-Arm Radial Arm Maze

Surprisingly, the poor performances of CKAMP44^{HCoex} mice on the T-Maze contrasted with the normal performance on the eight-arm RAM. In the latter test, CKAMP44^{HCoex} mice displayed normal spatial working memory performance and made the same number of both spatial reference working memory- (SRWM) and spatial non-reference working memory (SNRWM) -errors. The data derived from the RAM were further analysed to find out whether there was a difference in the spatial working memory mistakes (beyond what separation into SRWM errors and SNRWM error can reveal). The analysis was based on the assumption that the visit of an arm prevents re-entry into that very same arm in a recency-dependent manner, termed "recency dependent choice of arms". The most severe recency-dependent error ("type 0"-error) was defined as a direct re-entry into a previously visited arm without entering any other arm. A "type 3"-error represents any working memory mistake in which 3 arms were visited between the first entry to an arm and the re-entry to this very same arm (**Figure 3.21a**). The overall number of spatial working memory errors summed over all blocks was similar in Controls (n = 11) and CKAMP44^{HCoex} mice (n = 11) (mean number of working memory errors summed over all blocks: Controls 22.00 $\pm$ 3.17, CKAMP44^{HCoex} 22.09 $\pm$ 2.69, $t_{(20)} = 0.02$, $p = 0.983$ (**Figure 3.21b**)). The recency-dependent choice of arms in Controls differed significantly from the recency-dependent choice of arms in CKAMP44^{HCoex} mice (**Figure 3.21c**). Data-analysis by 2-way-ANOVA showed a significant effect for interaction ($F_{(6,140)} = 3.70$, $p = 0.003$) and for the types of spatial working memory errors ($F_{(6,140)} = 10.96$, $p = 0.001$). Because of the significant interaction, Bonferroni multiple comparison was applied and revealed equal performances of Controls and CKAMP44^{HCoex} mice in all recency-dependent working memory errors except in the "type 0"-error ($t_{(6)} = 3.93$, p = 0.001). Here the performance differed significantly (mean percent of working memory "type 0"-errors: Contols: 1.73 $\pm$ 0.51, CKAMP44^{HCoex} 3.82 $\pm$ 0.71, $t_{(20)} = 2.40$, p = 0.0001). $t_{(21)} = 3.93$, $p = 0.027$).

These data demonstrate that while expressing the same overall number of spatial working memory errors, CKAMP44^{HCoex} mice showed a significant impairment in avoidance of reentry of the most recently visited arm ("type-0"-error), hinting at impaired recency-dependent behavior as already seen in the T-Maze.

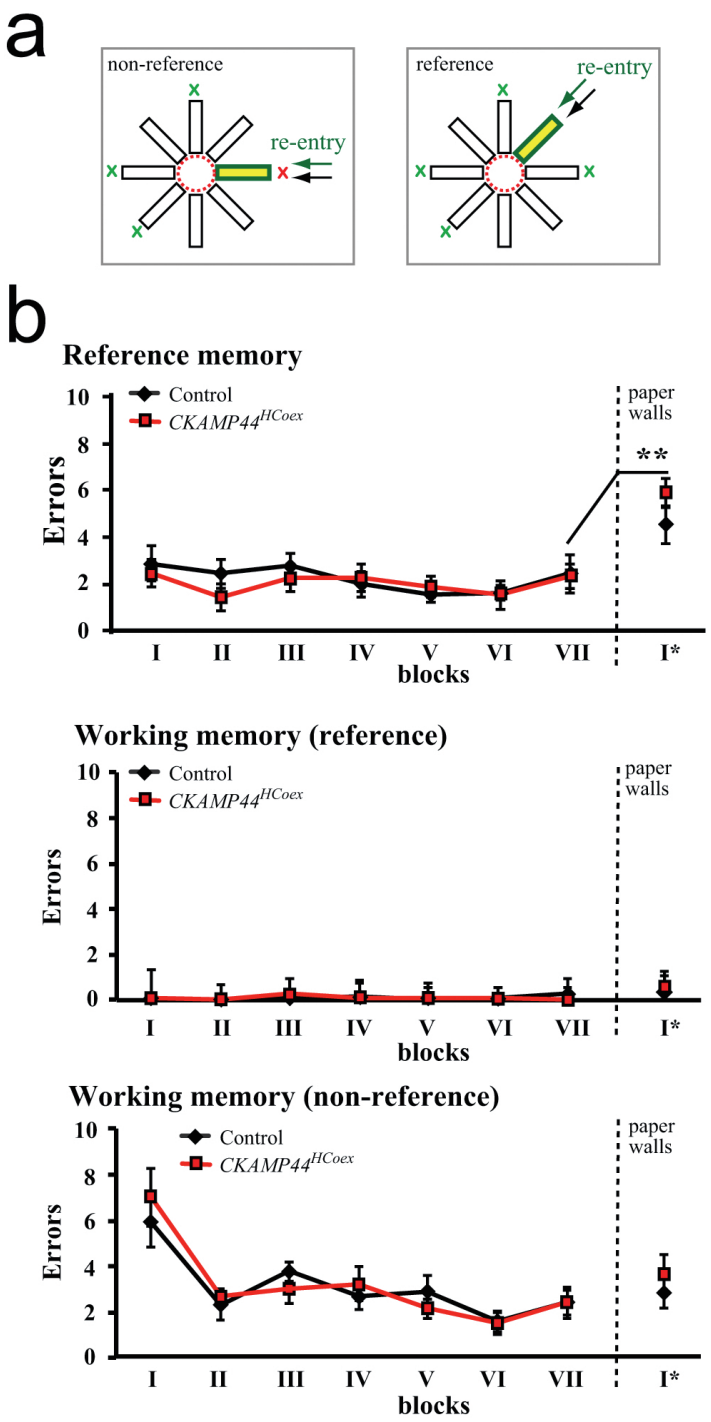

Figure 3.19: Dissection of Spatial Working Memory Performance on the Eight-Arm Radial Arm Maze (RAM) (a) Schemata depicting spatial non-reference working memory (SNRWM) and spatial reference working memory (SRWM) errors during spatial working memory test on the RAM. SNRWM errors (grey box, left): In a subsequent round of choice, all doors opened and the animal re-entered a previously visited previously baited arm. *Continued on page 61.*

Figure 3.19 (cont.): SRWM errors (grey box, right): In a subsequent round of choice, all doors opened and the animal re-entered a previously visited never baited arm. Red circle: all doors opened. Green X: baited arm. Red X: previously baited arm. Green rectangle: Twice visited arm (re-entry arm). Yellow filled arm: First visit of arm. Black arrow: First visit to an arm. Green arrow: Re-entry visit. (b) Top graph: Mean number of overall spatial reference memory errors (± SEM) during working memory test. Controls (n = 11) and CKAMP44^{HCoex} mice (n = 11) performed equally well. Middle graph: Mean number of SRWM errors (± SEM). Controls (n = 11) and CKAMP44^{HCoex} mice (n = 11) performed equally well. Bottom graph: Mean number of SNRWM errors (± SEM). Controls (n = 11) and CKAMP44^{HCoex} mice (n = 11) performed equally well.

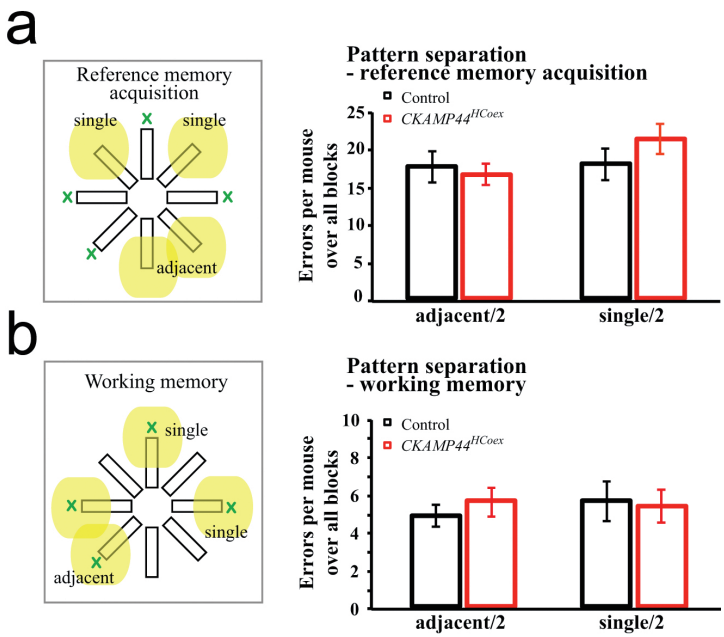

Figure 3.20: Unaltered Pattern Separation Performance of CKAMP44^{HCoex} Mice on the Eight-Arm Radial Arm Maze (RAM). (a) Pattern separation performance during spatial reference memory acquisition. Left panel: Schema depicting the pattern separation analysis of spatial reference memory acquisition. Identifying one of two adjacent baited arms with overlapping spatial cues is assumed to challenge the pattern separation ability of mice more than identifying a single baited arm with unique spatial cues [Niewoehner et al., 2007]. Graph: Mean spatial reference memory error per mouse (± SEM) over all blocks into adjacent/2 and single/2 arms showed no difference in pattern separation performances of Controls (n = 11) and CKAMP44^{HCoex} mice (n =11). (b) Pattern separation during spatial working memory. Left panel: Schema depicting the pattern separation analysis of spatial working memory test. Graph: Mean spatial working memory error per mouse (± SEM) over all blocks into adjacent/2 and single/2 arms showed no difference in pattern separation performances of Controls (n = 11) and CKAMP44^{HCoex} mice (n =11).

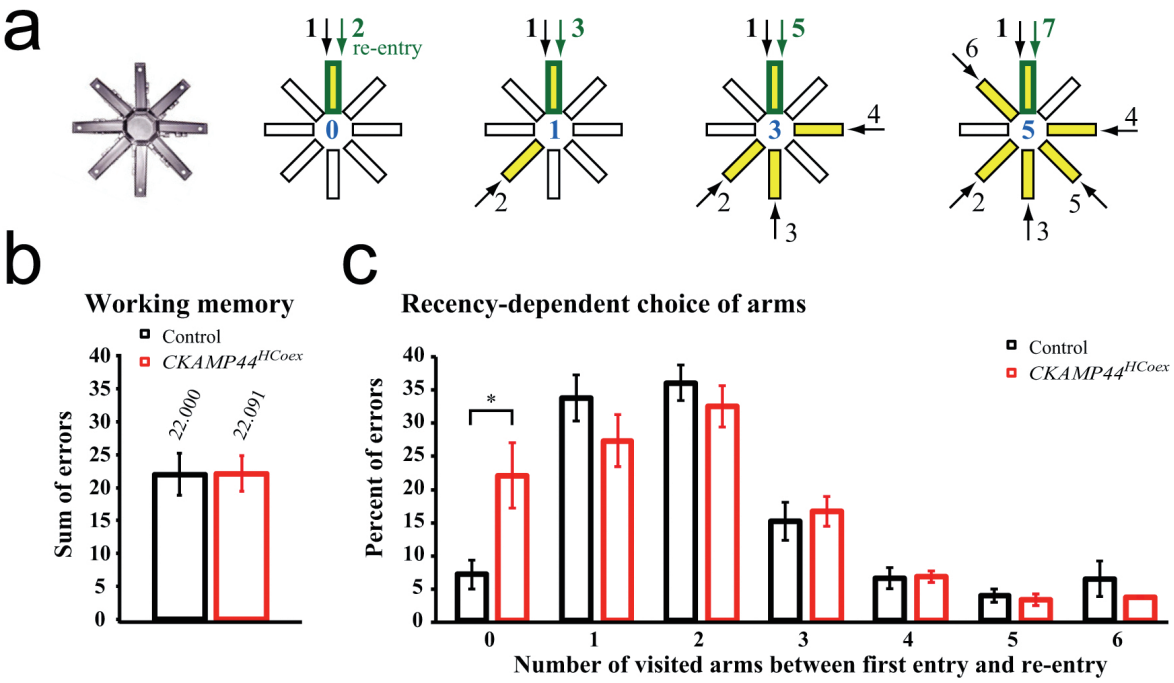

Figure 3.21: Impaired Recency-Dependent Choice of Arms while Spared Spatial Working Memory Performance of CKAMP44^{HCoex} Mice during Spatial Working Memory Test on the Eight-Arm Radial Arm Maze (RAM). (a) Schema depicting the analysis of recency-dependent choice of arms during the spatial working memory test on the RAM. Re-entries (spatial working memory errors) into any arm were analysed according to their recency. Recency was measured in number of visited arms (blue numbers) between first entry and re-entry (schemata given for "0"; "1"; "3" and "5"). Examples: "0": No other arm was visited between the first and the second visit (re-entry) of an arm. "3": After the first visit of an arm and before the second visit (re-entry) of the very same arm, 3 other arms were visited (numbered arrows show the sequence of visits). Black rectangles: Not visited arms. Green rectangle: Twice visited arm (re-entry arm). Yellow filled arm: First visit of arm. Black arrows with number: Sequence of visits (1 = first, 2 = second, 3 = third. . .). Green arrow with number: Last visit in sequence and thus re-entry (black arrow number 1, green rectangle). (b) Mean number of spatial working memory errors (± SEM) of Controls (n =11) and CKAMP44^{HCoex} mice (n = 11) summed over all blocks. There was no difference in spatial working memory performance. (c) Recency-dependent distribution of spatial working memory errors in mean percent of errors (± SEM). Compared to Controls (n =11), CKAMP44^{HCoex} mice (n = 11) displayed significantly more spatial working memory errors of "type-0" (gravest spatial working memory error: Direct re-entry into a previously visited arm without visiting any other arm). *p = 0.05.

4 Discussion

TARPs and other AMPAR auxiliary proteins were discovered only recently. Our knowledge about their diversity and function increases slowly. Nevertheless it becomes more and more apparent that these proteins provide multitudinous possibilities to influence AMPAR-trafficking and/or -transmission and thus have to be viewed as important modulators in shaping synaptic plasticity. The mouse models of altered CKAMP44 expression that were presented here, help to gain insight into the pivotal role that AMPAR modulating proteins have on spatial learning and memory.

In this project, it could be shown that overexpression of CKAMP44 following injection of an AAV construct into the hippocampus of adult C57Bl6 mice leads to impairments in hippocampus-dependent memory performances. The behavioral phenotype is comparable to that observed in GluA1$^{-/-}$ mice. Additionally, new aspects of spatial memory were demonstrated: Unaffected spatial working memory in the eight-arm RAM with simultaneously impaired recency-dependency is a new finding that has not been reported so far. Thus, CKAMP44^{HCoex} mice provide a novel tool to further investigate distinct memory processes.

Based on the hypothesis that the CKAMP44 overexpression influences hippocampal subfields differentially, given their native CKAMP44-expression levels, one can conclude that the behavioral deficits of CKAMP44^{HCoex} mice are mostly CA1-dependent. Indeed, the mice showed impaired performances on tests addressing the temporal component of memory separation, i.e. the rewarded alternation on the T-Maze and recency-dependent choice of arms on the eight-arm RAM (in contrast to spatial pattern separation which is assigned to the DG). Thus, data pertaining to the behavioral analysis of CKAMP44^{HCoex} mice support former evidence that the functional role of CA1 includes temporal pattern separation.

The specific memory defect shown by CKAMP44^{HCoex} mice underlines the necessity for re-evaluating the use of the rewarded alternation on the T-Maze (a dealyed non-matching-to-place task, hereafter referred to as “T-Maze”). The T-Maze has drawn much attention since it has been introduced by Dember and colleagues in 1961 [Dember and Fox, 1961] and was used as a classic approach to test spatial working memory in rodents. Recently, Sanderson and colleagues proposed to redefine this test as a tool to measure short-term, stimulus specific habituation

[Sanderson et al., 2011a]. The fact that CKAMP44^{HCoex} mice, compared to Controls, made the same number of working memory errors in the eight-arm RAM working memory test, but showed a deficit in recency-dependent behavior when tested on the RAM and T-Maze, supports this notion.

Furthermore, the CKAMP44 overexpression model underlines once more the important role of AMPAR modulating proteins. The herein discussed results suggest that in the adult mouse, CKAMP44 – by means of differential expression – modifies important memory functions in specific subfields in the hippocampus. Thus, the balance of CKAMP44 and other AMPAR auxiliary proteins or TARPs, might play a key-role in the expression of different forms of memory.

The findings summarized above are discussed in more detail in the subsequent chapters.

4.1 CKAMP44$^{-/-}$ Mice

4.1.1 Subfield-Specific Defects Dependent on CKAMP44 Expression: DG and Spatial Pattern Separation

In the adult mouse hippocampus, CKAMP44 is highly expressed in DG-neurons but shows very low expression in CA1- and no expression in CA3-neurons [Von Engelhardt et al., 2010]. Based on this finding, one predicts that overexpression or a global CKAMP44 knockout will influence the DG, CA1 and CA3 differentially. Overexpression should influence synaptic plasticity of CA1- and CA3-synapses (change from low expression to high expression) much more than synaptic plasticity of DG-synapses (change from high expression to even higher expression). Whereas –theoretically – in the CKAMP44$^{-/-}$, DG-synapses should be much more influenced than synapses of endogenous low expression in CA1. CKAMP44 is barely detectable in CA3. Thus, CKAMP44 knockout should not influence the function of CA3 synapses.

In the following paragraph, the CKAMP44$^{-/-}$ mice are discussed with focus on the subfield-specific deficits in learning and memory. The results derived from behavioral testing of CKAMP44^{HCoex} mice are discussed in the corresponding subchapter later in this work.

DG and Spatial Pattern Separation

Spatial pattern separation is defined as a mechanism for separating partially overlapping representations so that one representation may be retrieved as separate from others. Based on its

anatomy (many granule cells, sparse projection to CA3) the DG has been proposed to be the structure that enables the brain to perform spatial pattern separation.

Ongoing postnatal neurogenesis ensures that new DGCs continue to be added to the DG. Adult-born DGCs mature within the DG and eventually get integrated. These cells are supposed to provide new substrate for new patterns, thus creating neuronal space for improved "memory resolution" [Aimone et al., 2011]. Damage to the DG or disruption of adult neurogenesis affects spatial pattern separation. Deficits on spatial tasks may occur when there is increased overlap or similarity among distal cues. Spatial pattern separation performance can be tested on mazes that provide different degrees of overlap among critical spatial distal cues (e.g. RAM, MWM, Hole-Board/Cheeseboard, Barnes-Maze).

Results of studies with lesioned rats added proof to the involvement of the DG in spatial pattern separation [Gilbert et al., 2001]. With growing knowledge and refined methods, lesion studies were abandoned for the sake of more sophisticated and subtle manipulations. Fine-graded disturbances of the DG could be achieved by focally ablating adult neurogenesis via low-dose x-ray radiation [Clelland et al., 2009; Tronel et al., 2010; Sahay et al., 2011]. Using tests that require high spatial resolution (contextual fear-discrimination learning task and a two-choice touch screen spatial discrimination task), it was possible to show that new neurons are required for pattern separation. Sahay and colleagues subsequently designed a genetic approach to selectively increase adult neurogenesis in mice and showed improved spatial pattern separation in the mutants [Sahay et al., 2011].

Disturbed AMPAR transmission in the DG of CKAMP44$^{-/-}$ mice makes the animals theoretically prone to spatial pattern separation dysfunction. In 2007, Niewoehner and colleagues chose a sophisticated genetical approach to investigate the effect of altered synaptic plasticity in DG on the spatial pattern separation ability. Upon deletion of the main NMDAR subunit, NR1$^{\Delta DG}$ mice displayed impaired synaptic plasticity. The DG-specific knockout of NR1 resulted in impaired LTP in both inputs to the DG without influencing LTP in CA3-to-CA1 synapses. This led to impaired spatial working memory but normal spatial reference memory performance on a six-arm RAM. An analysis of pattern separation on the six-arm RAM was introduced. By choosing different baited arms (2 adjacent arms and 1 single arm), the grade of spatial resolution was defined. Unexpectedly, no pattern separation deficit was found in the NR1$^{\Delta DG}$ mice. An explanation for this could be the use of just 6 arms in the RAM. Thus, in the herein presented study, the use of the eight-arm (instead of the six-arm) RAM provided a higher spatial resolution. Dependent on the choice of baited arms, the grade between the arm openings were 45, 90, 135 and 180 degrees (compared to 60, 120, 180 degrees in the six-arm RAM). 45 degrees distance representing two adjacent arms, 180 degrees distance representing opposed arms. Despite this refined grading in pattern separation testing, CKAMP44$^{-/-}$ mice showed normal pattern-separation.

The failure in showing the expected disturbed spatial pattern separation could be due to insufficient spatial pattern grading on the eight-arm RAM and/or compensation of the lack of CKAMP44. By testing mice on a Cheeseboard/Hole-Board or Barnes Maze, the experimenter can choose much finer grades of spatial separations compared to the eight-arm RAM. Testing the CKAMP44$^{-/-}$ mice on those mazes promises to be more adequate for spatial pattern separation analysis.

In the CKAMP44$^{-/-}$ mice, compensatory mechanisms throughout development and/or compensation by other putative CKAMP44-like proteins cannot be excluded. Impairments might also derive from the lack of CKAMP44 in other brain regions (e.g. the cerebellum). The CKAMP44$^{-/-}$ mice showed a normal performance in the exploration tasks (open field test, novel object recognition test) and in the rewarded alternation on the T-Maze. In the spatial reference memory acquisition on the eight-arm radial arm maze, Wts and CKAMP44$^{-/-}$ mice learned over time to commit fewer spatial reference memory errors. Although CKAMP44$^{-/-}$ mice learned the task as well as Wts, even after 100 trials, they both failed to reach a level of spatial reference memory performance comparable to CKAMP44^{HCoex} mice and their Controls (baseline spatial reference memory errors: 5.57 $\pm$0.45 out of 16 possible mistakes per block for Wt; 5.56 $\pm$0.68 out of 16 possible mistakes perblock for CKAMP44$^{-/-}$; 2.18 $\pm$0.4 out of 16 mistakes per block for Controls; 2.24 $\pm$0.14 out of 16 possible mistakes per block for CKAMP44^{HCoex} mice). Given the normal performance in the rewarded alternation on the T-Maze, further testing of CKAMP44$^{-/-}$ mice in the spatial working memory paradigm on the eight-arm radial arm maze was not conducted.

The fact that Wts and CKAMP44$^{-/-}$ alike were unable to reach the necessary baseline performance on the test, hints at a problem idiosyncratic to the line. CKAMP44$^{-/-}$ mice were bred in our own facilities and the mice used to perform behavioral testings were not of a pure C57Bl6-background (F5/F6) whereas CKAMP44^{HCoex} mice were C57Bl6-mice purchased from Charles River.

To rule out compensatory mechanisms, generation of forebrain- or DG-specific CKAMP44 knockouts would be helpful. Another valid approach is the injection of sh-RNA constructs into the hippocampus to knock down the CKAMP44 expression. As explained in previous chapters, the endogenous expression level of CKAMP44 hints at a special function for the DG based on the CKAMP44-based manipulation of AMPARs . Hippocampus-specific knockdown of CKAMP44 (via usage of sh-RNA), would influence DG most. In theory, a CKAMP44-knockdown model would be more comparable to the CKAMP44^{HCoex} model because animals in both models ungergo the same treatment: operation and injection in adulthood. Mice for injections could be purchased from the same supplier (e.g. Charles River) and thus would be of the same background (or even littermates).

4.2 CKAMP44^{HCoex} Mice

4.2.1 CKAMP44^{HCoex} Mice versus GluA1$^{-/-}$ Mice

Based on its activity-dependent trafficking and de novo insertion, the AMPAR subunit GluA1 is of utmost importance in synaptic plasticity [Shi et al., 1999, 2001]. GluA1$^{-/-}$ mice have been subjected to many sophisticated behavioral experiments providing researchers with deeper insights into the mechanisms of spatial learning and memory. The selective spatial working memory impairment in GluA1$^{-/-}$ mice suggests that spatial working memory and spatial reference memory are based on two different mechanisms [Reisel et al., 2002; Schmitt et al., 2003]. Recently it was proposed that these mechanisms compete with one another [Sanderson et al., 2009]. CKAMP44^{HCoex} mice showed an even more graded level of spatial memory impairment than GluA1$^{-/-}$ mice. Hence direct comparison between the behavioral phenotypes of both models is the sensible step to take. The following table gives a detailed overview on spatial memory tests performed on both models (Table 4.1 on page 68).

Two important observations arise from comparing GluA1$^{-/-}$ mice to CKAMP44^{HCoex} mice:

Observation 1: Hippocampal overexpression of the AMPAR auxiliary protein CKAMP44 leads to a similar phenotype as that reported for GluA1$^{-/-}$ mice. Activity-dependent trafficking and insertion of GluA1-containing AMPARs into the synapse has been regarded as one of the main players in regulating synaptic strength. CKAMP44 was proven to be involved in this process by manipulating either AMPAR kinetics [Von Engelhardt et al., 2010] or/and AMPAR trafficking (personal communication about ongoing, unpublished work of Von Engelhardt and colleagues).

Observation 2: CKAMP44^{HCoex} mice displayed a very specific spatial learning deficit. GluA1$^{-/-}$ mice showed a bias in their performances in spatial working- (impaired) and spatial reference-memory (normal) and thus helped identifying the different substrates underlying these memory processes. CKAMP44^{HCoex} mice showed normal spatial working- and normal spatial reference-memory on the eight-arm RAM, but impairment in two tests addressing the temporal component of short-term memory (rewarded alternation on the T-Maze and recency-dependent choice of arms during the working memory paradigm on the eight-arm RAM). Thus, CKAMP44^{HCoex} mice provide a useful tool to allow a fine-graded resolution in testing spatial memory processes. The results of this study help to better delineate working memory in rodents and provide further evidence for subfield-dependent memory-processes.

4.2.2 Re-Evaluation of the Use of the T-Maze

Rewarded alternation on the T-Maze has long been regarded as a standard test for hippocampus dependent, spatial working memory [Olton and Papas, 1979]. Recently, Sanderson and

TEST	GluA1$^{-/-}$	CKAMP44^{HCoex}
OPEN FIELD		
• Squares & rearings	• **Hyperactive**[1]	• **Hyperactive**
NOVEL OBJECT RECOGNITION		
• Exploratory behavior	• **Hyperexploratory**[2]	• **Hyperexploratory**
• Recognition test performance	• Normal (preference for novel object)[2]	• Normal (preference for novel object)
• Object recency	• Normal (preference for less recent object)[2]	• Not tested
• Yoked object recognition	• **Impaired**[2]	• Not tested
• Yoked object recency	• **Impaired**[2]	• Not tested
T-MAZE		
• Reference memory	• Normal[3]	• Not tested
• Transfer test	• Normal[3]	• Not tested
MORRIS WATER MAZE		
• Working memory	• **Impaired**[4]	• **Impaired**
RADIAL ARM MAZE		
• Acquisition of reference memory	• Normal[5]	• Normal
• Working memory	• **Impaired**[5]	• Normal
• Pattern seperation	• Not tested	• Normal
• Recency-dependent choice of arms	• Not tested	• **Impaired**

Table 4.1: Comparison of Behavioral Phenotype in GluA1$^{-/-}$ Mice and CKAMP44^{HCoex} Mice. Bold writing indicates performances different from normal behavior. Behavioral testing of CKAMP44^{HCoex} mice is explained in detail in the results. Performances of GluA1$^{-/-}$ mice were taken from the following publikations:
[1]: Bannerman D.M., Deacon R.M.J., Brady S., Bruce A., Sprengel R., Seeburg P.H., J.N.P. Rawlins (2004) A comparison of GluR-A-deficient and wild-type mice on a test battery assessing sensorimotor, affective, and cognitive behaviors. Beh Neurosci 118(3).
[2]: Sanderson D.J., Hindley E., Smeaton E., Denny N., Taylor A., Barkus C., Sprengel R., Seeburg P.H., Bannerman D.M. (2011) Deletion of the GluA1 AMPA receptor subunit impairs recency-dependent object recognition memory. Learn Memory 18.
Continued on page 69

colleagues re-evaluated the use of the T-Maze and claimed that alternation behavior results from short-term, stimulus-specific habituation [Sanderson and Bannerman, 2011]. Based on results derived from a series of experiments with GluA1$^{-/-}$ mice, they postulated that the poor performances on the T-Maze and in the novel yoked object recognition task arose both from the inability to habituate to a very recently experienced stimulus (e.g. the previously visited arm, the previously encountered object). They argued that performance in habituation-based tasks does not rely on the hallmarks of working memory as they have been defined for humans: active maintenance and manipulation of information. This differentiation is not just mere hair-splitting about a definition. It is of highest importance when it comes to the transfer of the understanging of memory mechanisms, based on research done in rodent-models, to the human brain. As Sanderson and Bannerman pointed out, deficits in habituation might derive from a deficit in attention and thus would be more related to attentional processes in humans than to human working memory processes [Sanderson and Bannerman, 2011; Sanderson et al., 2011b].

Mice normally prefer novel stimuli to previously experienced stimuli. This can be tested in diverse novelty preference tests (continuous spontaneous alternation on the Y-maze [Drew et al., 1973], object recognition task [Rampon et al., 2000], novel-arm-test on the RAM [Sanderson and Bannerman, 2011] and has to be clearly distinguished from spatial working memory tests that are supposed to test for flexible memory. As mentioned above, according to Sanderson and Bannerman, rewarded alternation on the T-Maze addresses novelty preference based on habituation to a stimulus, just like the novel object recognition test. This is very important regarding the results of this work: Performances of CKAMP44^{HCoex} mice were impaired in the delayed non-matching-to-place task of the T-Maze and the recency-dependent choice of arms in the eight-arm RAM, but the animals showed normal performance in the working memory test on the eight-arm RAM.

When C576BL/6 mice were free to explore all arms of a six-arm RAM, the chance of re-entry into a previously explored arm rose with the time spent on the Maze: Arms that were visited in

Table 4.1 (cont.):
[3]: Zamanillo D., Sprengel R., Hvalby O., Jensen V., Burnaschev N., Rozov A., Kaiser K.M., Koster H.J., Borchardt T., Worley P., Lubke J., Frotscher M., Kelly P.H., Sommer B., Andersen P., Seeburg P.H., Sakmann B. (1999) Importance of AMPA receptors for hippocampal synaptic plasticity but not for spatial learning. Science 284.
[4]: Reisel D., Bannerman D.M., Schmitt W.B., Deacon R.M.J., Flint J., Borchardt T., Seeburg P.H., Rawlins J.N.P. (2002) Spatial memory dissociations in mice lacking GluR1. Nature Neurosci 5(9).
[5]: Schmitt W.B., Deacon R.M., Seeburg P.H., Rawlins J.N.P., Bannerman D.M. (2003) A within-subjects, within-task demonstration of intact spatial reference memory and impaired spatial working memory in glutamate receptor-A-deficient mice. J Neurosci 23(9).

the beginning of the experiment were most probably re-entered when some time passed and other arms have been visited inbetween. A direct re-entry into a once explored arm was least probable. This implies a greater memory of the recently explored arm and seemed to be due to the habituation to the most recent stimulus [Sanderson and Bannerman, 2010], similar to the novel object recognition test.

Based on these observations, one would assume that in the working memory test on the eight-arm RAM, the previously visited most recently explored arm will be entered the least likely at the next choice of arms. This held true for Controls, but not for CKAMP44^{HCoex} mice. CKAMP44^{HCoex} mice directly re-entered the most recently visited arm significantly more often than Controls (see results). This behavior represented a short-term, stimulus specific memory/habituation deficit and explained the bad performance on the T-Maze where the correct choice of arm-entry is based on the very previously entered arm.

In line with the proposal of Sanderson and Bannerman, the habituation-deficit of CKAMP44^{HCoex} mice in the working memory task on the eight-arm RAM together with their impairment on the T-Maze give reason to believe that the classical use of the T-Maze must be reconsidered.

4.2.3 Accurate Disintegration of Memory Processes via Behavioral Testing

Unlike GluA1$^{-/-}$ mice, CKAMP44^{HCoex} mice were exclusively impaired in their performance on the T-Maze, but showed no deficits in spatial working and spatial reference memory tested on the eight-arm RAM. By refining testing paradigms and analysis, more subtle and more specific impairments were found.

To investigate the short-term, stimulus-specific memory/habituation (temporal pattern separation), data obtained from the eight-arm RAM were analysed with regards to the number of arm entries that were made between the first entry and re-entry into a given non-baited arm. CKAMP44^{HCoex} mice showed a significantly different performance compared to Controls. But the deficit in short-term, stimulus-specific memory/habituation of CKAMP44^{HCoex} mice did not influence the overall performance shown in the working memory task. The flexible working memory, which is responsible for keeping track of the arms already visited during the trial is independent from the more simple reflex-like habituation memory. Results derived from this experiment show that the “short-term, stimulus-specific memory/habituation” is to be separated from “working memory”.

I want to propose the term “recency-dependent memory” for the “short-term, stimulus-specific memory/habituation” that is supposed to be tested on the T-Maze and that is responsible for the

recency-dependent choice of arms on the eight-arm RAM. Whereas recency-dependent memory seems to be influenced by the expression level of AMPAR auxiliary protein CKAMP44, working memory relies on GluA1- but not on CKAMP44-expression. Low expression of CKAMP44 in CA1-neurons is important in order to enable hippocampal AMPARs to shape synaptic plasticity in a way that allows mice to avoid already encountered environment based on the recency of the previous exploration.

Whether this effect is subunit-specific will be discussed in the next chapter.

4.2.4 Subfield Specific Defects Dependent on CKAMP44 Expression: CA1 and Temporal Pattern Separation

As already mentioned, hippocampal subfields are assumed to play a role in distinct hippocampal memory processes. The involvement of the DG in spatial pattern separation was discussed in a previous chapter. The following paragraph elaborates on the contribution of the CKAMP44^{HCoex} model to the investigation of the functional role CA1 plays in temporal pattern separation.

CA1 and Temporal Pattern Separation

CA1 receives input from different pathways (e.g. direct input from entorhinal cortex via temporoammonic pathway, input from CA3 via Schaffer Collaterals) and is believed to be the main output region of the hippocampus. Computational models suggested CA1 to be the mediator of temporal processing of information [Marr, 1971; Rolls, 1996]. Studies in humans showed that cues that occur further apart in a temporal sequence are remembered better than cues which are temporally adjacent [Madsen and Kesner, 1995]. To corroborate these results in rodents, behavioral task that require the separation of temporally patterned information were designed.

Lesion studies in rats confirmed the role of the hippocampus in temporally separating a sequence of visited arms in the RAM [Chiba et al., 1994]. Gilbert and colleagues presented a study to dissociate the function between DG and CA1. Till then, it had not been explicitly shown whether hippocampal subregions function as an ensemble to separate patterns of incoming information or whether specific subregions are responsible for this process. If the first assumption were true, lesions to either part of the hippocampus should produce a deficit in spatial and temporal spatial pattern separation tasks. Gilbert and colleagues restricted lesions to defined hippocampal subfields and could demonstrate that the DG is involved in spatial pattern separation, whereas (spatio-) temporal pattern separation is a function based on the CA1 region [Gilbert et al., 2001]. In 2008, Hunsaker and colleagues confirmed these results. Rats were trained on a temporal

pattern separation task in which the animals had to use the immediately preceding element in a sequence to choose a correct baited location. As soon as they succeeded in this task, they were treated with ibotenic acid to lesion either CA1 or CA3. To show the involvement of the lesioned region, postoperative animals were confronted again with the same task. CA1-lesioned animals were highly impaired. In order to prove that it is the temporal component of the task that hinders the lesioned animals in succeeding, they were subsequently tested under the same paradigm minus the temporal component. Here, all animals were able to manage the task [Hunsaker et al., 2008].

The recency-dependent choice of arms on the eight-arm RAM is a novel approach for the purpose of investigating temporal pattern separation. The correct decision (choice of the baited location) is recency-dependent as it is based on the immediate previously encountered stimulus. Thus, the impairment of recency-dependent memory upon CKAMP44 overexpression in the adult hippocampus supports the idea that CA1 controls (spatio-) temporal pattern separation.

Furthermore, the results suggest that the attribution of specific memory processes to a given hippocampal subfield might not be solely realized by the AMPAR composition but also (or even majorly) by the expression of auxiliary proteins. With increasing knowledge of their function, TARPs and other AMPAR auxiliary proteins are realized to be more important in manipualting AMPAR function and thus influencing synaptic plasticity than previously thought. The ability of these proteins to alter AMPAR-transmission and/or -trafficking together with their differential expression throughout development and throughout tissues and even subfields, adds a new dimension to the possibilities of shaping and refining the memory system.

The CKAMP44^{HCoex} mice provide the first model to specifically attribute a distinct memory function to a single AMPAR auxiliary protein. This also gives rise to questions about the possible functions of putative related proteins; about their redundancy and their possible roles during development. These questions could be addressed by generating specific overexpression- and knockout-models as realized for CKAMP44.

Interneurons and CA1 Function

Immunostainings revealed cells in CA1 of CKAMP44^{HCoex} mice that expressed both: GFP(and thus presumably CKAMP44) and the interneuron marker PV. Based on this, one could argue that the CKAMP44^{HCoex}-phenotype derived from dysfunctional inhibition in CA1. Additionally, it has been shown that fast spiking PV-positive cells (expression specifically GluA1 and GluA4) exert great influence on hippocampal function and related behavior [Fuchs et al., 2001, 2007]. Especially in the CA1 subfield, the functional ablation of PV-positive interneurons impaired spatial working memory performance as tested in the water maze version of the RAM (RAWM) and in a delayed matching to sample/place task [Murray et al., 2011].

Regarding the low number of GFP/PV-double-positive neurons, a correlation of the described CKAMP44^{HCoex} phenotype and CKAMP44-expressing interneuron is unlikely. Murray and colleagues claimed to affect roughly 80% of all PV-positive cells in CA1 [Murray et al., 2011]. In CKAMP44^{HCoex} mice, the number of double-positive cells varied between CKAMP44^{HCoex} individuals from as few as 1 cell per hemisphere to maximal 13 cells per hemisphere. All animals showed a similar degree of impairment. Still, regarding the results from Fuchs and Murray, it would be interesting to investigate the influence of CKAMP44 – or related proteins – on hippocampal interneurons and principal cells separately.

4.2.5 CKAMP44 versus TARPs and other AMPAR Auxiliary Proteins

In comparison with TARPs and other AMPAR auxiliary proteins, CKAMP44 has unique properties; it prolongs deactivation but accelerates desensitization. Furthermore it slows the rate of recovery from desensitization, as shown in hippocampal slices [Von Engelhardt et al., 2010]. CKAMP44 is widely expressed in the adult brain . In hippocampus, the protein is differentially expressed at high levels in DG, and lower levels in CA1. What possible role does the differential expression of CKAMP44 in the hippocampus play in learning and memory?

This question could not be answered by the investigation of CKAMP44$^{-/-}$ mice that showed no specific memory impairments. As discussed in a previous chapter, this could be either due to compensatory effects (developmental compensation or compensation by other members of the CKAMP-family) or due to the lack of fine-graded testing paradigms. Knockout or knockdown restricted to the hippocampus might serve as a more appropriate tool to investigate the role of CKAMP44 in the hippocampus and especially the region of high expression, namely the DG.

The CKAMP44^{HCoex} model is the only model of hippocampus-specific altered AMPAR auxiliary protein expression. *Stargazer* mice, in which the first TARP has been identified, displayed a phenotype based mainly on cerebellar dysfunction. The knockout of other TARPs like γ-3; γ-4; γ-7 and γ-8, was not associated with an overt behavioral phenotype [Menuz et al., 2008; Letts, 2005; Yamazaki et al., 2010; Rouach et al., 2005]. To circumvent the redundancy of the γ-family-members, double- and triple knockouts were generated (see **table 1.2** in the Introduction). These were mostly characterized by more severe ataxia and low bodyweight or seizure introduction into formerly seizure-free single-allele-mutants (γ-2/γ-3; γ2/γ7 and γ-2/γ4, respectively). Knockout models or models of altered expression of the other recently discovered AMPAR auxiliary proteins CNIH-2, CNIH-3 and SynDIG-1 have not been published.

CKAMP44^{HCoex} mice are thus the first model to prove altered memory function based on highly restricted alteration of AMPAR auxiliary protein expression. CKAMP44^{HCoex} mice introduced in this work, showed impairment in stimulus-specific, recency-dependent memory that derived from a restricted hippocampal region (CA1) and thus represent the very first model to dissect memory function with respect to the role of AMPAR auxiliary proteins.

The hippocampus is known to be involved in a broad range of neurophysiological diseases like Alzheimer's disease, temporal lobe epilepsy, cognitive ageing, post-traumatic stress disorder, transient global amnesia, schizophrenia, depressive and anxiety disorders – to name only a few of the most common and most frequently studied diseases [reviewed by: Small et al., 2011]. Unveiling the bits and pieces that eventually add up to build the memory system is of pivotal importance. Not only for the sake of pure knowledge but also for laying the ground for new methods and approaches targeting pathological dysfunctions. The discovery of the TARPs initiated the quest for more AMPAR auxiliary proteins. With the discovery of the protagonist of this work, CKAMP44, Von Engelhardt and colleagues introduced a new potentially powerful protein in memory regulation to the field. The herein presented proof of the implication of CKAMP44 in fine-graded memory processes adds an important piece of information towards the understanding of learning and memory.

Bibliography

J B Aimone, W Deng, and F H Gage. Resolving new memories: a critical look at the dentate gyrus, adult neurogenesis, and pattern separation. *Trends in Cognitive Sciences*, 70(4): 589–596, 2011. doi: 10.1016/j.neuron.2011.05.010. URL http://www.ncbi.nlm.nih.gov/pubmed/21609818.

J M Alarcon, R Hodgman, M Theis, Y S Huang, E R Kandel, and J D Richter. selective modulation of some forms of schaffer collateral-CA1 synaptic plasticity in mice with a disruption of the CPEB-1 gene. *Learning and Memory*, 11:318–327, 2004.

D G Amaral. A Golgi study of cell types in the hilar region of the hippocampus in the rat. *The Journal of Comparative Neurology*, 182(4 Pt 2):851–914, 1978. URL http://www.ncbi.nlm.nih.gov/pubmed/730852.

D G Amaral, H E Scharfman, and P Lavenex. The dentate gyrus: fundamental neuroanatomical organization (dentate gyrus for dummies). *Progression in Brain Research*, 163:3–22, 2007. doi: 10.1016/S0079-6123(07)63001-5. URL http://www.ncbi.nlm.nih.gov/pubmed/17765709.

P Andersen, T W Blackstad, and T Lomo. Location and identification of excitatory synapses on hippocampal pyramidal cells. *Experimental Brain Research*, 1(3):236–248, 1966. URL http://www.ncbi.nlm.nih.gov/pubmed/5920551.

B K Andrasfalvy, M A Smith, T Borchardt, R Sprengel, and J C Magee. Impaired regulation of synaptic strength in hippocampal neurons from GluR1-deficient mice. *Journal of Physiology*, 552:34–45, 2003.

M C Ashby, S R Maier, A Nishimune, and J M Henley. Lateral diffusion drives constitutive exchange of AMPA receptors at dendritic spines and is regulated by spine morphology. *The Journal of Neuroscience*, 26(26):7046–7055, 2006. doi: 10.1523/JNEUROSCI.1235-06.2006. URL http://www.ncbi.nlm.nih.gov/pubmed/16807334.

A Bakker, C B Kirwan, M Miller, and C E Stark. pattern separation in the human hippocampal CA3 and dentate gyrus. *Science*, 319:1640–1642, 2008.

D M Bannerman, M A Good, S P Butcher, M Ramsay, and R G Morris. Distinct components of spatial learning revealed by prior training and NMDA receptor blockade. *Nautre*, 378 (6553):182–186, 1995. doi: 10.1038/378182a0. URL http://www.ncbi.nlm.nih.gov/pubmed/7477320.

Z I Bashir, D E Jane, D C Sunter, J C Watkins, and G L Collingridge. Metabotropic glutamate receptors contribute to the induction of long-term depression in the CA1 region of the hippocampus. *European Journal of Pharmacology*, 239(1-3):265–266, 1993. URL http://www.ncbi.nlm.nih.gov/pubmed/8223907.

J T Becker, J A Walker, and D S Olton. Neuroanatomical bases of spatial memory. *Brain Research*, 200:307–320, 1980.

M A Bedoukian, A M Weeks, and K M Partin. Different domains of the AMPA receptor direct stargazin-mediated trafficking and stargazin-mediated modulation of kinetics. *The Journal of Biological Chemistry*, 281:23908–23921, 2006.

T W Blackstad. Commissural connections of the hippocampal region in the rat, with special reference to their mode of termination. *The Journal of Comparative Neurology*, 105(3): 417–537, 1956. URL http://www.ncbi.nlm.nih.gov/pubmed/13385382.

T V Bliss and A R Gardner-Medwin. Long-lasting potentiation of synaptic transmission in the dentate area of the unanaestetized rabbit following stimulation of the perforant path. *The Journal of Physiology*, 232(2):357–374, 1973. URL http://www.ncbi.nlm.nih.gov/pubmed/4727085.

J P Changeux and Laurence Garey. *Neuronal Man*. Pantheon Book, New York, first edit edition, 1985.

L Chen, S Bao, X Quiao, and R F Thompson. Impaired cerebellar synapse maturation in waggler, a mutant mouse with a disrupted neuronal calcium channel gamma subunit. *PNAS*, 96:12132 – 32137, 1999.

L Chen, D M Chetkovich, R S Petralia, N T Sweeney, Y Kawasaki, R J Wenthold, D S Bredt, and R A Nicoll. Stargazin regulates synaptic targeting of AMPA receptors by two distinct mechanisms. *Nature*, 408(6815):936–943, 2000. doi: 10.1038/35050030. URL http://www.ncbi.nlm.nih.gov/pubmed/11140673.

A A Chiba, R P Kesner, and A M Reynolds. Memory for spatial location as a function of temporal lag in rats: role of hippocampus and medial prefrontal cortex. *Behavioral and neural biology*, 61(2):123–131, 1994. URL http://www.ncbi.nlm.nih.gov/pubmed/8204078.

C H Cho, F St-Gelaus, W Zhang, S Tomita, and J R Howe. Two families of TARP isoforms that have distinct effects on the kinetic properties of AMPA receptors and synaptic currents. *Neuron*, 55:890–904, 2007.

C D Clelland, M Choi, C Romberg, G D Clemenson Jr., A Fragniere, P Tyers, S Jessberger, L M Saksida, R A Barker, F H Gage, and T J Bussey. A functional role for adult hippocampal neurogenesis in spatial pattern separation. *Science*, 325(5937):210–213, 2009. doi: 10.1126/science.1173215. URL http://www.ncbi.nlm.nih.gov/pubmed/19590004.

G L Collingridge, S J Kehl, and H McLennan. Excitatory amino acids in synaptic transmission in the Schaffer collateral-commissural pathway of the rat hippocampus. *The Journal of Physiology*, 334:33–46, 1983. URL http://www.ncbi.nlm.nih.gov/pubmed/6306230.

S Cull-Candy, S Brickley, and M Farrant. NMDA receptor subunits: diversity, development and disease. *Current Opinion in Neurobiology*, 11(3):327–335, 2001. URL http://www.ncbi.nlm.nih.gov/pubmed/11399431.

R L De No. Studies on the structure of the cerebral cortex II. Continuation of the study of ammonic system. *Journal für Psychologie und Neurologie*, 46:64, 1934.

R M Deacon, A Croucher, and J N Rawlins. Hippocampal cytotoxic lesion effects on species-typical behaviours in mice. *Behavioral Brain Research*, 132(2):203–213, 2002. URL http://www.ncbi.nlm.nih.gov/pubmed/11997150.

W N Dember and R Fox. A critical note on Thompson's two-factor theory of inhibition. *Psychological Review*, 68:416–419, 1961. URL http://www.ncbi.nlm.nih.gov/pubmed/13885298.

W Deng, J B Aimone, and F H Gage. New neurons and new memories: how does adult hippocampal neurogenesis affect learning and memory? *Nature Reviews. Neuroscience*, 11 (5):339–350, 2010. doi: 10.1038/nrn2822. URL http://www.ncbi.nlm.nih.gov/pubmed/20354534.

E Diaz. SynDIG1 regulation of excitatory synapse maturation. Ahead of Print, 2011. URL http://www.ncbi.nlm.nih.gov/pubmed/21878521.

E Diaz, Y Ge, Y H Yang, K C Loh, T A Serafini, Y Okazaki, Y Hayashizaki, T P Speed, J Ngai, and P Scheiffele. Molecular analysis of gene expression in the developing pontocerebellar projection system. *Neuron*, 36(3):417–434, 2002. URL http://www.ncbi.nlm.nih.gov/pubmed/12408845.

N Doidge. *The brain that changes itself: Stories of personal triumph from the frontiers of brain science*. Viking Adult, 2007.

W G Drew, L L Miller, and E L Baugh. Effects of delta9-THC, LSD-25 and scopolamine on continuous, spontaneous alternation in the Y-maze. *Psychopharmacologia*, 32(2):11, 1973.

I Ehrlich and R Malinow. Postsynaptic density 95 controls AMPA receptor incorporation during long-term potentiation and experience-driven synaptic plasticity. *The Journal of Neuroscience*, 24(4):916–927, 2004. doi: 10.1523/JNEUROSCI.4733-03.2004. URL http://www.ncbi.nlm.nih.gov/pubmed/14749436.

H Eichenbaum. The hippocampus and declarative memory: cognitive mechanisms and neural codes. *Behavioral Brain Research*, 127(1-2):199–207, 2001. URL http://www.ncbi.nlm.nih.gov/pubmed/11718892.

D Forrest, M Yuzaki, H D Soares, L Ng, D C Luk, M Sheng, C L Stewart, J I Morgan, J A Connor, and T Curran. Targeted disruption of NMDA receptor 1 gene abolishes NMDA response and results in neonatal death. *Neuron*, 13(2):325–338, 1994. URL http://www.ncbi.nlm.nih.gov/pubmed/8060614.

E C Fuchs, H Doheny, H Faulkner, A Caputi, R D Traub, A Bibbig, N Kopell, M A Whittington, and H Monyer. Genetically altered AMPA-type glutamate receptor kinetics in interneurons disrupt long-range synchrony of gamma oscillation. *PNAS*, 98(6):3571–3576, 2001. doi: 10.1073/pnas.051631898. URL http://www.ncbi.nlm.nih.gov/pubmed/11248119.

E C Fuchs, A R Zivkovic, M O Cunningham, S Middleton, F E Lebeau, D M Bannerman, A Rozov, M A Whittington, R D Traub, J N Rawlins, and H Monyer. Recruitment of parvalbumin-positive interneurons determines hippocampal function and associated behavior. *Neuron*, 53(4):591–604, 2007. doi: 10.1016/j.neuron.2007.01.031. URL http://www.ncbi.nlm.nih.gov/pubmed/17296559.

M Fukaya, A Kato, C Lovett, S Tonegawa, and M Watanabe. Retention of NMDA receptor NR2 subunits in the lumen of endoplasmic reticulum in targeted NR1 knockout mice. *PNAS*, 100(8):4855–4860, 2003. doi: 10.1073/pnas.0830996100. URL http://www.ncbi.nlm.nih.gov/pubmed/12676993.

M Fukaya, M Yamazaki, K Sakimura, and M Watanabe. Spatial diversity in gene expression for VDCCgamma subunit family in developing and adult mouse brains. *Neuroscience Research*, 53(4):376–383, 2005. doi: 10.1016/j.neures.2005.08.009. URL http://www.ncbi.nlm.nih.gov/pubmed/16171881.

M Fyhn, T Hafting, A Treves, M B Moser, and E I Moser. Hippocampal remapping and grid realignment in entorhinal cortex. *Nature*, 446(7132):190–194, 2007. doi: 10.1038/nature05601. URL http://www.ncbi.nlm.nih.gov/pubmed/17322902.

P E Gilbert and A M Brushfield. The role of the CA3 hippocampal subregion in spatial memory: a process oriented behavioral assessment. *Progress in Neuro-Psychopharmacology & Biological Psychiatry*, 33(5):774–781, 2009. doi: 10.1016/j.pnpbp.2009.03.037. URL http://www.ncbi.nlm.nih.gov/pubmed/19375477.

P E Gilbert, R P Kesner, and I Lee. Dissociating hippocampal subregions: double dissociation between dentate gyrus and CA1. *Hippocampus*, 11(6):626–636, 2001. doi: 10.1002/hipo.1077. URL http://www.ncbi.nlm.nih.gov/pubmed/11811656.

M B Gill, A S Kato, M F Roberts, H Yu, H Wang, S Tomita, and D S Bredt. Cornichon-2 modulates AMPA receptor-transmembrane AMPA receptor regulatory protein assembly to dictate gating and pharmacology. *The Journal of Neuroscience*, 31(18):6928–6938, 2011. doi: 10.1523/JNEUROSCI.6271-10.2011. URL http://www.ncbi.nlm.nih.gov/pubmed/21543622.

C M Gladding, S M Fitzjohn, and E Molnar. Metabotropic glutamate receptor-mediated long-term depression: molecular mechanisms. *Pharmacological Reviews*, 61(4):395–412, 2009. doi: 10.1124/pr.109.001735. URL http://www.ncbi.nlm.nih.gov/pubmed/19926678.

A E Gold and R P Kesner. The role of the CA3 subregion of the dorsal hippocampus in spatial pattern completion in the rat. *Hippocampus*, 15(6):808–814, 2005. doi: 10.1002/hipo.20103. URL http://www.ncbi.nlm.nih.gov/pubmed/16010664.

I H Greger and J A Esteban. AMPA receptor biogenesis and trafficking. *Current Opinion in Neurobiology*, 17(3):289–297, 2007. doi: 10.1016/j.conb.2007.04.007. URL http://www.ncbi.nlm.nih.gov/pubmed/17475474.

E W Harris and C W Cotman. Long-term potentiation of guinea pig mossy fiber responses is not blocked by N-methyl D-aspartate antagonists. *Neuroscience Letters*, 70(1):132–137, 1986. URL http://www.ncbi.nlm.nih.gov/pubmed/3022192.

K Hashimoto, M Fukaya, X Qiao, K Sakimura, M Watanabe, and M Kano. Impairment of AMPA receptor function in cerebellar granule cells of ataxic mutant mouse stargazer. *The Journal of Neuroscience*, 19(14):6027–6036, 1999. URL http://www.ncbi.nlm.nih.gov/pubmed/10407040.

D O Hebb. *The organization of behavior*. Wiley, New York, 1949.

S H Heinemann and E Leipold. Conotoxins of the O-superfamily affecting voltage-gated sodium channels. *Cellular and Molecular Life Sciences*, 64(11):1329–1340, 2007. doi: 10.1007/s00018-007-6565-5. URL http://www.ncbi.nlm.nih.gov/pubmed/17385074.

D A Henze, L Wittner, and G Buzsaki. Single granule cells reliably discharge targets in the hippocampal CA3 network in vivo. *Nature Neuroscience*, 5(8):790–795, 2002. doi: 10.1038/nn887. URL http://www.ncbi.nlm.nih.gov/pubmed/12118256.

M Hollmann and S Heinemann. Cloned glutamate receptors. *Annual Review of Neuroscience*, 17:31–108, 1994. doi: 10.1146/annurev.ne.17.030194.000335. URL http://www.ncbi.nlm.nih.gov/pubmed/8210177.

D H Wiesel T N Hubel. *Brain and visual perception: the story of a 25-year collaboration*. University Press, Oxford, 2004.

M R Hunsaker, B Lee, and R P Kesner. Evaluating the temporal context of episodic memory: the role of CA3 and CA1. *Behavioral Brain Research*, 188(2):310–315, 2008. doi: 10.1016/j.bbr.2007.11.015. URL http://www.ncbi.nlm.nih.gov/pubmed/18178264.

K Ibata, Q Sun, and G G Turrigiano. Rapid synaptic scaling induced by changes in postsynaptic firing. *Neuron*, 57(6):819–826, 2008. doi: 10.1016/j.neuron.2008.02.031. URL http://www.ncbi.nlm.nih.gov/pubmed/18367083.

M Ito, M Sakurai, and P Tongroach. Climbing fibre induced depression of both mossy fibre responsiveness and glutamate sensitivity of cerebellar Purkinje cells. *The Journal of Physiology*, 324:113–134, 1982. URL http://www.ncbi.nlm.nih.gov/pubmed/7097592.

A C Jackson and R A Nicoll. The expanding social network of ionotropic glutamate receptors: TARPs and other transmembrane auxiliary subunits. *Neuron*, 70(2):178–199, 2011. doi: 10.1016/j.neuron.2011.04.007. URL http://www.ncbi.nlm.nih.gov/pubmed/21521608.

L E Jarrard. Selective hippocampal lesions and behavior: effects of kainic acid lesions on performance of place and cue tasks. *Behavioral Neuroscien*, 97:873–889, 1983.

L E Jarrard. On the role of the hippocampus in learning and memory in rat. *Behavioral and Neural Biology*, 60:9–26, 1993.

V Jensen, K M Kaiser, T Borchardt, G Adelmann, A Rozov, N Burnashev, C Brix, M Frotscher, P Andersen, O Hvalby, B Sakmann, P H Seeburg, and R Sprengel. A juvenile form of postsynaptic hippocampal long-term potentiation in mice deficient for the AMPA receptor

subunit GluR-A. *The Journal of Physiology*, 553(Pt 3):843–856, 2003. doi: 10.1113/jphysiol.2003.053637. URL http://www.ncbi.nlm.nih.gov/pubmed/14555717.

J W Johnson and P Ascher. Glycine potentiates the NMDA response in cultured mouse brain neurons. *Nature*, 325(6104):529–531, 1987. doi: 10.1038/325529a0. URL http://www.ncbi.nlm.nih.gov/pubmed/2433595.

M W Jung and B L McNaughton. Spatial selectivity of unit activity in the hippocampal granular layer. *Hippocampus*, 3(2):165–182, 1993. doi: 10.1002/hipo.450030209. URL http://www.ncbi.nlm.nih.gov/pubmed/8353604.

E Kalashnikova, R A Lorca, I Kaur, G A Barisone, B Li, T Ishimaru, J S Trimmer, D P Mohapatra, and E Diaz. SynDIG1: an activity-regulated, AMPA- receptor-interacting transmembrane protein that regulates excitatory synapse development. *Neuron*, 65(1):80–93, 2010. doi: 10.1016/j.neuron.2009.12.021. URL http://www.ncbi.nlm.nih.gov/pubmed/20152115.

A S Kato, W Zhou, A D Milstein, M D Knierman, E R Siuda, J E Dotzlaf, H Yu, JE Hale, E S Nisenbaum, R A Nicoll, and D S Bredt. New transmembrane AMPA receptor regulatory protein isoform, gamma-7 differentially regulates AMPA receptors. *The Journal of Neuroscience*, 27:4969–4977, 2007.

A S Kato, E R Siuda, E S Nisenbaum, and D S Bredt. AMPA receptor subunit-specific regulation by a distinct family of type II TARPs. *Neuron*, 59:986–996, 2008.

A S Kato, M B Gill, H Yu, E S Nisenbaum, and D S Bredt. TARPs differentially decorate AMPA receptors to specify neuropharmacology. *Trends in Neurosciences*, 33(5):241–248, 2010. doi: 10.1016/j.tins.2010.02.004. URL http://www.ncbi.nlm.nih.gov/pubmed/20219255.

K Keinänen, W Wisden, B Sommer, P Werner, A Herb, T A Verdoorn, B Sakmann, and P H Seeburg. A family of AMPA-selective glutamate receptors. *Science*, 249(4968):556–560, 1990. URL http://www.ncbi.nlm.nih.gov/pubmed/2166337.

R P Kesner and R O Hopkins. Mnemonic functions of the hippocampus: a comparison between animals and humans. *Biological Psychology*, 73(1):3–18, 2006. doi: 10.1016/j.biopsycho.2006.01.004. URL http://www.ncbi.nlm.nih.gov/pubmed/16473455.

R P Kesner, M R Hunsaker, and P E Gilbert. The role of CA1 in the acquisition of an object-trace-odor paired associate task. *Behavioral Neuroscience*, 119(3):781–786, 2005. doi: 10.1037/0735-7044.119.3.781. URL http://www.ncbi.nlm.nih.gov/pubmed/15998199.

C Koerber, M Werner, S Kott, Z L Ma, and M Hollmann. The transmembrane AMPA receptor regulatory protein gamma 4 is a more effective modulator of AMPA receptor function than stargazin (gamma 2). *The Journal of Neuroscience*, 27:8442–8447, 2007.

S Kott, M Werner, C KÃ¶rber, and M Hollmann. Electrophysiological properties of AMPA receptors are differentially modulated depending on the associated member of TARP family. *The Journal of Neuroscience*, 27:3780–3789, 2007.

S Kott, C Sager, D Tapken, M Werner, and M Hollmann. Comparative analysis of the pharmacology of GluR1 in complex with transmembrane AMPA receptor regulatory proteins gamma2, gamma3, gamma4, and gamma8. *Neuroscience*, 158:78–88, 2009.

S Kügler, E Kilic, and M Bähr. Human synapsin 1 gene promoter confers highly neuron-specific long-term transgene expression from an adenoviral vector in the adult rat brain depending on the transduced area. *Gene Therapy*, 10(4):337 – 47, 2003.

I Lee and R P Kesner. Encoding versus retrieval of spatial memory: double dissociation between the dentate gyrus and the perforant path inputs into CA3 in the dorsal hippocampus. *Hippocampus*, 14(1):66–76, 2004. doi: 10.1002/hipo.10167. URL `http://www.ncbi.nlm.nih.gov/pubmed/15058484`.

I Lee, T S Jerman, and R P Kesner. Disruption of delayed memory for a sequence of spatial locations following CA1- or CA3-lesions of the dorsal hippocampus. *Neurobiology of Learning and Memory*, 84(2):138–147, 2005. doi: 10.1016/j.nlm.2005.06.002. URL `http://www.ncbi.nlm.nih.gov/pubmed/16054848`.

R A Lester and C E Jahr. NMDA channel behavior depends on agonist affinity. *The Journal of Neuroscience*, 12(2):635–643, 1992. URL `http://www.ncbi.nlm.nih.gov/pubmed/1346806`.

V A Letts. Stargazer–a mouse to seize! *Epilepsy currents / American Epilepsy Society*, 5 (5):161–165, 2005. doi: 10.1111/j.1535-7511.2005.00051.x. URL `http://www.ncbi.nlm.nih.gov/pubmed/16175212`.

V A Letts, R Felix, G H Biddlecome, J Arikkath, C L Mahaffey, A Valenzuela, F S 2nd Bartlett, Y Mori, K P Campbell, and W N Frankel. The mouse stargazer gene encodes a neuronal Ca2+-channel gamma subunit. *Nature Genetics*, 19:340–347, 1998.

J K Leutgeb and E I Moser. Enigmas of the dentate gyrus. *Neuron*, 55(2):176–178, 2007. doi: 10.1016/j.neuron.2007.07.002. URL `http://www.ncbi.nlm.nih.gov/pubmed/17640520`.

J K Leutgeb, S Leutgeb, M B Moser, and E I Moser. Pattern separation in the dentate gyrus and CA3 of the hippocampus. *Science*, 315(5814):961–966, 2007. doi: 10.1126/science.1135801. URL http://www.ncbi.nlm.nih.gov/pubmed/17303747.

S Leutgeb and J K Leutgeb. Pattern separation, pattern completion, and new neuronal codes within a continuous CA3 map. *Learning & Memory*, 14(11):745–757, 2007. doi: 10.1101/lm.703907. URL http://www.ncbi.nlm.nih.gov/pubmed/18007018.

S Leutgeb, J K Leutgeb, M B Moser, and E I Moser. Place cells, spatial maps and the population code for memory. *Current Opinion in Neurobiology*, 15(6):738–746, 2005. doi: 10.1016/j.conb.2005.10.002. URL http://www.ncbi.nlm.nih.gov/pubmed/16263261.

A B MacDermott, M L Mayer, G L Westbrook, S J Smith, and J L Barker. NMDA-receptor activation increases cytoplasmic calcium concentration in cultured spinal cord neurones. *Nature*, 321(6069):519–522, 1986. doi: 10.1038/321519a0. URL http://www.ncbi.nlm.nih.gov/pubmed/3012362.

J Madsen and R P Kesner. The temporal-distance effect in subjects with dementia of the Alzheimer type. *Alzheimer disease and associated disorders*, 9(2):94–100, 1995. URL http://www.ncbi.nlm.nih.gov/pubmed/7662329.

R C Malenka and M F Bear. LTP and LTD: an embarrassment of riches. *Neuron*, 44(1):5–21, 2004. doi: 10.1016/j.neuron.2004.09.012. URL http://www.ncbi.nlm.nih.gov/pubmed/15450156.

D Marr. Simple memory: a theory for archicortex. *Philosophical Transactions of the Royal Society of London*, 262(841):23–81, 1971. URL http://www.ncbi.nlm.nih.gov/pubmed/4399412.

T J McHugh, M W Jones, J J Quinn, N Balthasar, R Coppari, J K Elmquist, B B Lowell, M S Fanselow, M A Wilson, and S Tonegawa. Dentate gyrus NMDA receptors mediate rapid pattern separation in the hippocampal network. *Science*, 317(5834):94–99, 2007. doi: 10.1126/science.1140263. URL http://www.ncbi.nlm.nih.gov/pubmed/17556551.

B L McNaughton and L Nadel. *Hebb-Marr networks and the neurobiological representation of action in space*, chapter 1-64, page 64. Hillsdale, New York, neuroscien edition, 1990.

N McNaughton and R G Morris. Chlordiazepoxide, an anxiolytic benzodiazepine, impairs place navigation in rats. *Behavioral Brain Research*, 24(1):39–46, 1987. URL http://www.ncbi.nlm.nih.gov/pubmed/3580114.

K Menuz and R A Nicoll. Loss of inhibitory neuron AMPA receptors contributes to ataxia and epilepsy in stargazer mice. *The Journal of Neuroscience*, 28:10599–10603, 2008.

K Menuz, R M Stroud, R A Nicoll, and F A Hays. TARP auxiliary subunits switch AMPA receptor antagonists into partial agonists. *Science*, 318:815–817, 2007.

K Menuz, J L O'Brien, S Karmizadegan, D S Bredt, and R A Nicoll. TARP redundancy is critical for maintaining AMPA receptor function. *The Journal of Neuroscience*, 28(35): 8740–8746, 2008. doi: 10.1523/JNEUROSCI.1319-08.2008. URL `http://www.ncbi.nlm.nih.gov/pubmed/18753375`.

K Menuz, G A Kerchner, J L OBrien, and R A Nicoll. Critical role for TARPs in early development despite broad functional redundancy. *Neuropharmacology*, 56:22–29, 2009.

R Miles and R D Traub. Excitatory synaptic interactions between CA3 neurons in the guinea-pig hippocampus. *Journal of Physiology*, X(373):21, 1986.

A D Milstein and R A Nicoll. Regulation of AMPA receptor gating and pharmacology by TARP auxiliary subunits. *Trends in Pharmacological Sciences*, 29(7):333–339, 2008. doi: 10.1016/j.tips.2008.04.004. URL `http://www.ncbi.nlm.nih.gov/pubmed/18514334`.

A D Milstein, W Zhou, S Karimzadegan, D S Bredt, and R A Nicoll. TARP subtypes differentially and dose-dependently control synaptic AMPA receptor gating. *Neuron*, 55 (6):905–918, 2007. doi: 10.1016/j.neuron.2007.08.022. URL `http://www.ncbi.nlm.nih.gov/pubmed/17880894`.

H Monyer, R Sprengel, R Schoepfer, A Herb, M Higuchi, H Lomeli, N Burnashev, B Sakmann, and P H Seeburg. Heteromeric NMDA receptors: molecular and functional distinction of subtypes. *Science*, 256(5060):1217–1221, 1992. URL `http://www.ncbi.nlm.nih.gov/pubmed/1350383`.

H Monyer, N Burnashev, D J Laurie, B Sakmann, and P H Seeburg. Developmental and regional expression in the rat brain and functional properties of four NMDA receptors. *Neuron*, 12(3): 529–540, 1994. URL `http://www.ncbi.nlm.nih.gov/pubmed/7512349`.

K Moriyoshi, M Masu, T Ishii, R Shigemoto, N Mizuno, and S Nakanishi. Molecular cloning and characterization of the rat NMDA receptor. *Nature*, 354:31–37, 1991.

R G Morris, P Garrud, J N Rawlins, and J O'Keefe. Place navigation impaired in rats with hippocampal lesions. *Nature*, 297(5868):681–683, 1982. URL `http://www.ncbi.nlm.nih.gov/pubmed/7088155`.

R G Morris, E Anderson, G S Lynch, and M Baudry. Selective impairment of learning and blockade of long-term potentiation by an N-methyl-D-aspartate receptor antagonist, AP5. *Nature*, 319(6056):774–776, 1986. doi: 10.1038/319774a0. URL http://www.ncbi.nlm.nih.gov/pubmed/2869411.

R U Muller, J L Kubie, and R Saypoff. The hippocampus as a cognitive graph (abridged version). *Hippocampus*, 1(3):243–246, 1991. doi: 10.1002/hipo.450010306. URL http://www.ncbi.nlm.nih.gov/pubmed/1669298.

A J Murray, J F Sauer, G Riedel, C McClure, L Ansel, L Cheyne, M Bartos, W Wisden, and P Wulff. Parvalbumin-positive CA1 interneurons are required for spatial working but not for reference memory. *Nature Neuroscience*, 14(3):297–299, 2011. doi: 10.1038/nn.2751. URL http://www.ncbi.nlm.nih.gov/pubmed/21278730.

L Nadel and M Moscovitch. The hippocampal complex and long-term memory revisited. *Trends in Cognitive Sciences*, 5(6):228–230, 2001. URL http://www.ncbi.nlm.nih.gov/pubmed/11390282.

K Nakazawa, L D Sun, M C Quirk, L Rondi-Reig, M A Wilson, and S Tonegawa. Hippocampal CA3 NMDA receptors are crucial for memory acquisition of one-time experience. *Neuron*, 38 (2):305–315, 2003. URL http://www.ncbi.nlm.nih.gov/pubmed/12718863.

K Nakazawa, T J McHugh, M A Wilson, and S Tonegawa. NMDA receptors, place cells and hippocampal spatial memory. *Nature Reviews. Neuroscience*, 5(5):361–372, 2004. doi: 10.1038/nrn1385. URL http://www.ncbi.nlm.nih.gov/pubmed/15100719.

T Nakazawa, T Tezuka, and T Yamamoto. [Regulation of NMDA receptor function by Fyn-mediated tyrosine phosphorylation]. *Japanese Journal of Psychopharmacology*, 22(5): 165–167, 2002. URL http://www.ncbi.nlm.nih.gov/pubmed/12451687.

B Niewoehner, F N Single, O Hvalby, V Jensen, S Meyer Zum Alten Borgloh, P H Seeburg, J N Rawlins, R Sprengel, and D M Bannerman. Impaired spatial working memory but spared spatial reference memory following functional loss of NMDA receptors in the dentate gyrus. *The European Journal of Neuroscience*, 25(3):837–846, 2007. doi: 10.1111/j.1460-9568.2007.05312.x. URL http://www.ncbi.nlm.nih.gov/pubmed/17313573.

J L Noebels, X Qiao, R T Bronson, C Spencer, and M T Davisson. Stargazer: a new neurological mutant on chromosome 15 in the mouse with prolonged cortical seizures. *Epilepsy Research*, 7(2):129–135, 1990. URL http://www.ncbi.nlm.nih.gov/pubmed/2289471.

L Nowak, P Bregestovski, P Ascher, A Herbet, and A Prochiantz. Magnesium gates glutamate-activated channels in mouse central neurones. *Nature*, 307(5950):462–465, 1984. URL http://www.ncbi.nlm.nih.gov/pubmed/6320006.

J O'Keefe. Place units in the hippocampus of the freely moving rat. *Experimental Neurology*, 51(1):78–109, 1976. URL http://www.ncbi.nlm.nih.gov/pubmed/1261644.

J O'Keefe and D H Conway. Hippocampal place units in the freely moving rat: why they fire where they fire. *Experimental Brain Research*, 31(4):573–590, 1978. URL http://www.ncbi.nlm.nih.gov/pubmed/658182.

J O'Keefe and J Dostrovsky. The hippocampus as a spatial map. Preliminary evidence from unit activity in the freely-moving rat. *Brain Research*, 34(1):171–175, 1971. URL http://www.ncbi.nlm.nih.gov/pubmed/5124915.

D S Olton and B C Papas. Spatial memory and hippocampal function. *Neuropsychologia*, 17 (6):669–682, 1979. URL http://www.ncbi.nlm.nih.gov/pubmed/522981.

D S Olton and R F Samuelson. remembrance of places passed: spatial memory in rats. *Journal of Experimental Psychology: Animal Behavior Processes*, 2:97–116, 1976.

P Opazo and D Choquet. A three-step model for the synaptic recruitment of AMPA receptors. *Molecular and Cellular Neurosciences*, 46(1):1–8, 2011. doi: 10.1016/j.mcn.2010.08.014. URL http://www.ncbi.nlm.nih.gov/pubmed/20817097.

G Paxinos and K B J Franklin. *the mouse brain in stereotaxic coordinates*. University of Washington, 2001.

A Priel, A Kolleker, G Ayalon, M Gillor, P Osten, and Y Stern-Bach. Stargazin reduces desensitization and slows deactivation of the AMPA-type glutamate receptors. *The Journal of Neuroscience*, 25(10):2682–2686, 2005. doi: 10.1523/JNEUROSCI.4834-04.2005. URL http://www.ncbi.nlm.nih.gov/pubmed/15758178.

C Rampon, Y P Tang, J Goodhouse, E Shimizu, M Kyin, and J Z Tsien. Enrichment induces structural changes and recovery from nonspatial memory deficits in CA1 NMDAR1-knockout mice. *Nature Neuroscience*, 3(3):238–244, 2000. doi: 10.1038/72945. URL http://www.ncbi.nlm.nih.gov/pubmed/10700255.

J N Rawlins and D S Olton. The septo-hippocampal system and cognitive mapping. *Behavioral Brain Research*, 5(4):331–358, 1982. URL http://www.ncbi.nlm.nih.gov/pubmed/7126316.

D Reisel, D M Bannerman, W B Schmitt, R M Deacon, J Flint, T Borchardt, P H Seeburg, and J N Rawlins. Spatial memory dissociations in mice lacking GluR1. *Nature Neuroscience*, 5(9):868–873, 2002. doi: 10.1038/nn910. URL http://www.ncbi.nlm.nih.gov/pubmed/12195431.

G Riedel, J Micheau, A G Lam, E L Roloff, S J Martin, H Bridge, L de Hoz, B Poeschel, J McCulloch, and R G Morris. Reversible neural inactivation reveals hippocampal participation in several memory processes. *Nature Neuroscience*, 2(10):898–905, 1999. doi: 10.1038/13202. URL http://www.ncbi.nlm.nih.gov/pubmed/10491611.

R G Robertson, E T Rolls, and P Georges-Fran Ois. Spatial view cells in the primate hippocampus: effects of removal of view details. *Journal of Neurophysiology*, 79(3):1145–1156, 1998. URL http://www.ncbi.nlm.nih.gov/pubmed/9497397.

E T Rolls. A theory of hippocampal function in memory. *Hippocampus*, 6(6):601–620, 1996. doi: 10.1002/(SICI)1098-1063(1996)6:6\<601::AID-HIPO5\>3.0.CO;2-J. URL http://www.ncbi.nlm.nih.gov/pubmed/9034849.

E T Rolls and R P Kesner. A computational theory of hippocampal function, and empirical tests of the theory. *Progress in Neurobiology*, 79(1):1–48, 2006. doi: 10.1016/j.pneurobio.2006.04.005. URL http://www.ncbi.nlm.nih.gov/pubmed/16781044.

E T Rolls, A Treves, R G Robertson, P Georges-Francois, and S Panzeri. Information about spatial view in an ensemble of primate hippocampal cells. *Journal of Neurophysiology*, 79(4):1797–1813, 1998. URL http://www.ncbi.nlm.nih.gov/pubmed/9535949.

C Romberg, J Raffel, L Martin, R Sprengel, P H Seeburg, J N Rawlins, D M Bannerman, and O Paulsen. Induction and expression of GluA1 (GluR-A)-independent LTP in the hippocampus. *The European Journal of Neuroscience*, 29(6):1141–1152, 2009. doi: 10.1111/j.1460-9568.2009.06677.x. URL http://www.ncbi.nlm.nih.gov/pubmed/19302150.

N Rouach, K Byrd, R S Petralia, G M Elias, H Adesnik, S Tomita, S Karimzadegan, C Kealey, D S Bredt, and R A Nicoll. TARP gamma-8 controls hippocampal AMPA receptor number, distribution and synaptic plasticity. *Nature Neuroscience*, 8(11):1525–1533, 2005. doi: 10.1038/nn1551. URL http://www.ncbi.nlm.nih.gov/pubmed/16222232.

A Sahay, D A Wilson, and R Hen. Pattern separation: a common function for new neurons in hippocampus and olfactory bulb. *Neuron*, 70(4):582–588, 2011. doi: 10.1016/j.neuron.2011.05.012. URL http://www.ncbi.nlm.nih.gov/pubmed/21609817.

J Sambrook, E F Fritsch, and T Maniatis. *Molecular cloning: a laboratory manual.*, volume 3. Cold Spring Harbor Laboratory Press, New York, 2 edition, 1989.

D J Sanderson and D M Bannerman. The role of habituation in hippocampus-dependent spatial working memory tasks: Evidence from GluA1 AMPA receptor subunit knockout mice. *Hippocampus*, 2010. doi: 10.1002/hipo.20896. URL http://www.ncbi.nlm.nih.gov/pubmed/21125585.

D J Sanderson and D M Bannerman. Competitive short-term and long-term memory processes in spatial habituation. *Journal of Experimental Psychology*, 37(2):189–199, 2011. doi: 10.1037/a0021461. URL http://www.ncbi.nlm.nih.gov/pubmed/21319917.

D J Sanderson, C Cunningham, R M Deacon, D M Bannerman, V H Perry, and J N Rawlins. A double dissociation between the effects of sub-pyrogenic systemic inflammation and hippocampal lesions on learning. *Behavioral Brain Research*, 201(1):103–111, 2009. doi: 10.1016/j.bbr.2009.01.038. URL http://www.ncbi.nlm.nih.gov/pubmed/19428623.

D J Sanderson, E Hindley, E Smeaton, N Denny, A Taylor, C Barkus, R Sprengel, P H Seeburg, and D M Bannerman. Deletion of the GluA1 AMPA receptor subunit impairs recency-dependent object recognition memory. *Learning & Memory*, 18(3):181–190, 2011a. doi: 10.1101/lm.2083411. URL http://www.ncbi.nlm.nih.gov/pubmed/21378100.

D J Sanderson, R Sprengel, P H Seeburg, and D M Bannerman. Deletion of the GluA1 AMPA receptor subunit alters the expression of short-term memory. *Learning & Memory*, 18(3):128–131, 2011b. doi: 10.1101/lm.2014911. URL http://www.ncbi.nlm.nih.gov/pubmed/21325433.

W B Schmitt, R M Deacon, P H Seeburg, J N Rawlins, and D M Bannerman. A within-subjects, within-task demonstration of intact spatial reference memory and impaired spatial working memory in glutamate receptor-A-deficient mice. *The Journal of Neuroscience*, 23(9):3953–3959, 2003. URL http://www.ncbi.nlm.nih.gov/pubmed/12736365.

E Schnell, M Sizemore, S Karimzadegan, L Chen, D S Bredt, and R A Nicoll. Direct interactions between PSD-95 and stargazin control synaptic AMPA receptor number. *PNAS*, 99(21):13902–13907, 2002. doi: 10.1073/pnas.172511199. URL http://www.ncbi.nlm.nih.gov/pubmed/12359873.

J Schwenk, N Harmel, G Zolles, W Bildl, A Kulik, B Heimrich, O Chisaka, P Jonas, U Schulte, B Fakler, and N Klocker. Functional proteomics identify cornichon proteins as auxiliary subunits of AMPA receptors. *Science*, 323(5919):1313–1319, 2009. doi: 10.1126/science.1167852. URL http://www.ncbi.nlm.nih.gov/pubmed/19265014.

W B Scoville and B Milner. Loss of recent memory after bilateral hippocampal lesions. *Journal of Neurology, Neurosurgery, and Psychiatry*, 20(1):11–21, 1957. URL http://www.ncbi.nlm.nih.gov/pubmed/13406589.

P H Seeburg, N Burnashev, G Kohr, T Kuner, R Sprengel, and H Monyer. The NMDA receptor channel: molecular design of a coincidence detector. *Recent Progress in Hormone Research*, 50:19–34, 1995. URL http://www.ncbi.nlm.nih.gov/pubmed/7740157.

T J Sejnowski. Synaptic mechanisms for long-term depression. *Current Biology*, 1(1):38–40, 1991. URL http://www.ncbi.nlm.nih.gov/pubmed/15336203.

S Shi, Y Hayashi, J A Esteban, and R Malinow. Subunit-specific rules governing AMPA receptor trafficking to synapses in hippocampal pyramidal neurons. *Science*, 105(3):331–343, 2001. URL http://www.ncbi.nlm.nih.gov/pubmed/11348590.

S H Shi, Y Hayashi, R S Petralia, S H Zaman, R J Wenthold, K Svoboda, and R Malinow. Rapid spine delivery and redistribution of AMPA receptors after synaptic NMDA receptor activation. *Science*, 284(5421):1811–1816, 1999. URL http://www.ncbi.nlm.nih.gov/pubmed/10364548.

Y Shi, W Lu, A D Milstein, and R A Nicoll. The stoichiometry of AMPA receptors and TARPs varies by neuronal cell type. *Neuron*, 62:633–640, 2009.

Y Shi, Y H Suh, A D Milstein, K Isozaki, S M Schmid, K W Roche, and R A Nicoll. Functional comparison of the effects of TARPs and cornichons on AMPA receptor trafficking and gating. *PNAS*, 107(37):16315–16319, 2010. doi: 10.1073/pnas.1011706107. URL http://www.ncbi.nlm.nih.gov/pubmed/20805473.

G J Siegel, B W Agranoff, and R W Albers. *Basic Neurochemistry: Molecular, Cellular and Medical Aspects*. Lippincott-Raven, 1999.

S A Small, S A Schobel, R B Buxton, M P Witter, and C A Barnes. A pathophysiological framework of hippocampal dysfunction in ageing and disease. *Nature Reviews. Neuroscience*, 12(10):585–601, 2011. doi: 10.1038/nrn3085. URL http://www.ncbi.nlm.nih.gov/pubmed/21897434.

B Sommer, K Keinanen, T A Verdoorn, W Wisden, N Burnashev, A Herb, M Kohler, T Takagi, B Sakmann, and P H Seeburg. Flip and flop: a cell-specific functional switch in glutamate-operated channels of the CNS. *Science*, 249(4976):1580–1585, 1990. URL http://www.ncbi.nlm.nih.gov/pubmed/1699275.

B Sommer, M Kohler, R Sprengel, and P H Seeburg. RNA editing in brain controls a determinant of ion flow in glutamate-gated channels. *Cell*, 67(1):11–19, 1991. URL http://www.ncbi.nlm.nih.gov/pubmed/1717158.

D Soto, I D Coombs, L Kelly, M Farrant, and S G Cull-Candy. Stargazin attenuates intracellular polyamine block of calcium-permeable AMPA receptors. *Nature Neuroscience*, 10:1634, 2007.

D Soto, I D Coombs, M Renzi, M Zonouzi, M Farrant, and S G Cull-Candy. Selective regulation of long-form calcium-permeable AMPA receptors by an atypical TARP, gamma-5. *Nature Neuroscience*, 12:277–285, 2009.

R W Sperry. The problem of central nervous reorganization after nerve regeneration and muscle transposition. *The Quarterly Review of Biology*, 20:311–369, 1945. URL http://www.ncbi.nlm.nih.gov/pubmed/21010869.

L R Squire. memory and forgetting: long-term and gradual changes in memory storage. *International Review of Neurobiology*, 37:243–269, 1994.

V Stein, D R House, D S Bredt, and R A Nicoll. Postsynaptic density-95 mimics and occludes hippocampal long-term potentiation and enhances long-term depression. *The Journal of Neuroscience*, 23(13):5503–5506, 2003. URL http://www.ncbi.nlm.nih.gov/pubmed/12843250.

P Stern, P Behe, R Schoepfer, and D Colquhoun. Single-channel conductances of NMDA receptors expressed from cloned cDNAs: comparison with native receptors. *Proceedings. Biological Sciences/The Royal Society*, 250(1329):271–277, 1992. doi: 10.1098/rspb.1992.0159. URL http://www.ncbi.nlm.nih.gov/pubmed/1283639.

O Steward and S A Scoville. Cells of origin of entorhinal cortical afferents to the hippocampus and fascia dentata of the rat. *The Journal of Comparative Neurology*, 169(3):347–370, 1976. doi: 10.1002/cne.901690306. URL http://www.ncbi.nlm.nih.gov/pubmed/972204.

E Suzuki, M Kessler, and AC Arai. The fast kinetics of AMPA GluR3 receptors is selectively modulated by the TARPs gamma 4 and gamma 8. 38:117–123, 2008.

L W Swanson, J M Wyss, and W M Cowan. An autoradiographic study of the organization of intrahippocampal association pathways in the rat. *The Journal of Comparative Neurology*, 181(4):681–715, 1978. doi: 10.1002/cne.901810402. URL http://www.ncbi.nlm.nih.gov/pubmed/690280.

E C Tolman. Cognitive maps in rats and men. *Psychological Review*, 55(4):189–208, 1948. URL http://www.ncbi.nlm.nih.gov/pubmed/18870876.

S Tomita, L Chen, Y Kawasaki, R S Petralia, R J Wenthold, R A Nicoll, and D S Bredt. Functional studies and distribution define a family of transmembrane AMPA receptor regulatory proteins. *The Journal of Cell Biology*, 161(4):805–816, 2003. doi: 10.1083/jcb.200212116. URL http://www.ncbi.nlm.nih.gov/pubmed/12771129.

S Tomita, H Adesnik, M Sekiguchi, W Zhang, K Wada, J R Howe, R A Nicoll, and D S Bredt. Stargazin modulates AMPA receptor gating and trafficking by distinct domains. *Nature*, 435 (7045):1052–1058, 2005. doi: 10.1038/nature03624. URL http://www.ncbi.nlm.nih.gov/pubmed/15858532.

A Treves and E T Rolls. Computational constraints suggest the need for two distinct input systems to the hippocampal CA3 network. *Hippocampus*, 2(2):189–199, 1992. doi: 10.1002/hipo.450020209. URL http://www.ncbi.nlm.nih.gov/pubmed/1308182.

A Treves and E T Rolls. Computational analysis of the role of the hippocampus in memory. *Hippocampus*, 4(3):374–391, 1994. doi: 10.1002/hipo.450040319. URL http://www.ncbi.nlm.nih.gov/pubmed/7842058.

A Treves, A Tashiro, M E Witter, and E I Moser. What is the mammalian dentate gyrus good for? *Neuroscience*, 154(4):1155–1172, 2008. doi: 10.1016/j.neuroscience.2008.04.073. URL http://www.ncbi.nlm.nih.gov/pubmed/18554812.

S Tronel, L Belnoue, N Grosjean, J M Revest, P V Piazza, M Koehl, and D N Abrous. Adult-born neurons are necessary for extended contextual discrimination. *Hippocampus*, 2010. doi: 10.1002/hipo.20895. URL http://www.ncbi.nlm.nih.gov/pubmed/21049483.

J Z Tsien, P T Huerta, and S Tonegawa. The essential role of hippocampal CA1 NMDA receptor-dependent synaptic plasticity in spatial memory. *Cell*, 87(7):1327–1338, 1996. URL http://www.ncbi.nlm.nih.gov/pubmed/8980238.

D Turetsky, E Garringer, and D K Patneau. Stargazin modulates native AMPA receptor functional properties by two distinct mechanisms. *The Journal of Neuroscience*, 25(32):7438–7448, 2005. doi: 10.1523/JNEUROSCI.1108-05.2005. URL http://www.ncbi.nlm.nih.gov/pubmed/16093395.

G G Turrigiano and S B Nelson. Thinking globally, acting locally: AMPA receptor turnover and synaptic strength. *Neuron*, 21(5):933–935, 1998. URL http://www.ncbi.nlm.nih.gov/pubmed/9856445.

A Vazdarjanova and J F Guzowski. Differences in hippocampal neuronal population responses to modifications of an environmental context: evidence for distinct, yet complementary, functions of CA3 and CA1 ensembles. *The Journal of Neuroscience*, 24(29):6489–6496, 2004. doi: 10.1523/JNEUROSCI.0350-04.2004. URL http://www.ncbi.nlm.nih.gov/pubmed/15269259.

O S Vinogradova. Hippocampus as comparator: role of the two input and two output systems of the hippocampus in selection and registration of information. *Hippocampus*, 11(5):578–598, 2001. doi: 10.1002/hipo.1073. URL http://www.ncbi.nlm.nih.gov/pubmed/11732710.

J Von Engelhardt, V Mack, R Sprengel, N Kavenstock, K W Li, Y Stern-Bach, A B Smit, P H Seeburg, and H Monyer. CKAMP44: a brain-specific protein attenuating short-term synaptic

plasticity in the dentate gyrus. *Science*, 327(5972):1518–1522, 2010. doi: 10.1126/science.1184178. URL http://www.ncbi.nlm.nih.gov/pubmed/20185686.

C S Walker, P J Brockie, D M Madsen, M M Francis, Y Zheng, S Koduri, J E Mellem, N Strutz-Seebohm, and A V Maricq. Reconstitution of invertebrate glutamate receptor function depends on stargazin-like proteins. *PNAS*, 103(28):10781–10786, 2006a. doi: 10.1073/pnas.0604482103. URL http://www.ncbi.nlm.nih.gov/pubmed/16818877.

C S Walker, M M Francis, P J Brockie, D M Madsen, Y Zheng, and A V Maricq. Conserved SOL-1 proteins regulate ionotropic glutamate receptor desensitization. *PNAS*, 103(28):10787–10792, 2006b. doi: 10.1073/pnas.0604520103. URL http://www.ncbi.nlm.nih.gov/pubmed/16818875.

G V Wallenstein, H Eichenbaum, and M E Hasselmo. The hippocampus as an associator of discontiguous events. *Trends in Neurosciences*, 21(8):317–323, 1998. URL http://www.ncbi.nlm.nih.gov/pubmed/9720595.

R Wang, C S Walker, P J Brockie, M M Francis, J E Mellem, D M Madsen, and A V Maricq. Evolutionary conserved role for TARPs in the gating of glutamate receptors and tuning of synaptic function. *Neuron*, 59(6):997–1008, 2008. doi: 10.1016/j.neuron.2008.07.023. URL http://www.ncbi.nlm.nih.gov/pubmed/18817737.

S Williams and D Johnston. Muscarinic depression of long-term potentiation in CA3 hippocampal neurons. *Science*, 242(4875):84–87, 1988. URL http://www.ncbi.nlm.nih.gov/pubmed/2845578.

M A Wilson and B L McNaughton. Dynamics of the hippocampal ensemble code for space. *Science*, 261(5124):1055–1058, 1993. URL http://www.ncbi.nlm.nih.gov/pubmed/8351520.

M Yamazaki, T Ohno-Shosaku, M Fukaya, M Kano, M Watanabe, and K Sakimura. A novel action of stargazin as an enhancer of AMPA receptor activity. *Neuroscience Research*, 50:369–374, 2004.

Maya Yamazaki, Masahiro Fukaya, Kouichi Hashimoto, Miwako Yamasaki, Mika Tsujita, Makoto Itakura, Manabu Abe, Rie Natsume, Masami Takahashi, Masanobu Kano, Kenji Sakimura, and Masahiko Watanabe. Tarps gamma-2 and gamma-7 are essential for ampa receptor expression in the cerebellum. *Eur J Neurosci*, 31(12):2204–2220, Jun 2010. doi: 10.1111/j.1460-9568.2010.07254.x. URL http://dx.doi.org/10.1111/j.1460-9568.2010.07254.x.

R A Zalutsky and R A Nicoll. Comparison of two forms of long-term potentiation in single hippocampal neurons. *Science*, 248(4963):1619–1624, 1990. URL http://www.ncbi.nlm.nih.gov/pubmed/2114039.

D Zamanillo, R Sprengel, O Hvalby, V Jensen, N Burnashev, A Rozov, K M Kaiser, H J Koster, T Borchardt, P Worley, J Lubke, M Frotscher, P H Kelly, B Sommer, P Andersen, P H Seeburg, and B Sakmann. Importance of AMPA receptors for hippocampal synaptic plasticity but not for spatial learning. *Science*, 284(5421):1805–1811, 1999. URL http://www.ncbi.nlm.nih.gov/pubmed/10364547.

W Zhang, A Robert, S B Vogensen, and J R Howe. The relationship between agonist potency and AMPA receptor kinetics. *Biophysical Journey*, 91(4):1336–1346, 2006. doi: 10.1529/biophysj.106.084426. URL http://www.ncbi.nlm.nih.gov/pubmed/16731549.

Y Zheng, P J Brockie, J E Mellem, D M Madsen, C S Walker, M M Francis, and A V Maricq. SOL-1 is an auxiliary subunit that modulates the gating of GLR-1 glutamate receptors in Caenorhabditis elegans. *PNAS*, 103(4):1100–1105, 2006. doi: 10.1073/pnas.0504612103. URL http://www.ncbi.nlm.nih.gov/pubmed/16418277.

J Zuo, P L De Jager, K A Takahashi, W Jiang, D J Linden, and N Heintz. Neurodegeneration in Lurcher mice caused by mutation in delta2 glutamate receptor gene. *Nature*, 388(6644):769–773, 1997. doi: 10.1038/42009. URL http://www.ncbi.nlm.nih.gov/pubmed/9285588.

List of Figures

List of Tables

List of Abbreviations

AAV	—	adeno-associated virus
AMPAR	—	alpha-amino-3-hydroxy-5-methyl-4-isoxazolepropionicacid receptor
C. elegans	—	Caenorhabditis elegans
CA1	—	cornu ammonis 1
CA3	—	cornu ammonis 3
CA^{2+}	—	calcium
CB	—	calbindin
cDNA	—	copy deoxyribonucleic acid
CGC	—	cerebellar granule cells
CKAMP44	—	cystine knot AMPAR modulating protein, 44kDa
CNIH-2	—	cornichon homolog 2
CNIH-3	—	cornichon homolog 3
CR	—	calretinin
CTD	—	C-terminal domain
Ce STG-1	—	C. elegans stargazin-like protein 1
Ce STG-2	—	C. elegans stargazin-like protein 2
DG	—	dentate gyrus
DGC	—	dentate granule cell
dNTPs	—	deoxyribonucleo-triphosphate
EDTA	—	ethylenediaminetetraacetic acid
ES cell	—	embryonic stem cell
GFP	—	green fluorescent protein
GLR-1	—	C. elegans glutamate receptor 1
GluA1	—	AMPAR subunit 1
GluA2	—	AMPAR subunit 2
GluA3	—	AMPAR subunit 3
GluA4	—	AMPAR subunit 4
GluRδ1	—	glutamate receptor delta 1
GluRδ2	—	glutamate receptor delta 2
H_20_2	—	hydrogene peroxid
IHC	—	immunohistochemistry

iGluR	—	ionotropic glutamate receptor
IN	—	interneuron
IRES	—	internal ribosome entry site
KAR	—	kainate receptor
KO	—	knockout
LTD	—	long term depression
LTP	—	long term potentiation
MWM	—	Morris' water maze
MgCl	—	magnesium chloride
Mg^{2+}	—	magnesium
mGluR	—	metabotropic glutamate receptor
mRNA	—	messenger ribonucleic acid
NMDAR	—	N-methyl-D-aspartate receptor
NPY	—	neuronal peptide Y
NR1	—	NMDAR subunit 1
NaOH	—	sodium hydroxide
NeuN	—	neuronal nuclei
patient H.M.	—	Henry Gustav Molaison
PBS	—	phosphate buffered solution
PCR	—	polymerase chain reaction
PV	—	parvalbumin
Pr	—	primer
Q/R-site	—	glutamine/arginine site
RAM	—	radial arm maze
SDS	—	sodium dodecyle sulfate
SOL-1	—	surpressor of lurcher 1
SynDIG1	—	synapse differentially induced gene 1
TARP	—	transmembrane AMPAR regulating protein
TENS	—	buffer made of Tris, EDTA, NaOH and SDS
TRIS-HCl	—	Tris-hydrochloride
VGCC	—	voltage gated calcium channel
WB	—	western blot